

**Combined effects of interfaces and high pressure on
the activity and stability of α -chymotrypsin and
horseradish peroxidase**

Dissertation

zur Erlangung des akademischen Grades

Doktor der Naturwissenschaften

(Dr. rer. nat.)

eingereicht bei der

Fakultät für Chemie und Chemische Biologie

der Technischen Universität Dortmund

vorgelegt von

Vitor Diniz Schuabb

Aus Nova Friburgo, Brasilien

Dortmund 2016

**Combined effects of interfaces and high pressure on
the activity and stability of α -chymotrypsin and
horseradish peroxidase**

Thesis

For the achievement of the academic degree

Dr. rer. nat.

Submitted to

the Faculty of Chemistry and Chemical Biology

TU Dortmund University

by

Vitor Diniz Schuabb

From Nova Friburgo, Brazil

Dortmund 2016

Declaration/Erklärung

The work described in this Dissertation was performed from February 2013 to June 2016 at the Faculty of Chemistry and Chemical Biology, TU Dortmund University under the guidance of Prof. Dr. Claus Czeslik.

I hereby declare that I performed the work independently and did not use any other but the indicated aids.

Die vorliegende Arbeit wurde in der Zeit von Februar 2013 bis Juni 2016 an der Fakultät für Chemie und Chemische Biologie der Technischen Universität Dortmund unter der Anleitung von Prof. Dr. Claus Czeslik durchgeführt.

Hiermit versichere ich an Eides statt, dass ich die vorliegende Arbeit selbstständig und nur mit den angegebenen Hilfsmitteln angefertigt habe.

Dortmund 2016

Vitor Diniz Schuabb

Note

This thesis is based in part on the following two publications:

- 1) V. Schuabb, C. Czeslik Activation volumes of enzymes adsorbed on silica nanoparticles *Langmuir* (2014) 30, 15496-15503.
- 2) V. Schuabb, S. Cinar, C. Czeslik Effects of interfacial properties on the activation volume of adsorbed enzymes *Colloids and Surfaces B: Biointerfaces* (2016) 140, 497-504.

It contains sentences, phrases and figures taken from these publications in agreement with the publishers.

1st Examiner

Prof. Dr. Claus Czeslik

Faculty of Chemistry and Chemical Biology

Physical Chemistry

TU Dortmund University

Dortmund

2nd Examiner

Prof. Dr. Heinz Rehage

Faculty of Chemistry and Chemical Biology

Physical Chemistry II

TU Dortmund University

Dortmund

"Everything we hear is an opinion, not a fact.

Everything we see is a perspective, not the truth."

-M.A.

Agradecimentos

Gostaria de agradecer, primeiramente, ao querido Prof. Dr. Claus Czeslik pela incrível oportunidade a mim dada de ser seu aluno de doutorado e pelo projeto a mim confiado. Inúmeras foram as vezes em que enfrentei dificuldades, mas sempre pude contar com seu vasto conhecimento, com sua paciência e pronta disponibilidade para me atender. Muito obrigado, Claus. Serei eternamente grato.

Agradeço também ao Prof. Dr. Roland Winter por me receber em seu laboratório abertamente. Em muitas ocasiões pude desfrutar de seu conhecimento, de suas aulas e também de suas experiências enológicas e gastronômicas.

Um muito obrigado muito especial vai para a querida Andrea Kreusel. Andrea desde as primeiras trocas de emails já esbanjava sua simpatia e eficiência, e com o convívio mais próximo só me fez a comprovar o quanto a Alemanha se tornava mais fácil com seu auxílio.

Um envolvente muito obrigado a todos os membros e participantes do grupo PCI pela agradável convivência, pelas boas risadas e comemorações. Em especial gostaria de agradecer a Süleyman Cinar por nosso trabalho colaborativo, e a Mimi Gao por me auxiliar na versão alemã do sumario deste trabalho.

Agradeço a toda minha família por sempre me apoiar e incentivar durante todo esse longo caminho, especialmente ao meu irmão Vinícius. Ele que por inúmeras vezes esteve aqui comigo em minha casa durante esses anos e, mesmo distante a quase 10000 quilômetros, se mantém presente virtualmente para que continuemos a desfrutar de nossa amizade/irmandade e nossos sonhos. Te amo, meu irmão.

Como agradecer o apoio, o amor, a dedicação, a presença, os conselhos e o grande exemplo às duas pessoas que a quase trinta anos te deram a vida? Pai e Mãe, tudo isso só esta se realizando, porque em grande parte é fruto do carinho, do cuidado e do incansável trabalho que vocês dedicaram a mim. Agradeço do fundo do meu coração tudo o que vocês fizeram e fazem por mim. Amo muito vocês.

Por ultimo dedico um par de palavras à pessoa mais especial da minha vida. À minha esposa, à minha companheira, à minha amiga de todas as horas, à pessoa com quem divido a minha vida. Caroline, muito obrigado por tudo. Por seu apoio dia após dia, por nossos sonhos que nos inspiram, por nossas celebrações a cada avanço e por nosso amor que nos guia sempre em frente. Comecei seu parágrafo de agradecimento prometendo apenas um par de palavras e acabei me estendendo. Não importa, consertarei escrevendo o que digo todos os dias a você: Te amo.

Acknowledgments

I would like to thank, first, dear Prof. Dr. Claus Czeslik for the amazing opportunity given to me to be your doctoral student and the project entrusted to me. Many were the times when I faced difficulties, but I could always count on his vast knowledge, his patience and ready availability to help me. Thank you, Claus. I will be forever grateful.

I also thank Prof. Dr. Roland Winter to receive me in his laboratory openly. On many occasions I was able to enjoy his knowledge, his classes, also his wine-expertise and gastronomic experiences.

A very special thanks goes to dear Andrea Kreusel. Andrea from the first email exchanges already demonstrated her friendliness and efficiency and the daily-basis contact only has proven how Germany became easier to me with her assistance.

An engaging thanks to all members and participants of the PCI group for the pleasant working atmosphere, the good laughs and celebrations. In particular I would like to thank Süleyman Cinar for our collaborative work and Mimi Gao for assisting me in the German version of the summary in this work.

I thank all my family for always supporting me and encouraging throughout this long way, especially my brother Vinicius. He has numerous times been here with me in my house over these years and even far almost 10,000 kilometers, remains present in my life continuing to enjoy our friendship / brotherhood and our dreams. I love you my brother.

How to acknowledge the support, love, dedication, presence, advice and the great life example to the two people who almost thirty years ago have given to you the gift of life? Father and Mother, everything is just taking place, because it is largely the result of affection, care and tireless work that you have dedicated to me. Thank you from the bottom of my heart everything that you have done and do for me. Love you so much.

Finally I dedicate a couple of words to the most special person in my life. To my wife, my companion, my all-time friend, the person with whom I share my life. Caroline, thank you for everything. For your daily support, for our dreams that inspire us, for our celebrations in every advance we make and for our love that always guided us forward. I started this paragraph dedicated to you promising literally just a couple of words and I just extended it too much. It doesn't matter, I will fix it now by writing what I say every day to you: Love you.

Abbreviations

7-AMC	7- Amino- 4 - methylcoumarin
Ala-Ala.Phe-7-AMC	Alanine-alanine-phenyalanine-7-amid-4-methylcoumarin
ATR-FTIR	Attenuated total reflection fourier transform infrared spectroscopy
Da	Dalton
E	Enzyme
E+P	Enzyme plus product
E+S	Enzyme plus substrate
ES*	Transition state
FRET	Föster resonance energy transfer
FTIR	Fourier transform infrared spectroscopy
HP-SF	High pressure stopped-flow
HRP	Horseradish peroxidase
IR	Infrared
kDa	kilo Daltons
MW	Molecular weight
PDB	Protein data bank
PEG	Polyethylene glycol
PEI	Poly(ethyleneimine)
Phe	Phenylalanine
PS	Poly(styrene)

PSS	Poly(styrene) sulfonate
r	Kinetic rate at higher pressures
r ₀	Kinetic rate at 1 bar
RPM	Rotations per minute
SDS-PAGE	Sodium-dodecyl-sulfate polyacrylamide gel electrophoresis
TIRF	Total internal reflection fluorescence spectroscopy
Trp	Tryptophan
Tyr	Tyrosin
UV	Ultraviolet light
UV-VIS	Ultraviolet-visible light spectroscopy
XRR	X-ray reflectometry
α-CT	Alpha-chymotrypsin

Content

Declaration	I
Note	III
Examiners	V
<i>Agradecimientos</i>	IX
Acknowledgements	XI
Abbreviations	XIII
List of figures	XXIII
List of tables	XXXI
List of fluorophores	XXXIII
List of polymers	XXXV
1. Introduction	1
1.1. Immobilization of enzymes at aqueous-solid interfaces	3
1.2. Current strategies to overcome loss of enzyme function at interfaces	4
1.3. Effect of pressure on enzymes in solution	5
1.4. Motivation of the work	9
1.5. Alpha-chymotrypsin	10
1.6. Horseradish peroxidase	12
1.7. Physical adsorption on surfaces	13
1.8. Silica nanoparticles	14
1.8.1. Ludox CL®	15
1.8.2. Ludox AM®	15
1.9. Planar surfaces	16
2. Materials & methods	19
2.1. List of materials	21
2.2. Methods	24
2.2.1. Fluorescence spectroscopy	24
2.2.2. FTIR spectroscopy	25
2.2.3. UV-VIS spectroscopy	27
2.2.4. TIRF spectroscopy	27

2.2.5. Surface techniques	29
2.2.5.1. Spin-coating	29
2.2.5.2. Polyelectrolyte multilayer deposition	30
2.2.6. X-ray reflectivity	31
2.2.7. High pressure stopped-flow system	32
2.2.8. SDS-PAGE	33
3. Activation volumes of enzymes adsorbed on silica particles	35
3.1. Background	37
3.2. Experimental details	38
3.2.1. Enzymes and substrates	38
3.2.2. Enzymatic assays	39
3.2.3. Degree of adsorption	40
3.2.4. Data collection and analyses	43
3.2.5. FTIR spectroscopy	45
3.3. Results and discussion	46
3.3.1. Pressure stability of HRP and α -CT	46
3.3.2. Pressure effects on enzymatic activity of free and adsorbed α -CT	48
3.3.3. Pressure effects on enzymatic activity of free and adsorbed HRP	53
3.4. Conclusions	57
4. Effect of interfacial properties on the activation volume of adsorbed enzymes	59
4.1. Background	61
4.2. Experimental details	62
4.2.1. Proteins and chemicals	62
4.2.2. Enzymatic assays	62
4.2.3. Interfaces	63
4.2.4. Instrumental techniques	63
4.3. Results and discussion	65
4.3.1. Sample characterization	65
4.3.2. Enzyme activities at different interfaces	68

4.3.3. Activation volume of α -CT	69
4.3.4. Activation volume of HRP	75
4.4. Conclusions	81
5. Advantages of adsorbing α -CT on silica nanoparticles – A high-pressure stopped-flow study	83
5.1. Background	85
5.2. Experimental details	85
5.2.1. Proteins and chemicals	85
5.2.2. Enzymatic assays	85
5.2.3. Autolysis and SDS-PAGE	88
5.3. Results and discussion	89
5.3.1. Determination of K_M and k_{cat}	89
5.3.2. High-pressure stopped-flow experiments	93
5.3.3. Activation volumes	95
5.3.4. Reversibility	100
5.3.5. Autolysis	101
5.4. Conclusions	103
6. Global Summary	105
7. <i>Zusammenfassung</i>	111
8. Bibliography	119
9. Publications and presentations	127
10. <i>Curriculum Vitae</i>	131

List of Figures

- 1. Proteins adsorbed on planar surface. Ex.: Scheme of a biochip**
- 2. Volume change diagram of a hypothetical enzymatic reaction**
- 3. Free and adsorbed protein under pressure.**
- 4. α -CT crystal structure (PDB: 1GL0) and its kinetic mechanism**
- 5. Reaction between α -CT and Ala-Ala-Phe-7-AMC releasing the product 7-AMC**
- 6. HRP crystal structure (PDB: 1HCH) and its kinetic mechanism**
- 7. Reaction between HRP and Amplex Red® releasing the product resorufin.**
- 8. Examples of fixing proteins on surfaces with physical adsorption technique**
- 9. Ludox CL® interface scheme**
- 10. Ludox AM® interface scheme**
- 11. Protein adsorbed on modified planar surfaces**
- 12. High pressure fluorescence spectroscopy**
- 13. High pressure Fourier transform infrared spectroscopy**
- 14. UV-VIS spectroscopy**
- 15. High pressure total internal fluorescence spectroscopy**
- 16. Modification of a planar surface using the spin-coating technique**
- 17. Modification of a planar surface using the layer-by-layer technique**
- 18. X-ray reflectivity of a planar surface**
- 19. Single mixing stopped-flow system**
- 20. Polyacrylamid gel electrophoresis**
- 21. Amicon® ultrafiltration devices**

- 22. Activity measurements of adsorbed α -CT and HRP before and after ultrafiltration**
- 23. Typical fluorescence data recorded to probe the enzymatic activity of α -CT and HRP.**
- 24. Pressure dependence of fluorescence intensity of the assay product EnzChek and resorufin**
- 25. Amide I' band in the FTIR spectra of free and adsorbed α -CT and HRP (selected data)**
- 26. Tryptophan fluorescence of α -CT as a function of pressure and temperature**
- 27. Pressure dependence of the enzymatic activity of free α -CT**
- 28. Pressure dependence of the enzymatic activity of adsorbed α -CT**
- 29. Activation volumes of free and adsorbed α -CT**
- 30. Pressure dependence of the enzymatic activity of free HRP**
- 31. Pressure dependence of the enzymatic activity of adsorbed HRP**
- 32. Activation volumes of free and adsorbed HRP**
- 33. Pressure dependence of total internal reflection fluorescence intensity of the assay products**
- 34. X-ray reflectivity of quartz surfaces modified with PS film and polyelectrolyte multilayers ending with PSS and PAH**
- 35. Amide I' bands of α -CT and HRP, recorded both free in solution and irreversibly adsorbed at various aqueous-solid interfaces**
- 36. Total internal reflection fluorescence intensity as a function of time showing enzymatic activity of α -CT at water-quartz interface**
- 37. α -CT pressure dependent enzymatic activity when adsorbed on quartz**

38. α -CT pressure dependent enzymatic activity when adsorbed on PS film
39. α -CT pressure dependent enzymatic activity when adsorbed on PSS ending multilayers
40. α -CT pressure dependent enzymatic activity when adsorbed on PAH ending multilayers
41. Activation volumes of α -CT adsorbed on quartz, a PS film, a PSS ending and a PAH ending multilayers
42. HRP pressure dependent enzymatic activity when adsorbed on quartz
43. HRP pressure dependent enzymatic activity when adsorbed on PS film
44. HRP pressure dependent enzymatic activity when adsorbed on PSS ending multilayers
45. HRP pressure dependent enzymatic activity when adsorbed on PAH ending multilayers
46. Activation volumes of HRP adsorbed on quartz, a PS film, a PSS ending and a PAH ending multilayers
47. Enzymatic activity of α -CT measured with different Ala-Ala-Phe-7-AMC concentrations
48. Enzymatic activity of α -CT adsorbed on Ludox AM® with different Ala-Ala-Phe-7-AMC concentrations
49. Michaelis-Menten plot of α -CT free and adsorbed on Ludox AM® for Ala-Ala-Phe-7-AMC
50. High pressure stopped-flow kinetics of α -CT free and adsorbed on Ludox AM® with 500 μ M of Ala-Ala-Phe-7-AMC
51. High pressure stopped-flow kinetics of α -CT free and adsorbed on Ludox AM® with 1500 μ M of Ala-Ala-Phe-7-AMC

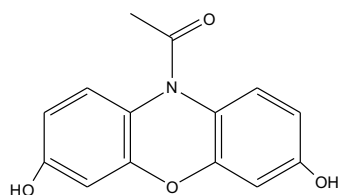
- 52. Pressure dependence of free α -CT enzymatic activity with 500 μ M of Ala-Ala-Phe-7-AMC**
- 53. Pressure dependence of α -CT enzymatic activity when adsorbed on Ludox AM® with 500 μ M of Ala-Ala-Phe-7-AMC**
- 54. Pressure dependence of the enzymatic activity of free α -CT with 1500 μ M of Ala-Ala-Phe-7-AMC**
- 55. Pressure dependence of the enzymatic activity of α -CT when adsorbed on Ludox AM® with 1500 μ M of Ala-Ala-Phe-7-AMC**
- 56. Activation volumes of α -CT free and adsorbed on Ludox AM® with 500 and 1500 μ M of Ala-Ala-Phe-7-AMC**
- 57. Reversibility test of α -CT free and adsorbed on Ludox AM® before and after pressurization up to 2000 bar**
- 58. Autolysis test of α -CT free and adsorbed on Ludox AM®**

List of Tables

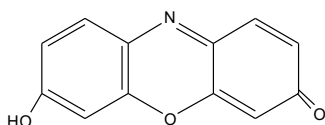
- 1. Activities of α -CT and HRP adsorbed on quartz, a PS film, a PSS and a PAH ending multilayer.**

List of fluorophores

- **Amplex Red®**

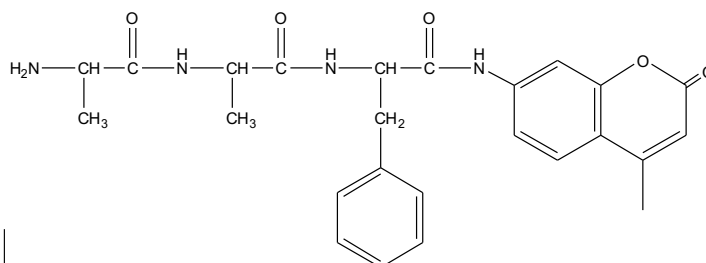


- **Resorufin**

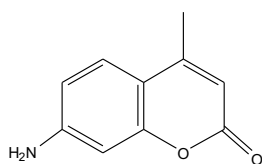


- **Enzchek® – Structure under patent protection.**

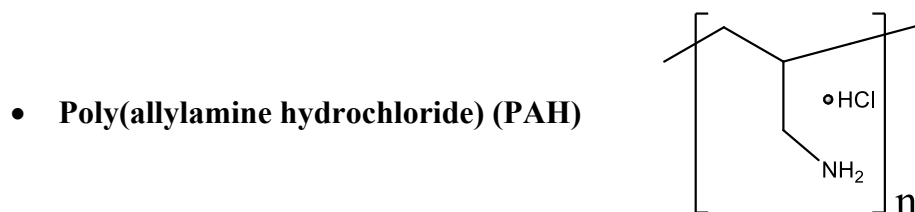
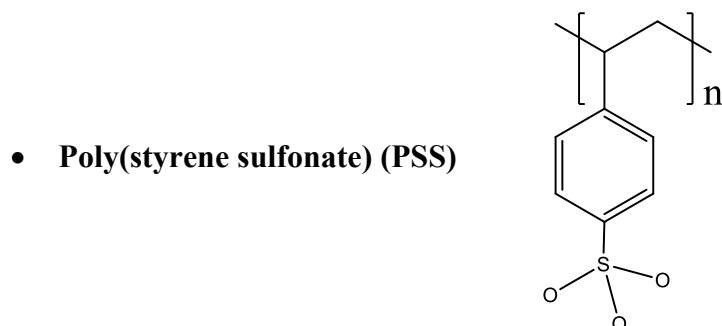
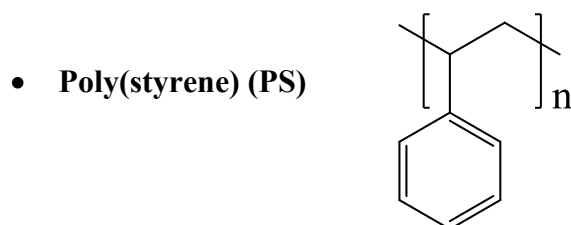
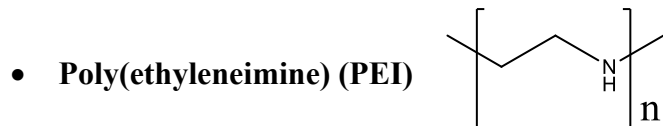
- **Ala-Ala-Phe-7-AMC**



- **7-AMC**



List of polymers



1. Introduction

1. Introduction

1.1. Immobilization of enzymes at aqueous-solid interfaces

Enzymes are mainly proteins with catalytic properties. They are responsible for accelerating biochemical reactions at optimal environmental conditions, which usually are neutral pH values, ambient pressure and more often ambient temperature. Usually an enzyme mechanism is very specific for a particular reaction pathway enabling yields with high enantiomeric excess [1]. Therefore, enzymes are very attractive to use in biotechnological, pharmaceutical, and biomedical processes. The greatest disadvantage of using enzymes, compared to chemical catalysts, is their relatively low stability and their relatively high cost. There are many examples of expensive enzymes that are worth being recovered from the reaction media to be reused in many cycles. Using filtration or centrifugation, enzymes are easily removed from a reaction mixture, when the enzymes are immobilized on carrier particles large enough to be retained or sedimented [2-3]. Particles are preferred over planar surfaces where a high amount of enzymes is needed. These particles may have a rough surface or are porous to increase the specific surface area. In research, biological samples are often immobilized on planar solid supports for imaging and spectroscopic analysis, even with single-molecule resolution [4]. It is of great interest to study the structure, dynamics and biological function of such samples. In this case, enzymatic activity might also be interesting to happen in the region of an aqueous-solid interface.

Enzymes are adapted to a certain type of cell environment, even though their native folded tertiary structure is only marginally stable in relation to an unfolded state [1,5]. The standard Gibbs energy change of unfolding, ΔG° , of many proteins is around 20 – 60 kJ mol⁻¹, similar to the strength of a few hydrogen bonds. This means that any deviation from the protein's natural environment can lead to structural change or even complete unfolding of the protein. Since any biological activity, in particular with enzymes, is strongly related to the native structure of the protein, even partial unfolding has to be avoided. Perturbation of the natural environment of a protein can be caused by a change of the solvent composition, *e.g.*, the pH-value, the ionic strength, or the presence of co-solvents. Consequently, the contact of a protein with an aqueous-solid interface represents a major perturbation of the protein environment. The aqueous-solid interface interaction can cause the replacement of water molecules by the artificial interface at the protein surface, especially when it is a hydrophobic

surface. In addition, an aqueous-solid interface may provide different pH-values, when dissociated chemical groups are present, or different ionic strength, when it has charged groups. Thus, any adsorption and/or immobilization of enzymes at aqueous-solid interfaces may lead to some changes in the protein's conformation [6-8]. The interaction with a solid surface can slow down the dynamics of a protein, and the overall enzymatic activity may be decreased by an unfavorable orientation of the enzyme molecules, since the active site can be blocked either by the material surface or by neighboring enzyme molecules [9]. As seen in figure 1.

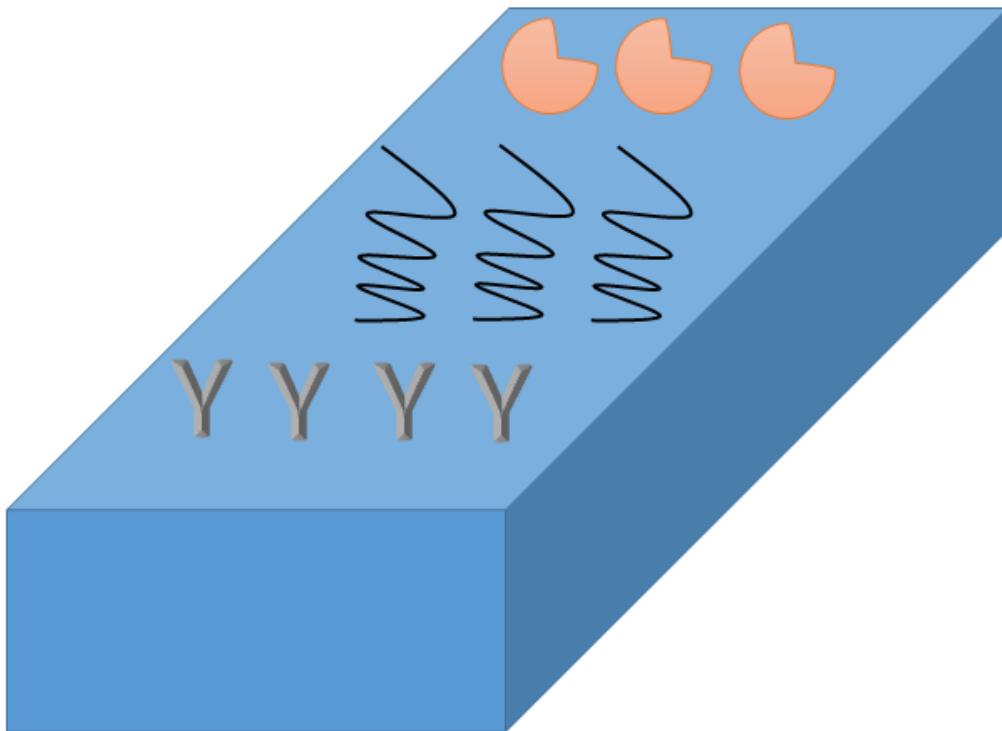


Figure 1. Proteins adsorbed on planar surface. Ex.: Scheme of a biochip. Different proteins can be adsorbed on a planar surface creating a biochip. At the bottom line the Y shaped figures represent antibodies, at the middle line coil shaped proteins are represented and at the top line there are globular enzymes with the active site exposed.

1.2. Current strategies to overcome loss of enzyme function at interfaces

As written in the section above, there are some advantages of enzyme immobilization on carrier particles [2,3]. It allows the removal of the enzymes from reaction mixtures and then their reutilization, and it prevents enzyme aggregation [3]. Even lipophilic enzymes can be

used in the aqueous phase, when they are attached to hydrophobic surfaces [10]. Some disadvantages of using immobilized enzymes appear from a low mass transfer to and from the interface and partitioning effects controlling the distribution of substrate and product molecules in the bulk phase and the interfacial layer. These factors can be reduced by stirring the solution and using carrier particles with a high specific surface area. Interestingly, charged interfaces can have a beneficial effect, when attractive forces to the substrate molecules are present, *e.g.* the enzymatic activity of α -chymotrypsin was found to be enhanced on a negatively charged polyelectrolyte layer compared to a positively charged one [11]. The curvature of the adsorbent surface also seems to have an effect on the enzymatic activity, since high curvature surfaces, *e.g.* smaller carrier particles, cause less denaturation [12]. Despite that, maybe the most important issue regarding the preservation of protein conformation and enzyme activity upon immobilization is the surface hydrophobicity. Proteins strongly adsorb on hydrophobic surfaces [13]. In this case, conformational changes are more likely to happen due to hydrophobic interactions between the protein side chains and the adsorbent surface. Therefore, hydrophilic surfaces are more often required in order to preserve enzymatic activities. This can be achieved by a surface modification, for example, with poly(ethylene glycol), collagen, chitosan, poly(acrylic acid), or heparin, and by tethering the enzymes with a flexible chain to the material surface [2,14]. Genetic engineering could also be applied to virtually create any mutant enzyme that is perfectly adapted to the interfacial environment.

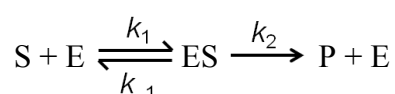
It will be detailed in this work, besides all these strategies already listed here, that application of pressure can be a new complementary, synergistic or even compensating tool to increase the activity of enzymes immobilized at aqueous-solid interfaces.

1.3. Effect of pressure on enzymes in solution

Pressure can have two major effects on enzymes, since enzymes have a folded conformation and are also reaction catalysts. Although a folded protein has a very well packed and dense structure, some void volumes and cavities can remain inside, which are filled by water upon unfolding [15]. Therefore, there is a negative volume change, ΔV , related to the unfolding of proteins, at least at ambient temperatures. Other contributions to ΔV are discussed in the literature, such as electrostriction upon exposure of charged and polar residues to the solvent [16-18]. In fact, the standard Gibbs energy change of unfolding, ΔG° , is lowered as the pressure is increased according to $(\Delta G^\circ/\Delta p)_T = \Delta V$. This destabilization

very often leads to protein unfolding at pressures of several 1000 bar and the correspondent loss of enzyme activity. The native state of proteins covers an elliptical region in the p,T -diagram; i.e., any movement away from the center of this region by a change in temperature and/or pressure is destabilizing the native state (decrease of ΔG°) and vice versa.

On the other hand, it has been shown that the catalytic properties of enzymes are pressure sensitive. Below the pressure of unfolding enzymatic reactions can be accelerated or decelerated [19,20]. In a simple case, Michaelis-Menten kinetics can be used to explain the mechanism of product formation [21]:



where S is the substrate, E the enzyme, ES the enzyme-substrate complex, and P the product. The rate of product formation is then given by:

$$v = k_2 [E]_{total} \frac{[S]}{[S] + K_M}$$

where k_2 is the rate constant of the second step, K_M is the Michaelis constant, $[S]$ is the substrate concentration, and $[E]_{total}$ is the total enzyme concentration.

Under pressure, low volume states are preferred over high volume states. Thus, a chemical equilibrium is shifted in the direction of negative volume change of reaction. This may apply to the equilibrium (first step) of the Michaelis-Menten mechanism. In addition, a transition state is favored under pressure, when it has a smaller volume than the reactants. This is expressed as negative activation volume. The activation volume, ΔV^\ddagger , is related to the change of the rate constant, k , with pressure, p , according to [18-19]:

$$\left(\frac{\partial \ln k}{\partial p} \right)_T = - \frac{\Delta V^\ddagger}{RT}$$

Applying Michaelis-Menten kinetics, $k = k_2$, when the substrate concentration is large, and $k = k_2/K_M$, when $[S]$ is small. The corresponding activation volumes are illustrated in

figure 2. ΔV^\ddagger can be obtained from a plot of $\ln k$ vs. p . In the literature, positive and negative activation volumes are reported for enzymes under various conditions [19].

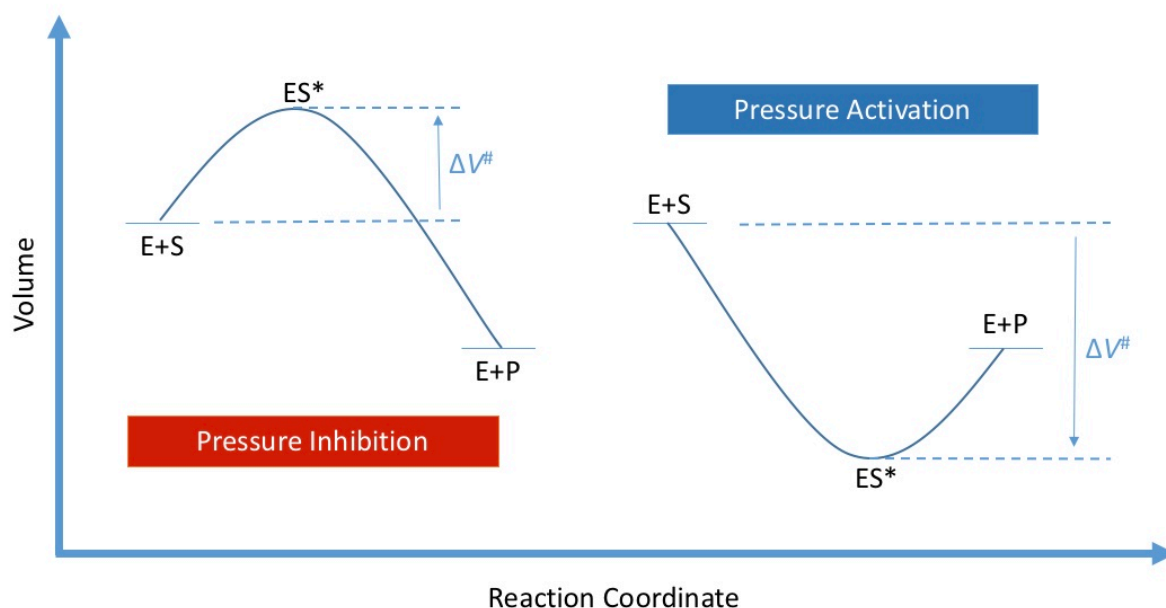


Figure 2. Volume change diagram of a hypothetical enzymatic reaction. When the transition state, ES^\ddagger , has a larger volume than the enzyme-substrate complex, $E+S$, the activation volume, ΔV^\ddagger , is positive, and the transition state is disfavored by pressure. In contrast, a negative activation volume is existent, when the transition state, ES^\ddagger , has a smaller volume than $E+S$. ΔV^\ddagger is negative, and the transition state is favored by pressure, i.e., an acceleration of the enzymatic reaction is observed.

At higher pressures, the reaction mechanism will probably change, if a reaction pathway of lower volume exists. Pressure selects reaction mechanisms, where strong hydrogen bonds occur or polar groups become hydrated. Even the hydration of non-polar groups is facilitated by pressure [18].

Finally, there are some selected examples from the literature that must be explored. Pressure experiments on the enzymatic activity of the strawberry peroxidase, which catalyzes the oxidation of substrate by H_2O_2 , have shown that pressurization at 4000 bar for five minutes increased the rate of oxidation [22]. In a similar way, pressurization caused an impressive activation of carrot peroxidase after a one-minute treatment at 4000-5000 bar [23]. It is important to note that in these studies enzyme activity has been measured at ambient pressure after pressure treatment. Thus, only irreversible pressure-induced structural changes are probed. In situ measurements, i.e., studying the enzyme activity under pressure, would provide much larger effects and more significant findings. The enzymatic activity at high pressures of α -chymotrypsin (α -CT), which hydrolyses peptide bonds, has also been studied. In the temperature range of 10-65 °C, a maximum rate constant of hydrolysis by α -CT has

been found at 45 °C and 2000 bar [24]. Moreover, an increase in pressure at 20 °C results in acceleration of the hydrolysis catalyzed by α -CT, reaching a 6.5-fold increase in activity at 4700 bar. At 50 °C and 3600 bar, the activity is more than 30 times higher [25].

1.4. Motivation of the work

In the present work, the effects of pressure on HRP and α -CT free and adsorbed at aqueous-solid interfaces, such as silica nanoparticles (figure 3) and chemically modified planar surfaces, were explored. Using well-chosen models, we aim to understand the way pressure influences enzymatic reactions at interfaces as well as to explore how pressure can be used to compensate limitations in enzyme activity at interfaces by favoring low-volume transition states and reaction pathways. Another target of this study is the role surface geometry and chemistry could play for the activation volume. The results of these investigations may help to optimize enzyme's catalytic activity at interfaces in biotechnological processes.

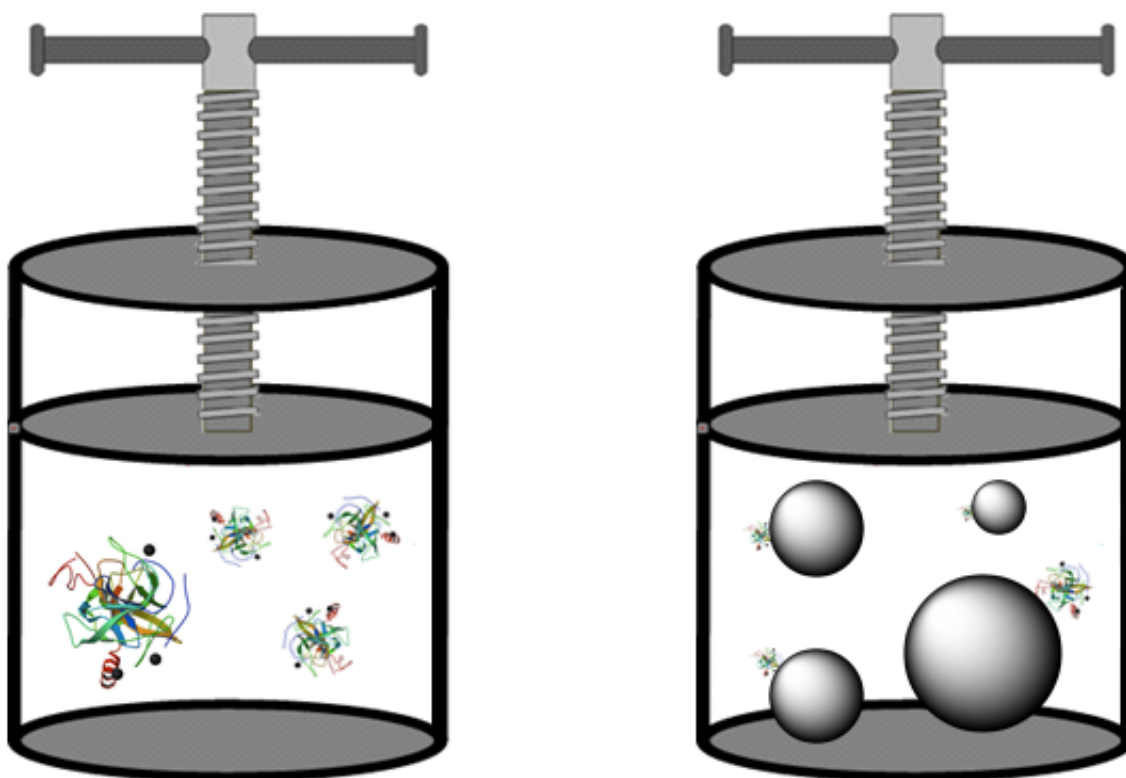


Figure 3. Free and adsorbed protein under pressure. On the left side, a protein solution is pressurized and all pressure effects are related to the natural pressure sensibility of this protein. On the right side, an adsorbed protein solution is pressurized and, in this case, the effect of the interface on the protein stability and dynamics should also be taken in account.

1.5. Alpha-chymotrypsin

α -Chymotrypsin (α -CT) is a protease of the subgroup of the serine proteases. Having 246 amino acid residues and a molar mass around 25 kDa, α -CT has one active site per enzyme molecule. In nature, α -CT is produced by the mammalian pancreas, starting from a zymogen called α -chymotrypsinogen. When this zymogen enters the intestine, it is converted into α -CT by trypsin, and active α -CT starts its own cleavage reactions. [26]

α -CT promotes the cleavage of peptide bonds by hydrolysis preferentially with substrates that have tryptophan, tyrosine, phenylalanine and leucine amino acids residues, which are cleaved at the carboxyl terminal. [26].

Being a member of the serine proteases, α -CT starts its hydrolysis reaction through a nucleophilic attack against a carbonyl group. This attack is made by the serine 195 residue, which is located in the active pocket, and α -CT binds covalently with the substrate creating the intermediate state complex. The catalytic triad of α -CT is constituted by the serine 195, histidine 57 and aspartic acid 102. [27]

One can divide the activity of α -CT into two steps: an initial fast reaction and a steady-state phase, where it follows the Michaelis-Menten kinetics. The α -CT two-step activity is also known as Ping-Pong mechanism (Figure 4). At first, α -CT promotes the acylation reaction and then the slow deacylation reaction, which is the rate limiting step of the global reaction. [26] The acetylated enzyme state is very stable and it can even be isolated [28]. According to literature, it has an isoelectric point about 9, with a positive net charge at neutral pH values and it has 6 tryptophans residues, according to PDB 1GL0.

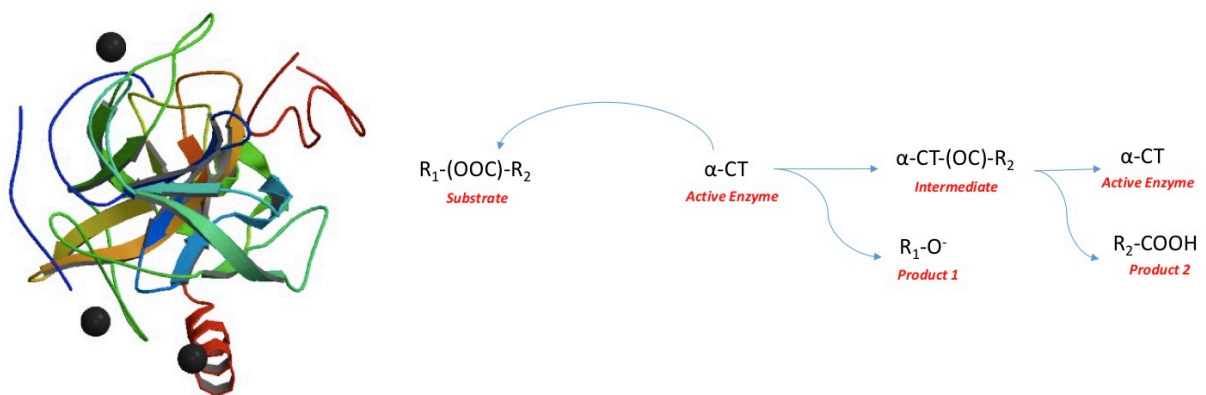


Figure 4. α -CT crystal structure (PDB: 1GL0) and its kinetic mechanism.

Since α -CT hydrolysis happens preferentially close to aromatic amino acid residues, several synthetic substrates were developed to probe its activity, such as the Ala-Ala-Phe-7-amid-4-methylcoumarin [29]. The enzyme recognizes the peptide sequence and cleaves the peptide bond between the phenylalanine residue and the 7-amino-4-methylcoumarin (7-AMC) group (Figure 5). After the hydrolysis, the 7-AMC molecule is released and it is highly fluorescent [29].

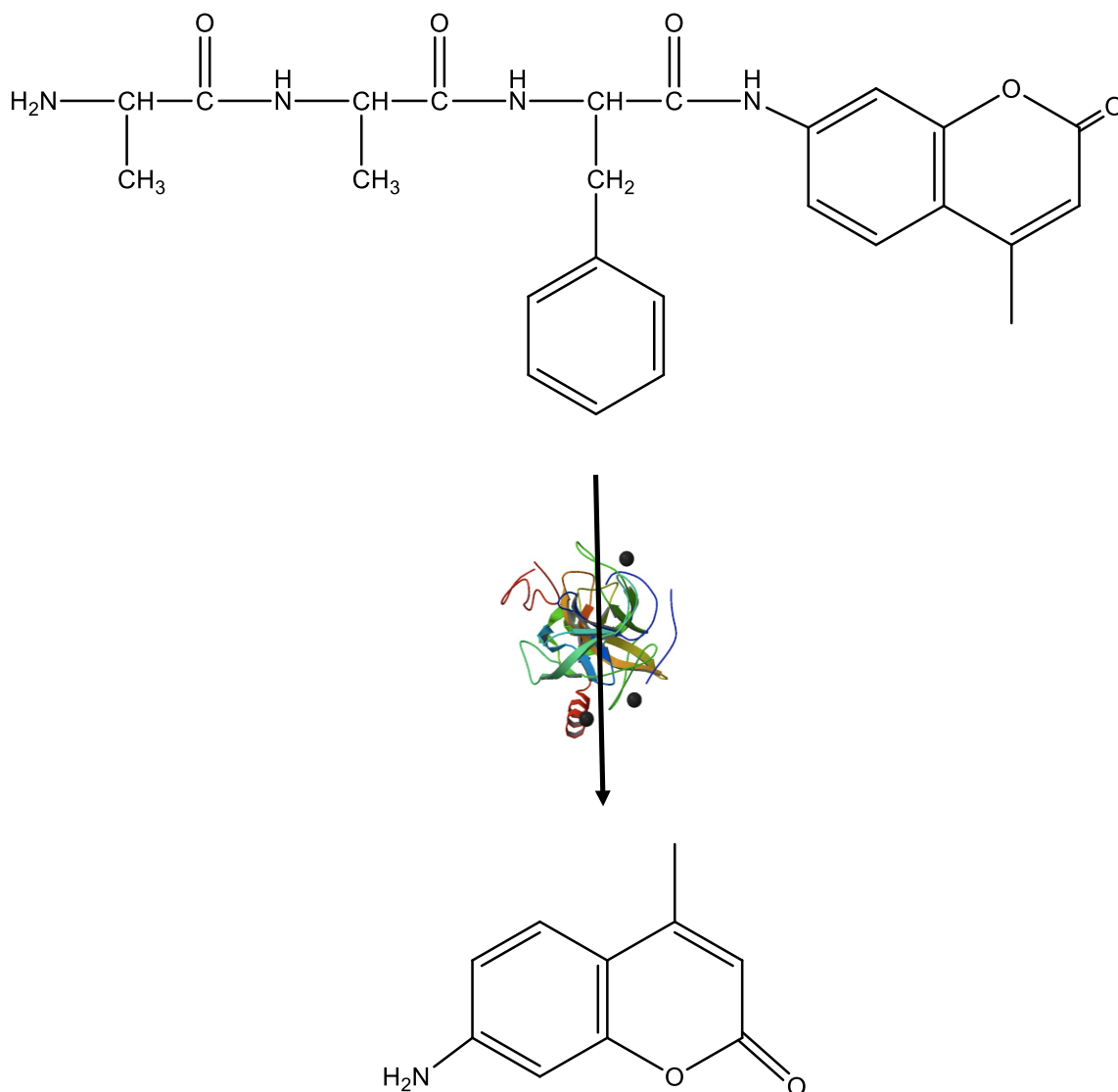


Figure 5. Reaction between α -CT and Ala-Ala-Phe-7-AMC releasing the product 7-AMC.

1.6. Horseradish peroxidase

Horseradish peroxidase (HRP) is a metalloenzyme, carrying a prosthetic heme group, and it is found in the root of the horseradish plant. [30, 31]. With 308 amino acid residues, the HRP molecule has a molar mass of around 33 kDa, but one 33 kDa polypeptide chain is bonded with 8 neutral carbohydrates chains, making the native HRP structure to have a total of 44 kDa. The net charge of HRP at neutral pH-values is very close to 0 [61, 62] and one tryptophan residue, according to PDB 1HCH.

HRP has in its structure one iron atom, located in the middle of the porphyrin ring of the heme group, and two additional calcium atoms. The iron atom has two binding sites available, one under the heme group and one above. The sixth position of the iron's octahedral is the active site of HRP [30]. The HRP's histidine 170 (His170) forms coordinate bond to the heme iron atom. When HRP is catalyzing a reaction, one oxygen from the hydrogen peroxide binds to the iron atom, then two electrons are transferred from a given substrate to the heme group, and finally a water molecule is released after uptake of two protons [30,32], as seen in figure 6.

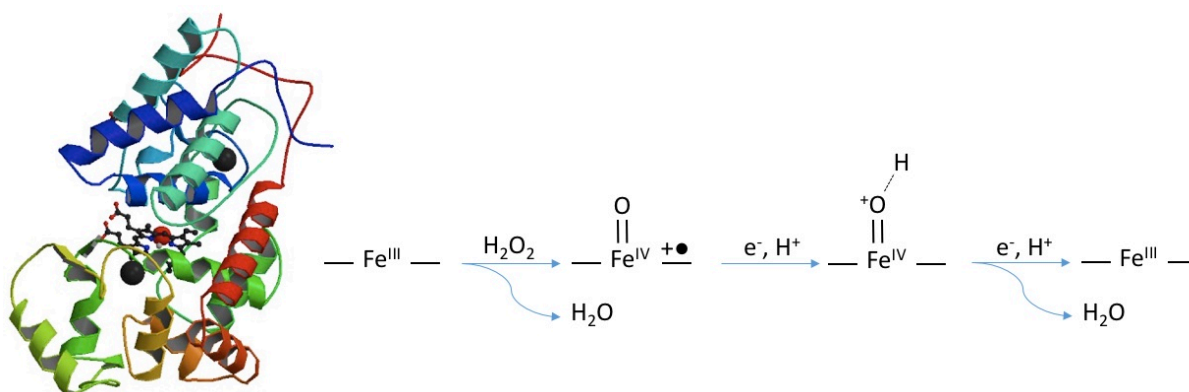


Figure 6. HRP crystal structure (PDB: 1HCH) and its mechanism.

A very good and efficient substrate for HRP is the commercial Amplex Red®. In the presence of HRP, the Amplex® Red molecule reacts with hydrogen peroxide, in a 1:1 stoichiometry, producing the oxidation product called resorufin, that can be measured by fluorescence or absorbance spectroscopy [33], as seen in figure 7.

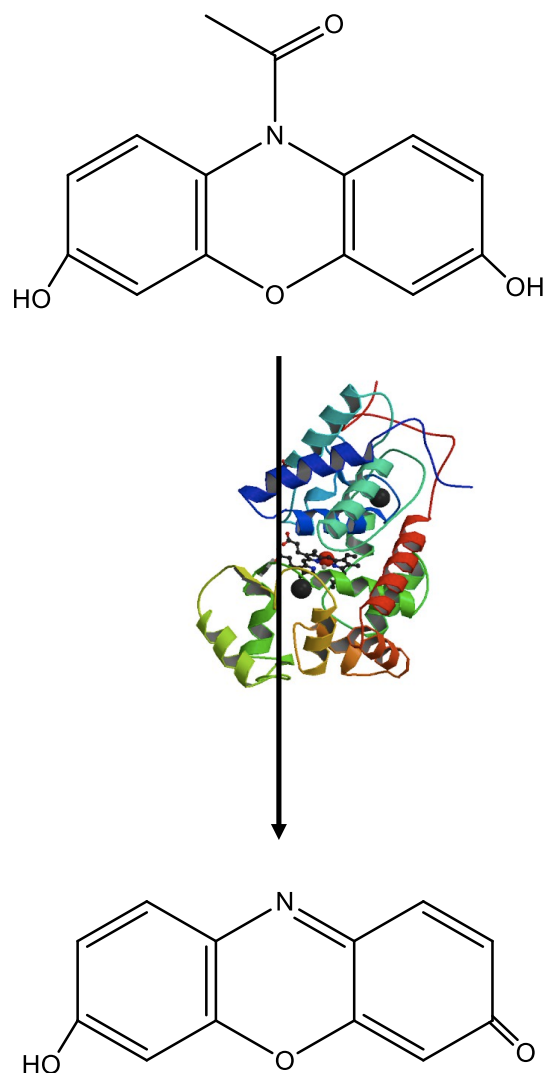


Figure 7. Reaction between HRP and Amplex Red® releasing the product resorufin.

1.7. Physical adsorption on surfaces

Reversible immobilization of enzymes on surfaces can be achieved using a very simple method, physical adsorption (Figure 8). It is induced by very weak non-specific interaction, *e.g.* van der Waals, hydrogen bond and hydrophobic interactions [34-36]. Reversible immobilized enzymes are easily removed from the surfaces and this allows the support to be recycled and reloaded with new enzymes [34]. To this end, physical adsorption requires just the incubation of the enzyme solution on the surface during a certain amount of time [37]. The pH of the enzyme solution is very relevant, since the enzyme surface has charges [38]. This can induce adsorption on any ion exchange carrier [39]. But when the surface is highly

charge, it can also create some distortions in the kinetics, due to partitioning and/or diffusion problems [34].

Overall, the physical adsorption technique is commercially attractive and a renewable method to fix enzymes due to its low cost and simplicity [34].

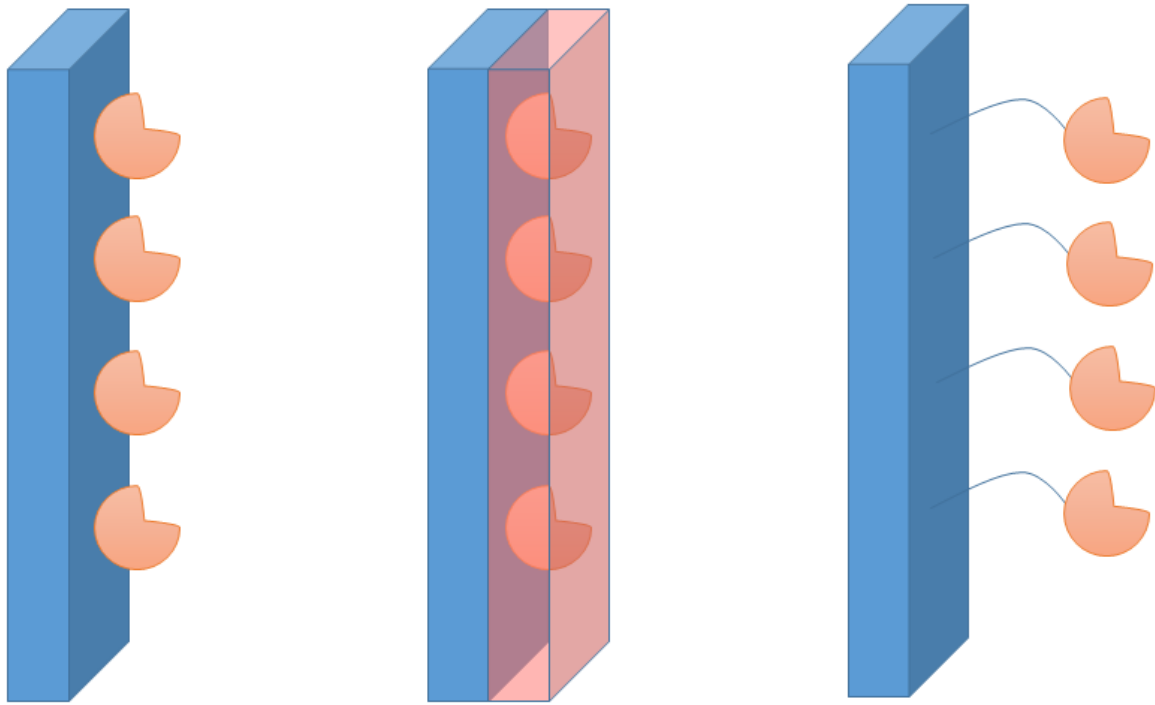


Figure 8. Examples of fixing proteins on surfaces with physical adsorption technique. From left to right: adsorption, entrapment and cross-linking. Adapted from Mohamed *et al*, 2015 [34].

1.8. Silica nanoparticles

Ludox® is a commercial trademark for all types of silica nanoparticles from DuPont. There are several types of modifications, sizes and properties of these particles, with a unique name for each of them.

The particles are discrete uniform spheres of silica which have no internal surface area or detectable crystallinity. Most are dispersed in an alkaline medium, which reacts with the silica surface to produce a negative charge. Because of the negative charge, the particles repel one another resulting in a stable suspension.

1.8.1. Ludox CL®

Ludox CL® is a colloidal silica in which each particle is coated with a layer of alumina. This coat converts the charge of the particle from negative to positive. It is also freeze stable and can be recovered after being frozen by thawing and remixing. It has 12 nm of diameter, 230 m²/g of specific surface area and it is stored at pH 4.5 at 30% wt%. (DuPont data sheet).

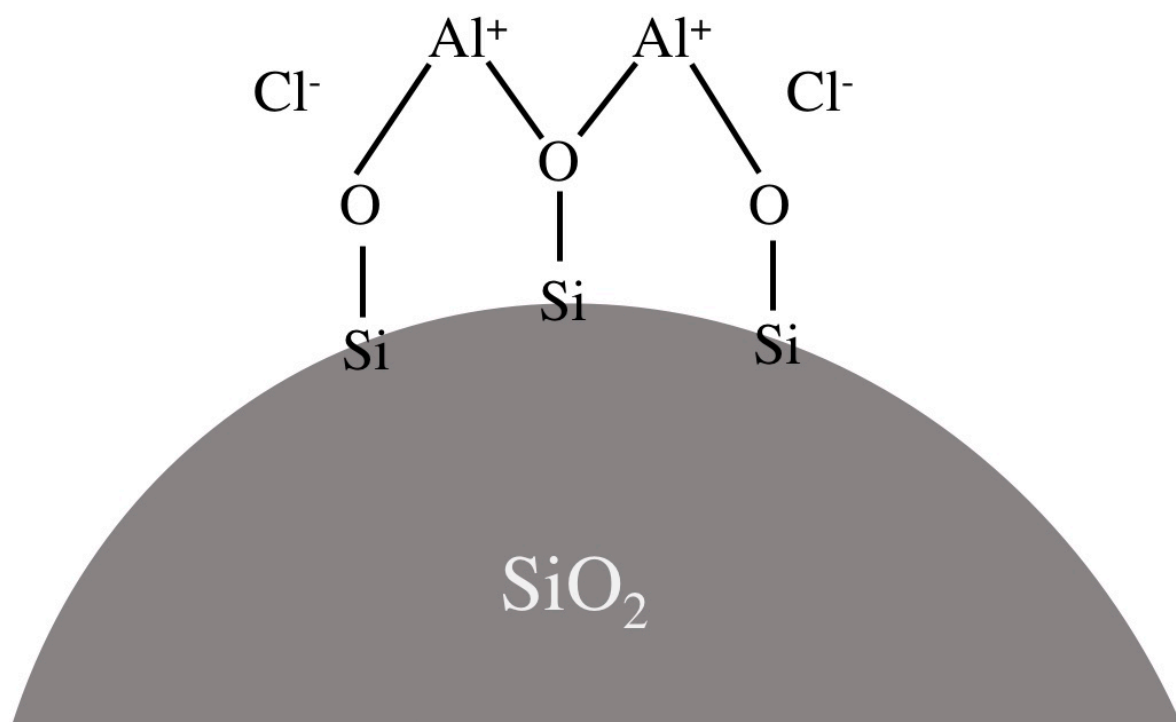


Figure 9. Ludox CL® interface scheme.

1.8.2. Ludox AM®

Ludox AM® is a colloidal silica in which some silicon atoms have been replaced by aluminum atoms. This creates a fixed negative charge independent of pH, resulting in particles very stable in neutral pH range. It has 12 nm of diameter, 220 m²/g of specific surface area and it is stored at pH 8.9 at 30% wt% (DuPont data sheet).

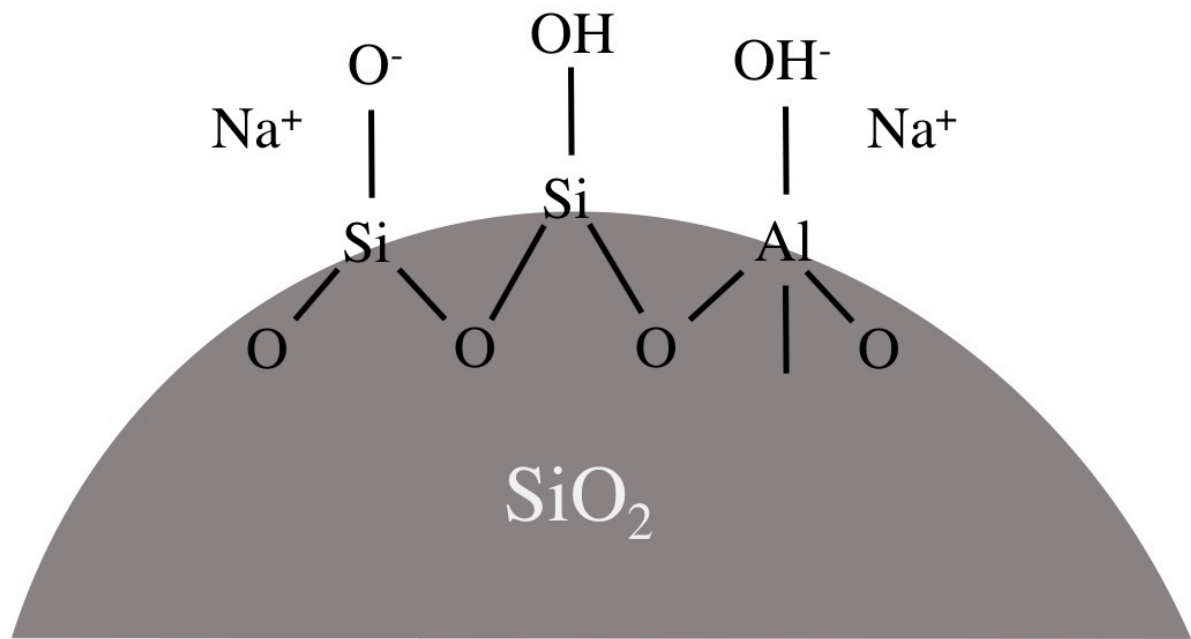


Figure 10. Ludox AM® interface scheme.

1.9. Planar surfaces

In contrast to the nanoparticles, which have a spherical surface, a planar solid substrate creates a different geometry for adsorption and it has its own advantages.

The planar surfaces are easily modified by chemicals and therefore many types of surfaces can be created on the same solid substrate [40]. For example, planar quartz can be modified to receive either a poly(styrene) (PS) film as well as polyelectrolyte multilayers, creating hydrophobic and hydrophilic surfaces, respectively (Figure 11).

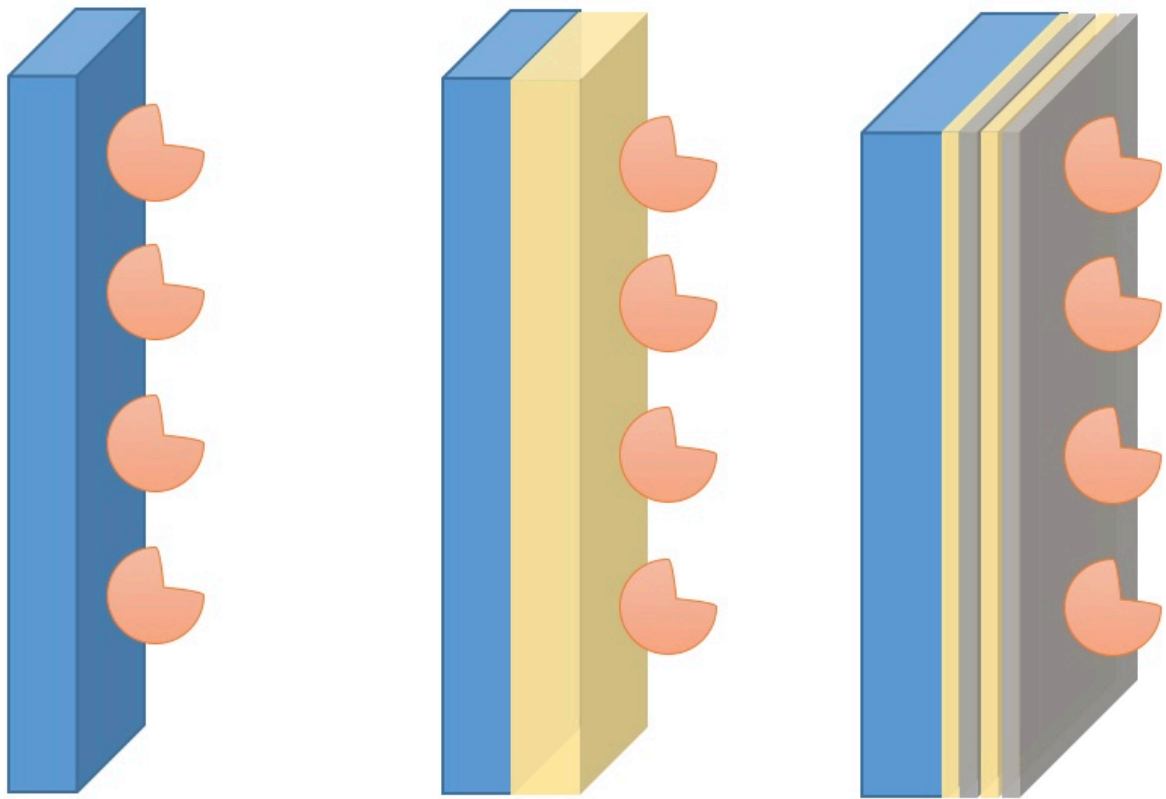


Figure 11. Proteins adsorbed on modified planar surfaces. From left to right: proteins adsorbed on a bare quartz, on a PS modified quartz and on a polyelectrolyte multilayer modified quartz.

2. Materials and methods

2. Materials & methods

2.1. List of materials

<i>Chemical / Code</i>	<i>Manufacturer</i>
Amplex Red® Hydrogen Peroxide/Peroxidase Assay Kit / A22188	Thermo Fisher
Alpha-chymotrypsin from bovine pancreas / C7762	Sigma-Aldrich
Calcium chloride / 1.02378.0500	Merck
Hydrochloric acid 25% / 1.00316.1000	Merck
EnzChek ® Peptidase/Protease Assay Kit / E33758	Thermo Fisher
Ludox AM / 420875 colloidal silica particles	Sigma-Aldrich
Ludox CL / 420883 colloidal silica particles	Sigma-Aldrich
Trizma® (TRIS base) / T1503	Sigma-Aldrich
Sodium phosphate monobasic/ 33198-8	Sigma-Aldrich
Di-sodium hydrogen phosphate dodecahydrate / 1.06579.0500	Merck
Hydrogen peroxide / 216763	Sigma-Aldrich
Amplex Red® / A12222	Thermo Fisher

Amicon[®] Ultra 0.5 mL centrifugal filter / Ultracel[®] 50k	Millipore
Deuterium oxide / 41648	Sigma-Aldrich
Horseradish peroxidase / 01-2001	Thermo Fisher
Ala-Ala-Phe-7-amido-4-methylcoumarin / A3401	Sigma-Aldrich
N-p-tosyl-L-phenylalanine chloromethyl ketone / T4376	Sigma-Aldrich
Poly(styrene) / 331651	Sigma-Aldrich
Poly(ethyleneimine) / P3142	Sigma-Aldrich
Poly(allylamine hydrochloride) / 28322-3	Sigma-Aldrich
Poly(styrene sulfonate) / 243051	Sigma-Aldrich
Sodium azide / S2002	Sigma-Aldrich
PlusOne[®] Silver staining kit, protein / 17-1150-01	GE Healthcare
SigmaMarker[™] low range, mol wt 6,500-66,000 Da / M3913	Sigma-Aldrich
Ammonium persulfate / A3678	Sigma-Aldrich
Rotiphorese[®] Gel 40 (29:1) / A515.2	Carl Roth
N,N,N',N'-Tetramethylethylenediamine / T9281	Sigma-Aldrich
Sodium dodecyl sulfate / L3771	Sigma-Aldrich

<i>Equipment and Software</i>	<i>Manufacturer</i>
K2 fluorimeter	ISS
High pressure fluorescence cell	ISS
Centrifuge	Eppendorf
UV-VIS spectrometer / UV-1800	Shimadzu
Nicolet IR Spectrometer / 6700	Thermo Fisher
GRAMS 8.0	Thermo Fisher
Origin 9.0	Origin Labs
ImageJ	NIH USA
Quartz prism / Corning 7980	Micros Präzisionsoptik
High pressure TIRF cell	House made (Koo & Czeslik 2012)
X-ray reflectometer / Seifert XRD 3000TT	GE Inspection Technologies
Spin Coater / KW-4A	CHEMAT TECHNOLOGY
Mini-Protean[®] Kit	Bio-Rad
High pressure stopped-flow system / HPSF-56	HiTech Scientific

2.2. Methods

2.2.1. Fluorescence spectroscopy

Fluorescence methods are based on the excitation of molecules, by UV or visible light, which are able to dissipate this energy by emitting electromagnetic radiation. Molecules with this ability are known as fluorophores. Fluorescence methods are well known for requiring very few amounts of sample and/or very diluted concentrations to be detected, if compared with other spectroscopies methods, such as UV-VIS spectroscopy [41,42].

The fluorescence experiments were done using K2 fluorimeters from ISS. A high-pressure stainless steel vessel, also from ISS, was used to pressurize liquid samples up to 3000 bar. Samples were placed in cylindrical quartz bottles and sealed with a flexible plastic foil fixed by a rubber O-ring. Then, the bottle was placed in the middle of the high pressure vessel. This vessel has three sapphire windows and was connected to a manual pump and gauge. In all experiments, water was used as pressure medium. For temperature control, a water bath was connected to the high-pressure vessel. There was a dead time of maximum 2 minutes between the sample mixing, *e.g.* substrate with enzyme, and data collection. The excitation light hits and crosses the sample cuvette, and the fluorophor emission light is collected at 90° in relation to the excitation beam, as seen in figure 12.

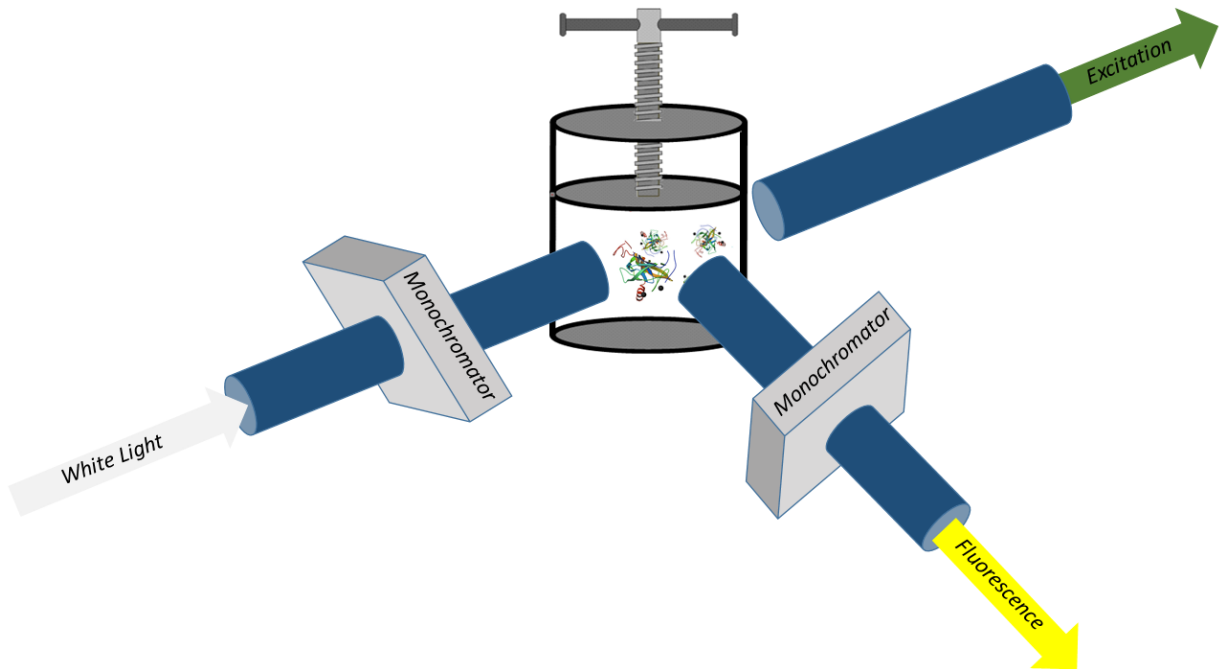


Figure 12. High pressure fluorescence spectroscopy. The white light enters the monochromator, which is set to a specific wavelength. This selected beam leaves the monochromator and hits the sample, passing through it. The fluorophores are excited and start emitting fluorescence in all directions. There is an output, placed 90° in relation to the excitation beam, which leads to a second monochromator. This last monochromator will select the specific wavelength of the fluorescence emitted that will hit the detector.

2.2.2. FTIR spectroscopy

The Fourier transform infrared spectroscopy (FTIR) method takes advantage that infrared light is absorbed by molecular vibrations. This occurs exactly when the light frequency and the molecular vibration frequency coincide. These frequencies of absorption and their intensities can be altered with minimal changes in the chemical environment, where these molecular vibrations are located, *e.g.* polarity, inter- and intramolecular interactions, etc. This makes the FTIR method a very powerful tool to follow, for example, any changes in secondary structure that may occur with a given protein. In this case, the amide I band can be used to probe the secondary structure of proteins [43,44].

The infrared absorption spectra were recorded using a Nicolet 6700 Fourier transform infrared spectrometer from Thermo Fisher Scientific with a resolution of 2 cm^{-1} . The sample solutions were analyzed in a diamond anvil cell, which is connected to a water bath circuit for temperature control. Fine powdered barium sulfate was added to the sample as an internal pressure calibrant. Pressure changes were quantified by the shift of the barium sulfate

stretching vibration band, at 983 cm^{-1} , to higher wavenumbers, which is related to the pressure in the system. [45]. Deuterium dioxide was used as the solvent for all experiments, and the background with buffer was collected and subtracted from all spectra.

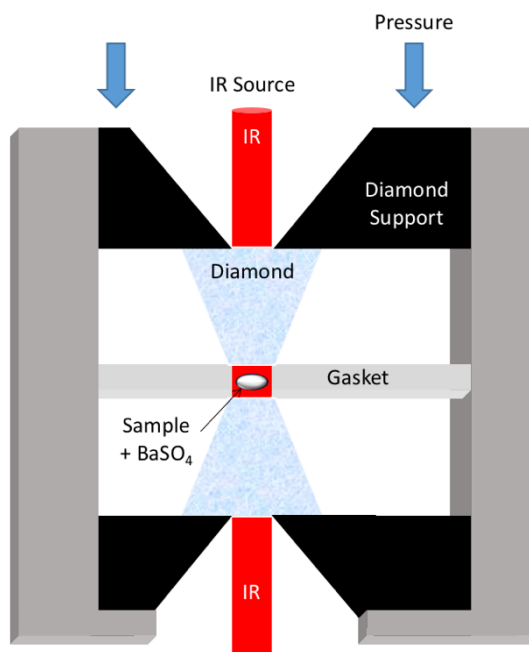


Figure 13. High pressure Fourier transform infrared spectroscopy. The IR beam crosses the diamond anvil cell hitting the sample with the pressure calibrant, BaSO₄. Some chemical bond vibrations will attenuate the IR radiation, and this difference is seen in the absorbance of each wavenumber in the spectrum. Pressure can be used to perturb this system and may cause some absorbance changes in the spectrum as well as wavenumber shifts.

2.2.3. UV-VIS spectroscopy

A UV-1800 UV-VIS spectrometer from Shimadzu was used to collect absorbance kinetics or spectra. During the measurements, a water bath connected to the cuvette holder kept the temperature constant. The cuvettes were all made of quartz.

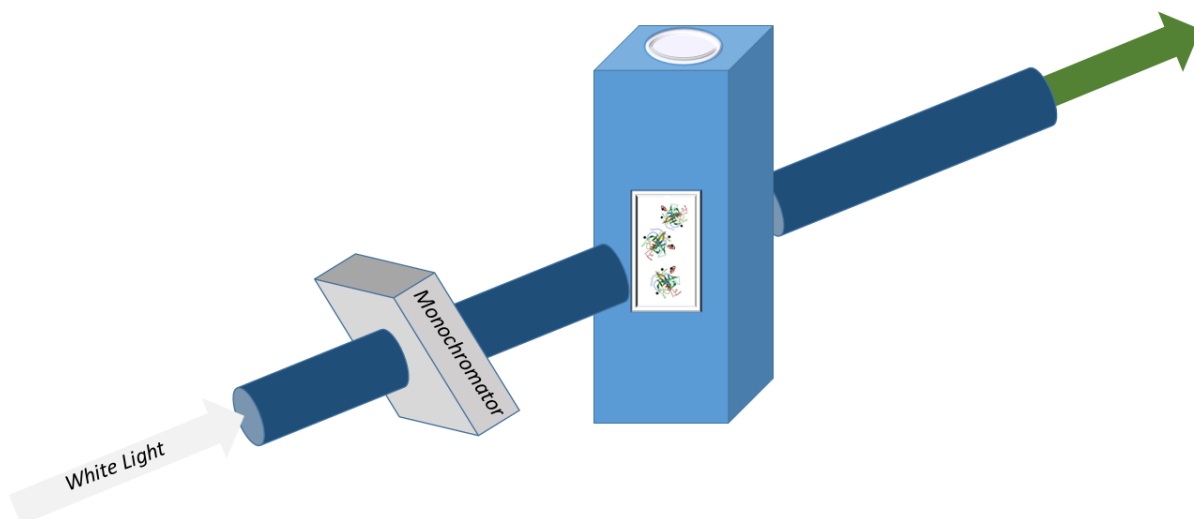


Figure 14. UV-VIS spectroscopy. A white light passes through a monochromator, which will select a specific wavelength. The monochromatic light hits the sample and some light can be absorbed by the sample, reducing the transmission. The detector is positioned after the sample and it will detect the amount of light transmitted from different samples in relation to a control.

2.2.4. TIRF spectroscopy

Total internal reflection fluorescence (TIRF) spectroscopy is a very useful method to study molecules and events at planar liquid-solid interfaces. In TIRF, as well as in conventional fluorescence, fluorophores are excited, but in different ways. In conventional fluorescence, the excitation beam hits directly the sample solution and passes through it. On the other hand, in TIRF, the excitation beam enters in an optical prism and it is internally totally reflected, because the prism has a higher index of refraction than the liquid phase ($n_1 > n_2$). Total internal reflection occurs below the critical angle θ_c (measured from the interface, $n_1 \cos \theta_c = n_0$). The totally reflected beam generates an evanescent wave, which penetrates the

liquid phase hitting the fluorophores at this surface. The penetration depth of this evanescent wave is given by an exponential decay of the electrical field amplitude:

$$E(z) = E_0 \exp(-z / d) \quad [6]$$

where d is the penetration depth:

$$d = \frac{\lambda}{2 \sqrt{n_1^2 \cos^2 \theta_1 - n_0^2}}$$

[7]

λ is the wavelength of the excitation, and θ_1 is the angle of the exciting beam from the interface.

In this way, d depends on the excitation wavelength, and this also shows how close the fluorophores must be to the solution-prism interface to get excited by the evanescence wave. This is also called the sensitive area of a TIRF experiment. This makes TIRF a very interesting method, since it excludes most part of the interference caused by the adjacent solution [46].

To perform high-pressure TIRF experiments, a high-pressure TIRF cell was used to pressurize samples up to 2500 bar [47]. The cell has 3 output windows made of sapphire. Through the first window comes the excitation beam. A second window is the output of the totally reflected beam. And through the last one comes out the fluorescence generated by the fluorophores excited by the evanescent wave. This cell hosts a 0.6 cm³ sample cuvette, which completely separates the sample from the external pressure medium, water. The sample interface has an active area of around 1.5 cm².

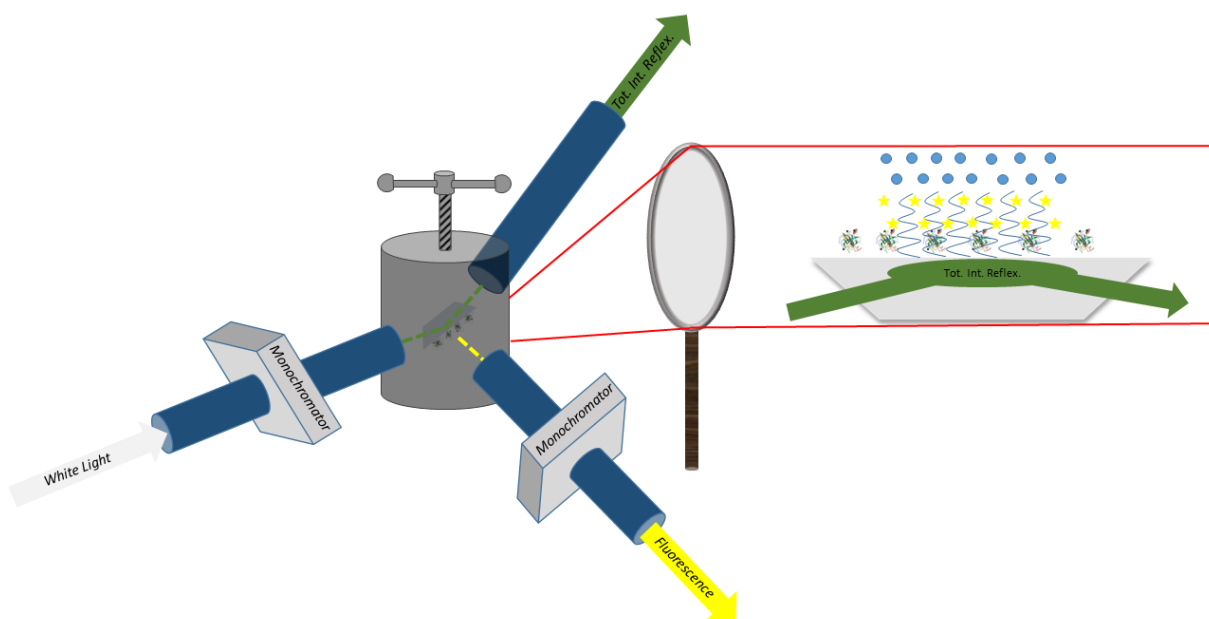


Figure 15. High pressure total internal reflection fluorescence spectroscopy. A white light passes through a monochromator, where monochromatic light is selected. Then, this monochromatic light hits the prism placed inside the high pressure cell (left), and the light is totally reflected (right). By this total reflection, an evanescent wave is created on the surface of the prism and excites fluorophores close to the surface. These fluorophores emit fluorescence that passes through a second monochromator and hits the detector. [47].

The cell was assembled in a K2 fluorimeter for data collection. The cell was connected to a water bath circuit to maintain the internal temperature constant. The dead time of this HP-TIRF experiment was 4 minutes, and the pressurization process was always in the rate +250 bar in 10 seconds.

2.2.5. Surface techniques

2.2.5.1. Spin-coating

Spin-coating is a simple and useful technique applied to modify a planar surface. It can quickly produce very uniform films of various thickness. Using a spin-coater KW-4A from Chemat Technology, a well clean planar substrate, such as a dove quartz prism, is positioned in the center plate of the machine. A solution containing a given polymer, *e.g.* poly(styrene), is added on the top of the prism for a first step of adsorption. Then a spin of around 2000 RPM is applied to create a very thin and homogeneous film on the substrate.

Then, this coated substrate is incubated at 110 °C to dry the surface and smooth out any imperfection.

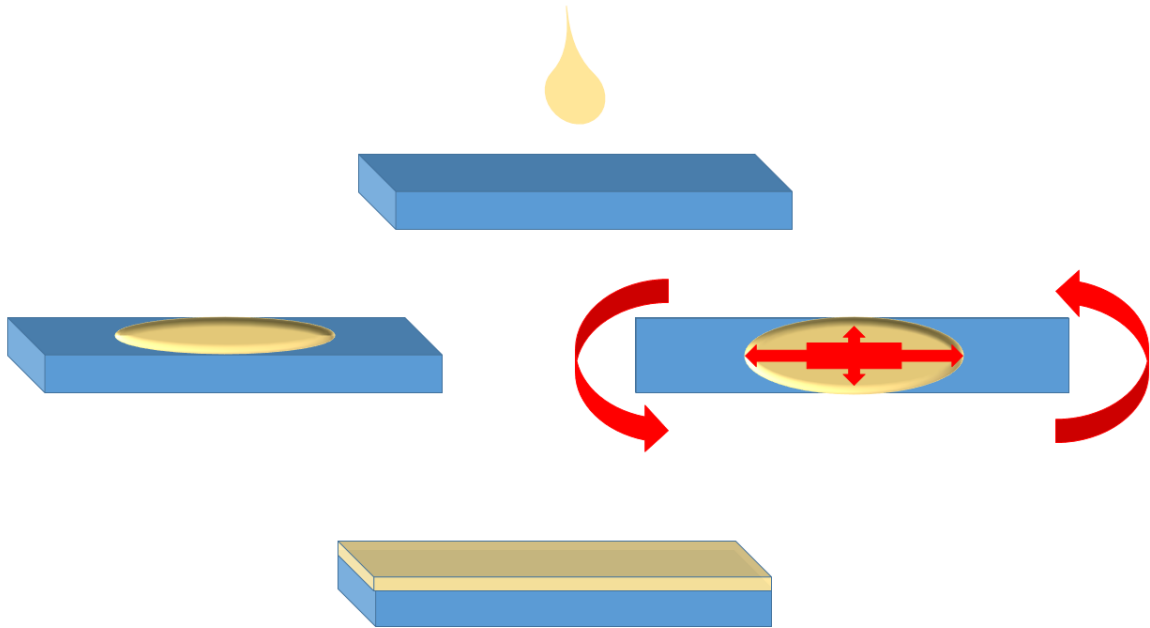


Figure 16. Modification of a planar surface using the spin-coating technique.

2.2.5.2 Polyelectrolyte multilayer deposition

Thin polymer films can be assembled by simply using the layer-by-layer technique [48-50]. In this method, the film is made just by dipping a substrate, *e.g.* quartz prism, into solutions containing a polycation and a polyanion multiple times, interchangeably. From the polycation to polyanion solution, the sample must be rinsed extensively with water. Each step adds a few polyelectrolyte molecules that adsorb on the surface of the substrate, allowing a controlled assembling of a polyelectrolyte multilayer. This kind of modified surface permits a strong immobilization of proteins and, due to its fluid and hydrated properties, creates a very mild environment for biomolecules, such as proteins.

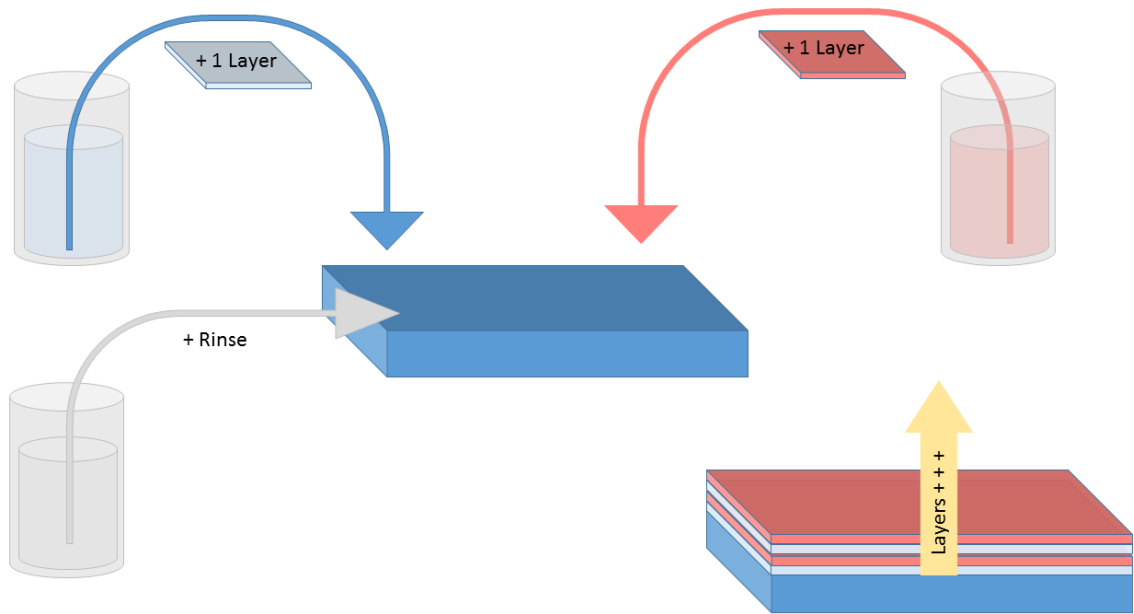


Figure 17. Modification of a planar surface with the layer-by-layer technique.

2.2.6. X-ray reflectivity

The characterization of surfaces, films and multilayers can be done by X-ray reflectivity experiments. The principle of this technique is based on an X-ray beam pointed to a given surface, where the incident angle is the same as the reflected angle. If the reflected X-ray is different from the incident beam, there are imperfections on the surface or, in the case of an interface placed over the surface of the solid substrate, oscillation fringes will be formed. This shows the constructive and destructive interference of two different reflected beams hitting the detector. Thus, the thickness and the roughness of the interface can be estimated [51].

The X-ray reflectometer used was a Seifert XRD 3000 TT from GE Inspection Technologies operated with the Mo-K α wavelength (0.71 Å). The raw data is converted to reflectivity curves by normalization of the reflected X-ray intensity to the incident intensity. Then, the curves are scaled as a function of wavevector transfer $Q = (4\pi/\lambda) \sin\theta$, where λ is the wavelength and θ is the angle of incidence.

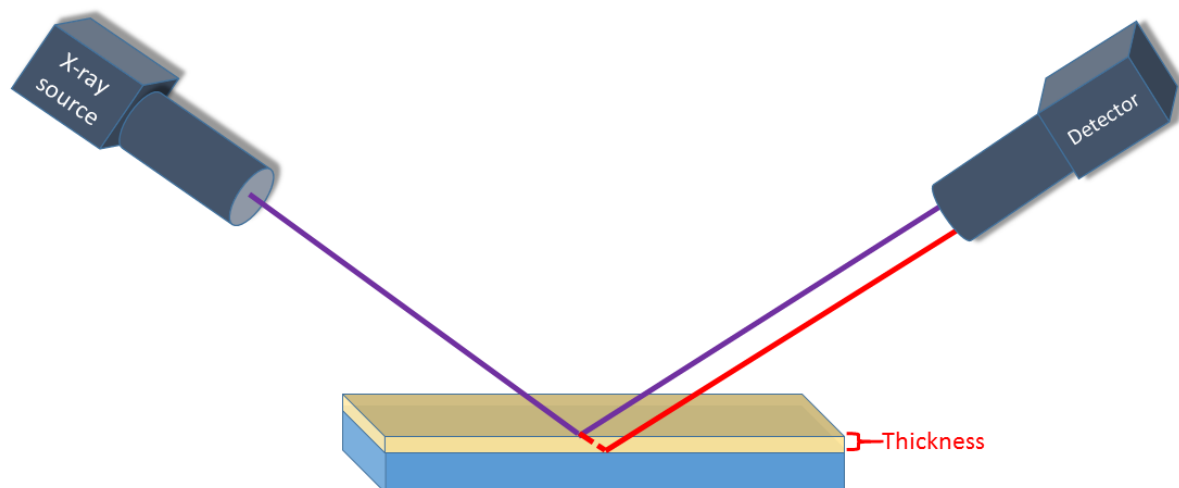


Figure 18. X-ray reflectivity of a planar surface.

2.2.7. High pressure stopped-flow system

The stopped-flow technique is suited to follow fast processes that happen right after mixing two or more components, such as enzymatic reactions, which start when enzyme and substrate are mixed together. It generates a signal that changes with time, *e.g.* in enzyme kinetics studies, binding of molecules, FRET experiments, etc. The principle is that very small volumes of at least two solutions are injected by sample syringes into a mixer chamber to start the process. Also rapidly, this recently mixed solution enters into the observation cell. This liquid influx stops by the limit set in the so-called stop-syringe. Before stopping, a very homogenized solution is generated in the observation chamber. The dead time between sample mixing and data collection is in the order of milliseconds.

In a high pressure stopped-flow system (HP-SF), the observation chamber has 3 sapphire windows. Each window is connected to one optical fiber cable. The first one is used for the input of light that comes from the excitation monochromator. A second fiber is set 180° in relation to the input, used for UV-VIS transmittance/absorbance detection. Finally, there is a third fiber, 90° in relation to the input window, used for fluorescence detection. In all studies in this work, the transmittance/absorbance output window was used. All this apparatus is confined inside a stainless steel autoclave vessel that can be pressurized up to 2000 bar (Figure 19).

This instrument permits the investigation of the very first seconds of enzyme reaction bringing to light more details that are hidden in other more conventional techniques, such as the high pressure fluorescence, described above. In addition, and also very important, the

mixing of a substrate and an enzyme happens already under pressure rather than pressurizing a reaction that has already started.

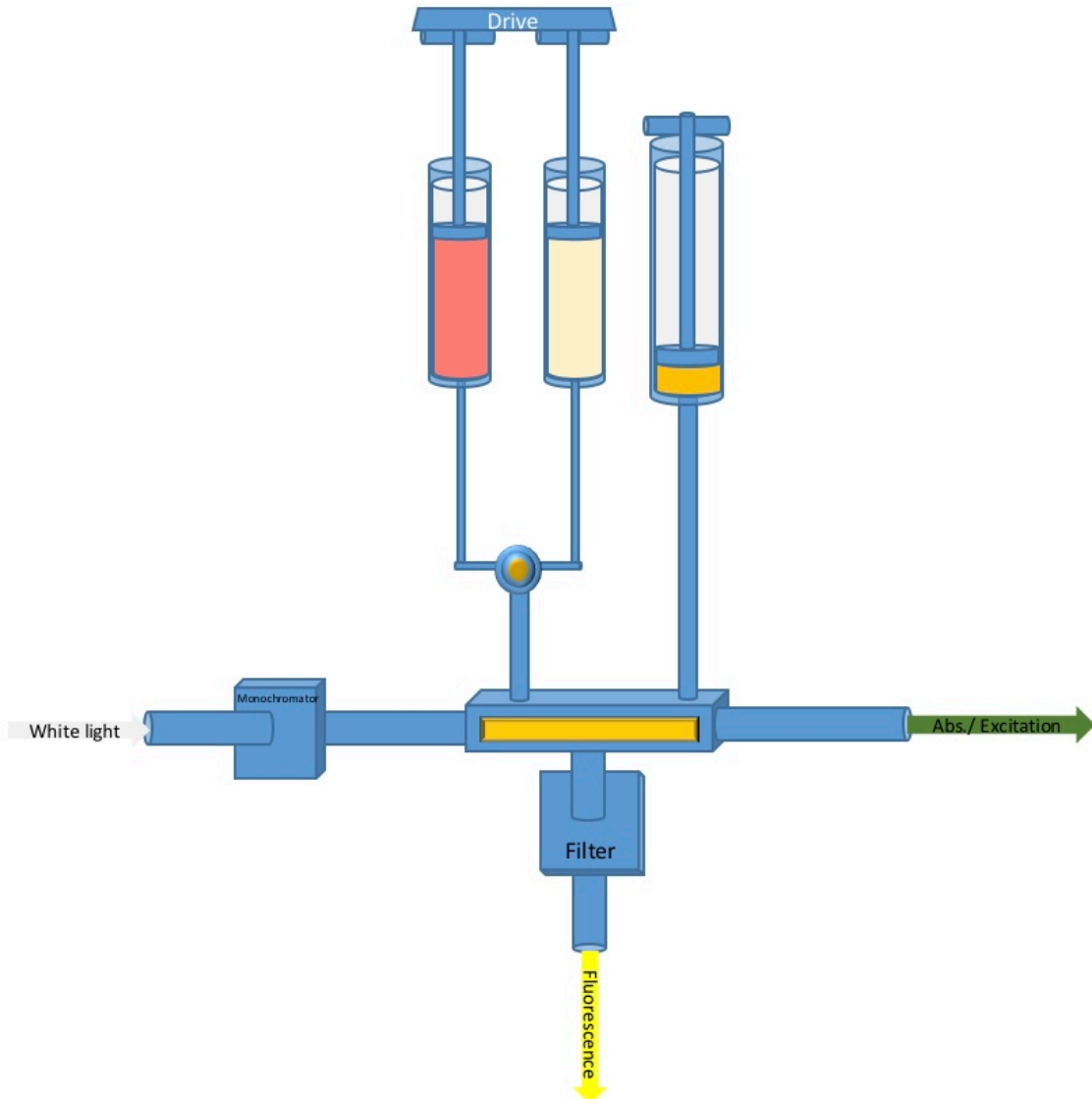


Figure 19. Single mixing stopped-flow system.

2.2.8. SDS-PAGE

Polyacrylamide gel electrophoresis (PAGE) is a widely used technique. It separates and helps to estimate/visualize the length and weight of proteins as well as other biomolecules. PAGE experiments can be performed in two different ways, with or without denaturant. When a chemical denaturant is added, *e.g.* sodium dodecyl sulfate (SDS), the protein will unfold, creating an unordered linear chain. Each protein will have different

mobility in the gel, and therefore small proteins will migrate faster and reach down the gel, while larger proteins will migrate slower and stay on upper areas of the gel [52]. This technique is suitable for visualizing the cleavage of proteins. The native state band will have reduced intensity while bands corresponding to smaller sizes will appear.

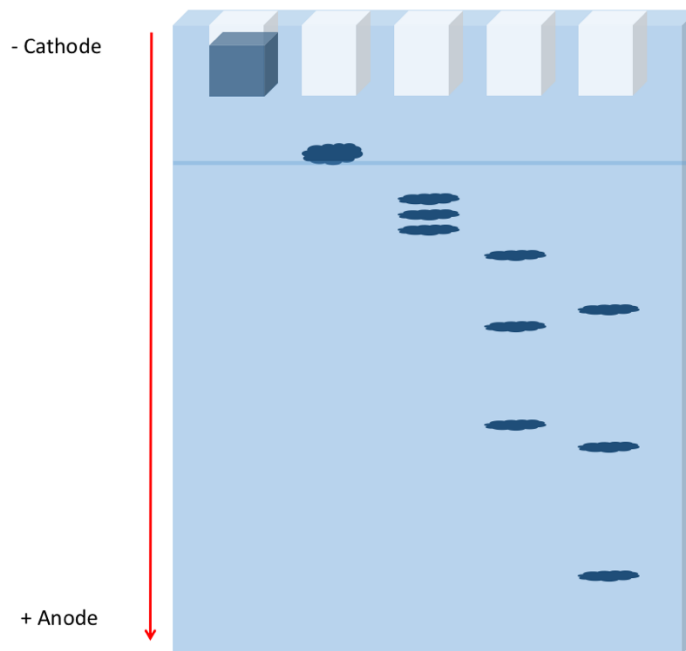
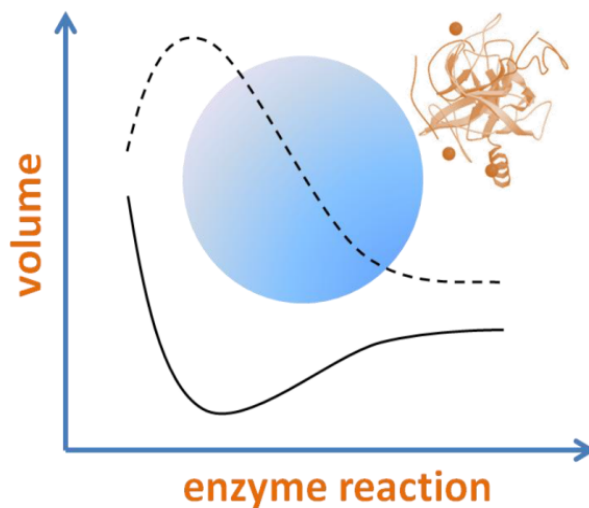


Figure 20. Polyacrylamide gel electrophoresis. The protein sample is denatured and negatively charged by the denaturant sample buffer at the cathode side of the gel. When inside the electrophoresis chamber, a voltage is applied and the proteins migrate to the positive end (anode). Different lengths will develop different mobility, and therefore larger protein will find more resistance to migrate through the gel.

3. Activation volumes of enzymes adsorbed on silica particles

*Reprinted with permission from V. Schuabb, C. Czeslik, Langmuir 2014, 30, 15496-15503.
Copyright 2014 American Chemical Society.*



3.1. Background

Enzymes are very special proteins that can catalyze reactions, but one disadvantage of enzymes is their low stability and the high costs associated with their use and maintenance, if compared with other chemical catalysts. One good strategy is to recover and reuse these enzymes in several reaction cycles. This can be possible when these enzymes are immobilized on carrier particles that would easily help in filtration or sedimentation processes [2,3]. However, this attachment on particles could change the protein's chemical environment and structure, which could lead to denaturation [6]. Besides that, the interaction between the enzyme and the solid substrate could change the dynamics [53], and/or the enzyme's active site could be orientated in a way that blocks the income of substrate molecules.

Many strategies were proposed to preserve the enzymatic activity at interfaces. [2,3], e.g. the use of hydrophilic surfaces, the incorporation of an enzyme into porous materials, and genetic engineering can be helpful to overcome limited enzymatic activity at aqueous-solid interfaces. In this work, pressure will be explored as a new tool to control and maybe enhance the activity of enzymes. Before that, it is good to remember that pressure can act in two different ways on proteins. First, it can induce protein denaturation and, second, it can alter the reaction rate acting on the enzyme's catalytic properties. Even a well folded and densely packed protein has some void volumes and cavities, which can be filled by water upon unfolding. Thus, there is a negative volume change, ΔV , associated with the unfolding of proteins (at least at ambient temperatures) [16,17]. In addition, electrostriction upon exposure of charged and polar residues to the solvent can contribute to ΔV [16]. There is a volume decrease, unfolding of the protein and loss of activity at several kbar.

Interestingly, the catalytic properties of enzymes have been shown to sensitively depend on pressure below the pressure of unfolding [19, 20, 54]. The transition state of the reaction is favored under pressure, when it has a smaller volume than the enzyme-substrate complex. This is also known as a negative activation volume, ΔV^\ddagger . The ΔV^\ddagger is related to the change of the rate constant, k , with pressure p [20, 54]:

$$\left(\frac{\partial \ln k}{\partial p}\right)_T = -\frac{\Delta V^\ddagger}{RT}$$

Positive and negative activation volumes are illustrated in figure 2. Depending on the sign of the activation volume enzymatic reactions can be accelerated (negative activation volume) or slowed down (positive activation volume) if pressure is applied on this system.

In this chapter, two enzymes were studied, horseradish peroxidase (HRP) and α -chymotrypsin (α -CT). The catalytic property of peroxidases is the oxidation of a substrate by H_2O_2 . Some reports have shown that the carrot peroxidase loses its activity up to 2000 bar, but displayed higher activity at 5000 bar [23]. In the case of HRP, an inactivation is observed up to 5000 bar, but it seems this pressure effect depends on the type of substrate used [55]. One report shows increased activity of HRP, when this enzyme is immobilized in a phospholipid film [56]. The second model studied here, as mentioned above, is α -CT. This enzyme is a protease and has the property of hydrolyzing peptide bonds. This enzyme is very well known to have its activity increased by high pressure [24, 25]. It is increased by a factor of 6.5 when pressurized to 4700 bar at 20 °C [25]. Besides that, α -CT can also be activated by simply fixing it on a polyelectrolyte surface with opposite charge in relation to the substrate [57]. If α -CT adsorbs on oppositely charged particles, positively charged substrates are preferred, showing that electrostatic interactions are very important for the binding of a substrate and the release of a product [58].

Thus, HRP and α -CT are good candidates for the study of combined effects of high pressure and aqueous-solid interfaces.

3.2. Experimental details

3.2.1. Enzymes and substrates

HRP and Amplex Red® substrate (10-acetyl-3,7-dihydroxyphenoxazine) were purchased from Thermo Fisher Scientific (Assay Kit A22188).

α -CT from bovine pancreas was purchased from Sigma-Aldrich (C7762). The EnzCheck® Peptidase/Protease Assay Kit from Thermo Fisher Scientific (Assay Kit E33758) was used to probe the protease activity of α -CT.

Ludox AM and Ludox CL colloidal silica particles were purchased from Sigma-Aldrich and used for immobilization of the enzymes. From dynamic light scattering experiments, diameters of about 30 nm and 180 nm have been found for Ludox AM and Ludox CL silica particles, respectively [59]. Ludox AM silica particles have a negative

surface charge, and Ludox CL silica particles are coated with alumina converting their charge from negative to positive.

3.2.2. Enzymatic assays

The experiments were done with α -CT free in solution as well as with it adsorbed on Ludox AM silica nanoparticles. α -CT was adsorbed on silica particles by mixing stock solutions of α -CT (40 μ L of a 6.8 mg mL⁻¹ solution) and Ludox AM (100 μ L of a 1.21 g mL⁻¹ solution) in 1 mL buffer solution (20 mM Tris-HCl, pH = 7.8) and incubating the mixed solution at 4 °C for 3 hours. This time was set to achieve maximum protein adsorption and better reproducibility of kinetic results.

The total area of Ludox AM was calculated for 100 μ L of a 1.31 g mL⁻¹ solution. From the density of 1.31 g mL⁻¹ and the surface area of 288 m² g⁻¹, a surface area of 26.1 m² in 100 μ L solution of silica particles can be calculated. 250 μ L of a 2 mg mL⁻¹ α -CT solution were applied to adsorb. α -CT has a molar mass of 25000 g mol⁻¹ that corresponds to a mean radius of $r = 1.9$ nm using a specific volume of 0.7 cm³ g⁻¹. From this radius, a footprint area of $\pi r^2 = 1.1 \cdot 10^{-17}$ m² per molecule can be estimated. There are $1.2 \cdot 10^{16}$ molecules in 250 μ L that have a total footprint area of 0.13 m². The surface coverage is then $0.13/26.1 = 5.10^{-3}$.

To probe the enzymatic activity of free or adsorbed α -CT (in the absence or presence of silica particles), samples contained 5 μ g mL⁻¹ of α -CT, 20 mM Tris-HCl buffer (pH = 7.8), and 1.57 mg mL⁻¹ EnzCheck substrate. This substrate consists of a fluorophore and a quencher moiety that are covalently connected via an amino acid chain. Upon chain cleavage by α -CT, the quencher separates from the fluorophore that is then free to emit fluorescence [60]. Experiments were carried out with a K2 fluorescence spectrometer from ISS (Champaign, Illinois, USA) with a high pressure sample cell from ISS. Fluorescence was excited at 502 nm with a Xe arc lamp and detected at 528 nm in photon counting mode. All measurements were performed at 20 °C.

HRP was also probed free and adsorbed on Ludox CL silica nanoparticles. The adsorbed HRP was prepared by mixing stock solutions of HRP (1.1 μ L of a 23 μ g mL⁻¹ solution) and Ludox CL (100 μ L of a 1.23 g mL⁻¹ solution) in 1 mL buffer solution (50 mM sodium phosphate, pH = 7.4) and incubating the mixed solution at 4 °C for 3 hours.

The total surface area available for adsorption of HRP was calculated for 100 μ L of Ludox CL solution with a density of 1.23 g mL⁻¹. From the density of 1.23 g mL⁻¹ and the surface area of 230 m² g⁻¹, a surface area of 28 m² in 100 μ L solution of silica particles was

calculated. Then, 1.1 μL HRP solution of a $23 \mu\text{g mL}^{-1}$ was added. HRP has a molar mass of 44000 g mol^{-1} that corresponds to a mean radius of $r = 2.3 \text{ nm}$ using a specific volume of $0.7 \text{ cm}^3 \text{ g}^{-1}$. From this radius, a footprint area of $\pi r^2 = 1.7 \cdot 10^{-17} \text{ m}^2$ per molecule can be estimated. There are $3.5 \cdot 10^{11}$ molecules in 1.1 μL that have a total footprint area of $6 \cdot 10^{-6} \text{ m}^2$. The surface coverage is then $6 \cdot 10^{-6} / 28 = 2 \cdot 10^{-7}$.

To probe the enzymatic activity of free or adsorbed HRP (in the absence or presence of silica particles), samples contained $1.16 \mu\text{g mL}^{-1}$ of HRP ($0.026 \mu\text{M}$), 50 mM sodium phosphate buffer ($\text{pH} = 7.4$), $50 \mu\text{M}$ Amplex Red substrate, and $1 \text{ mM H}_2\text{O}_2$. HRP catalyzes the oxidation of the Amplex Red substrate to the resorufin product by H_2O_2 . Because resorufin is fluorescent, it can be quantified easily [60]. Fluorescence was also measured using the K2 fluorescence spectrometer. Fluorescence of resorufin was excited at 530 nm and detected at 585 nm . All measurements were performed at $25 \text{ }^\circ\text{C}$.

3.2.3. Degree of adsorption

Ludox CL silica particles have a positive surface charge due to alumina coating and interact with negatively charged amino acid residues of HRP. The net charge of HRP at neutral pH-values is very close to 0 [61, 62]. α -CT, which has a small positive net charge at neutral pH-values (the isoelectric point is at $\text{pH} = 9$) [63,64] can bind to the negatively charged Ludox AM silica particles. To determine the degree of enzyme adsorption on the silica particles, we have used Millipore Amicon Ultra centrifugal filters 50.000 MW (50 kDa or $7\text{-}10 \text{ nm}$). Only free, non-adsorbed enzyme molecules, can pass the filter. Consequently, silica particles with adsorbed enzyme molecules are retained by the filter (Figure 21).

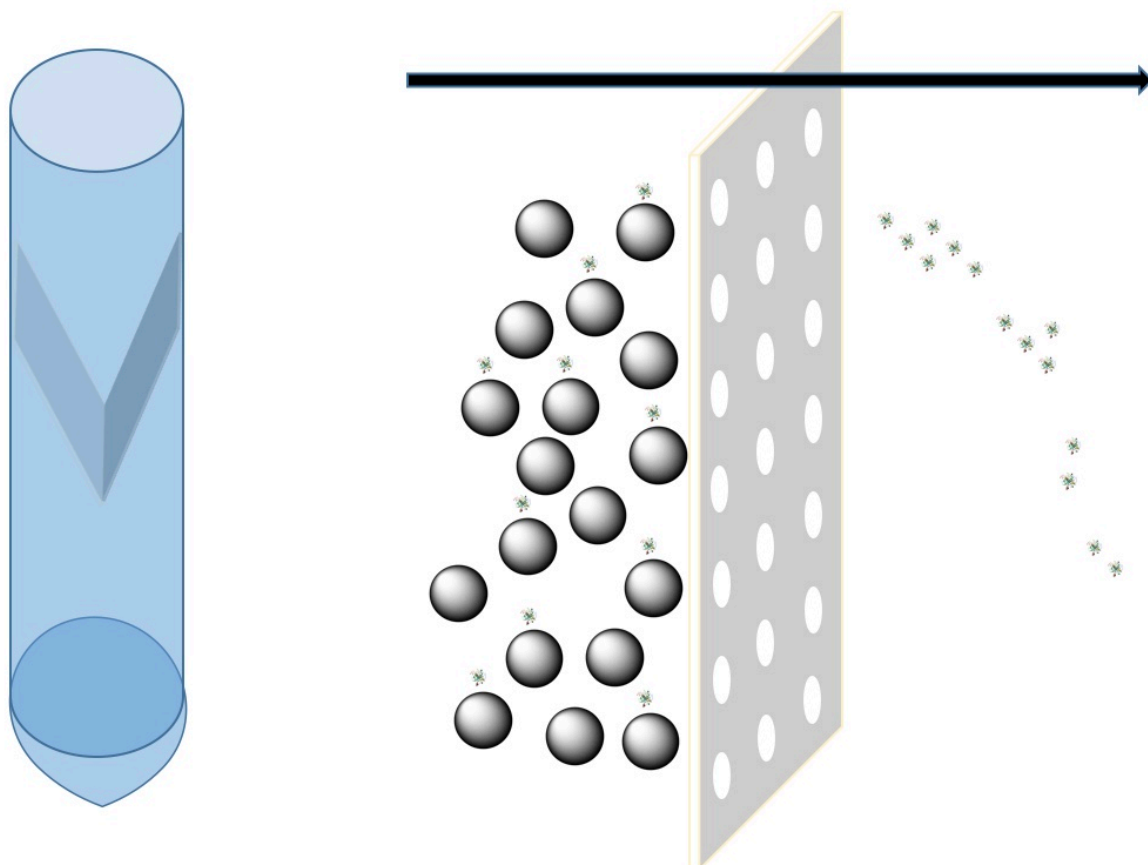


Figure 21. Amicon® ultrafiltration devices. In this centrifugal devices, there is a membrane, which has a very defined pore size. During the centrifugation, only molecules smaller than the pore size can pass and bigger molecules will be retained. As seen above, free enzymes can easily pass the membrane. However adsorbed enzymes are retained because the nanoparticle is larger than the pore.

The filters were loaded with the mixed solutions of enzymes and silica particles. After centrifugation at 14000 g for 10 min at 4 °C, the filtrates were analyzed for free enzymes. By UV-spectroscopy, no free HRP or α -CT could be detected. Moreover, no enzymatic activity of HRP or α -CT could be detected in the filtrate when carrying out the enzymatic assays described above. The fluorescence intensity did not change with time upon addition of the corresponding substrate (Figure 22). Thus, within the results obtained using UV- and fluorescence spectroscopy, it can be said that all enzyme molecules are adsorbed in the presence of the silica particles.

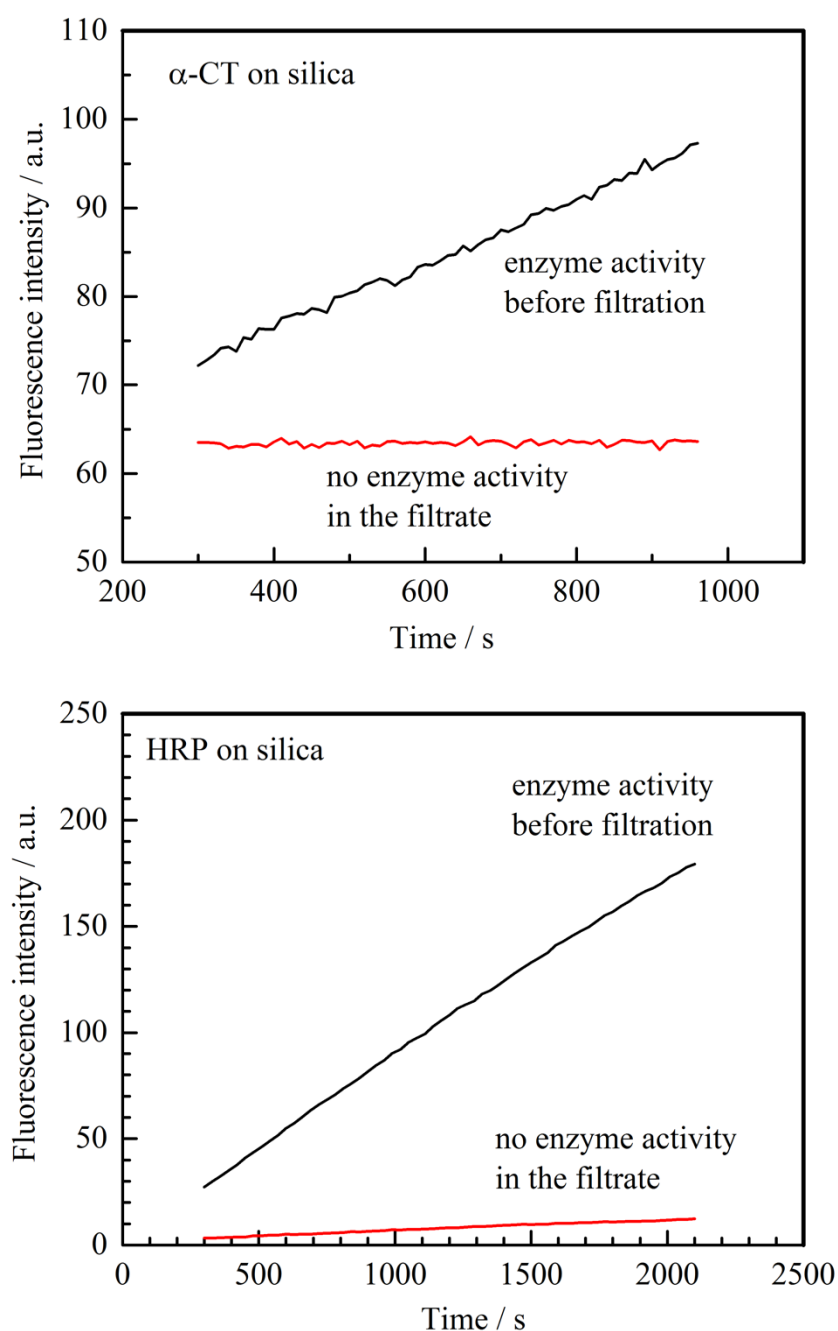


Figure 22. Activity measurements of adsorbed α -CT and HRP before and after ultrafiltration. The degree of enzyme adsorption on silica particles has been tested by activity measurements. The mixed solution of enzyme molecules with silica particles has been centrifuged through Millipore Amicon Ultra centrifugal filters with a pore size of 50 kDa. Free, non-adsorbed enzyme molecules can pass this filter. However, no significant enzymatic activity has been detected in the filtrates indicating that all enzyme molecules are adsorbed on the silica particles. In the case of HRP on silica, the small increase of the fluorescence intensity of the filtrate must be assigned to the direct oxidation of Amplex Red by H_2O_2 . The same increasing fluorescence intensity is observed, when Amplex Red and H_2O_2 are added to a pure buffer solution.

3.2.4. Data collection and analysis

Fluorescence intensity is proportional to the fluorophore concentration, c . Thus, the rate of product formation, dc/dt , is proportional (not equal) to the slope of the fluorescence intensity plotted as a function of time (Figure 23). To remove all instrumental factors affecting the fluorescence intensity, the slope observed under pressure, r , has been normalized to the slope observed under ambient pressure, r_0 . Each fluorescence assay started with a few minutes of data collection at 1 bar followed by a 1-2 min period, during which the pressure has been increased, and a further time period under high pressure. The ratio of the slopes measured directly before and after the pressure change can be related to the ratio of the corresponding rate constants, because the concentrations are very similar before and after the pressure change:

$$\frac{r}{r_0} = \frac{k}{k_0}$$

The meaning of the rate constants is discussed below. It follows from the equation below that a plot of $\ln(r/r_0)$ as a function of pressure, p , should yield a curve, whose slope contains the activation volume:

$$\left(\frac{\partial \ln(r/r_0)}{\partial p}\right)_T = -\frac{\Delta V^\ddagger}{RT}$$

This equation can be applied to all pressures, p , and does not require a constant activation volume. When the activation volume is pressure dependent, a change in the slope of $\ln(r/r_0)$ vs. p is observed.

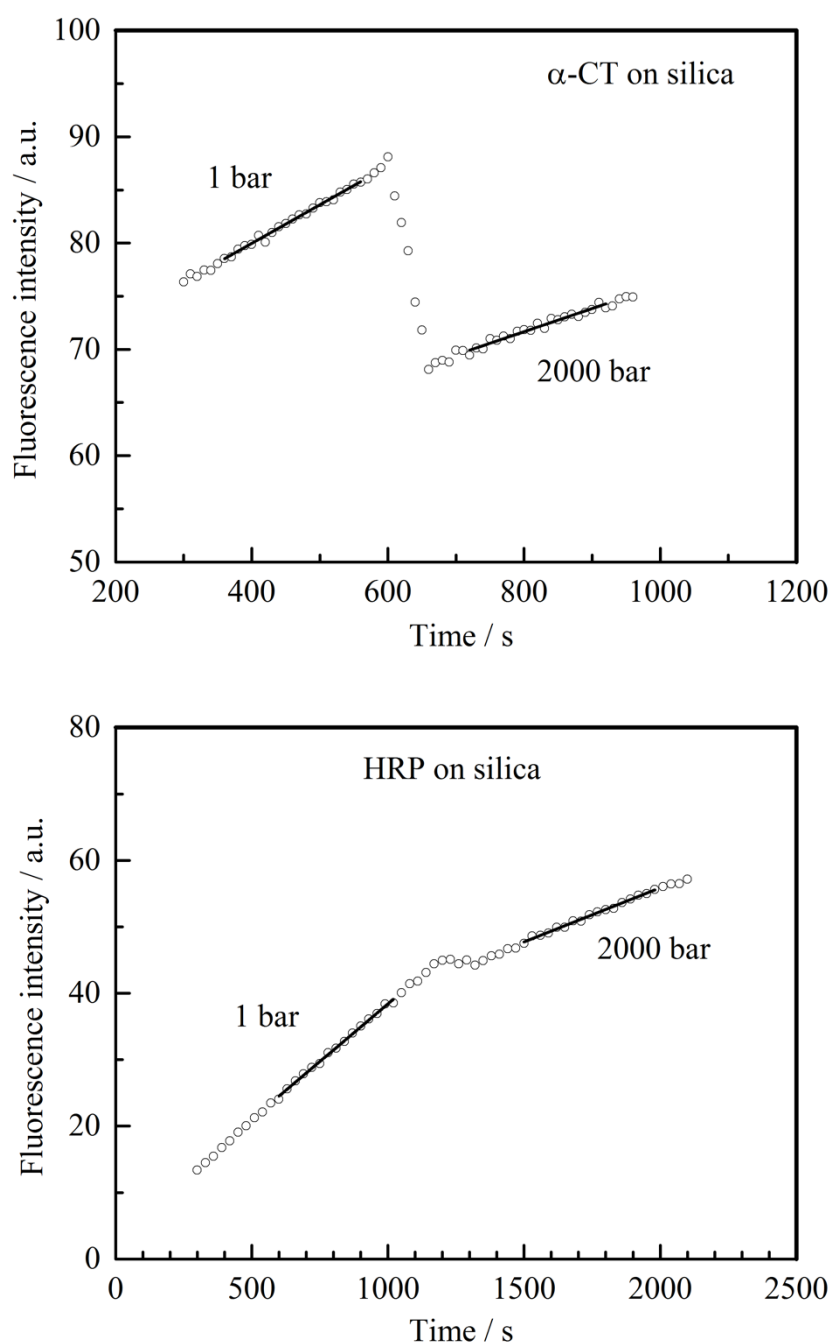


Figure 23. Typical fluorescence data recorded to probe the enzymatic activity of α -CT and HRP. The fluorescence intensity has been measured at 1 bar and after pressure increase. The slope of the data is proportional to the rate of the enzymatic reaction. The slopes before and after the pressure increase have been determined by linear fits.

In addition, the raw slope, $r_{\text{raw}}(p)$, taken from the fit under high pressure (Figure 24), has been corrected for the pressure dependence of the fluorescence quantum yield of the product. This has been measured using an enzymatic assay with free HRP or α -CT (without

silica particles) that was allowed to run for about five hours until the fluorescence intensity of the product has reached a constant value, and no additional product was formed anymore. Then, the fluorescence intensity of this assay was measured as a function of pressure. After normalization to 1 bar (Figure 24), the fluorescence intensity, $I(p)$, was used to correct the raw slope, $r_{\text{raw}}(p)$, by calculating $r(p) = r_{\text{raw}}(p)/I(p)$.

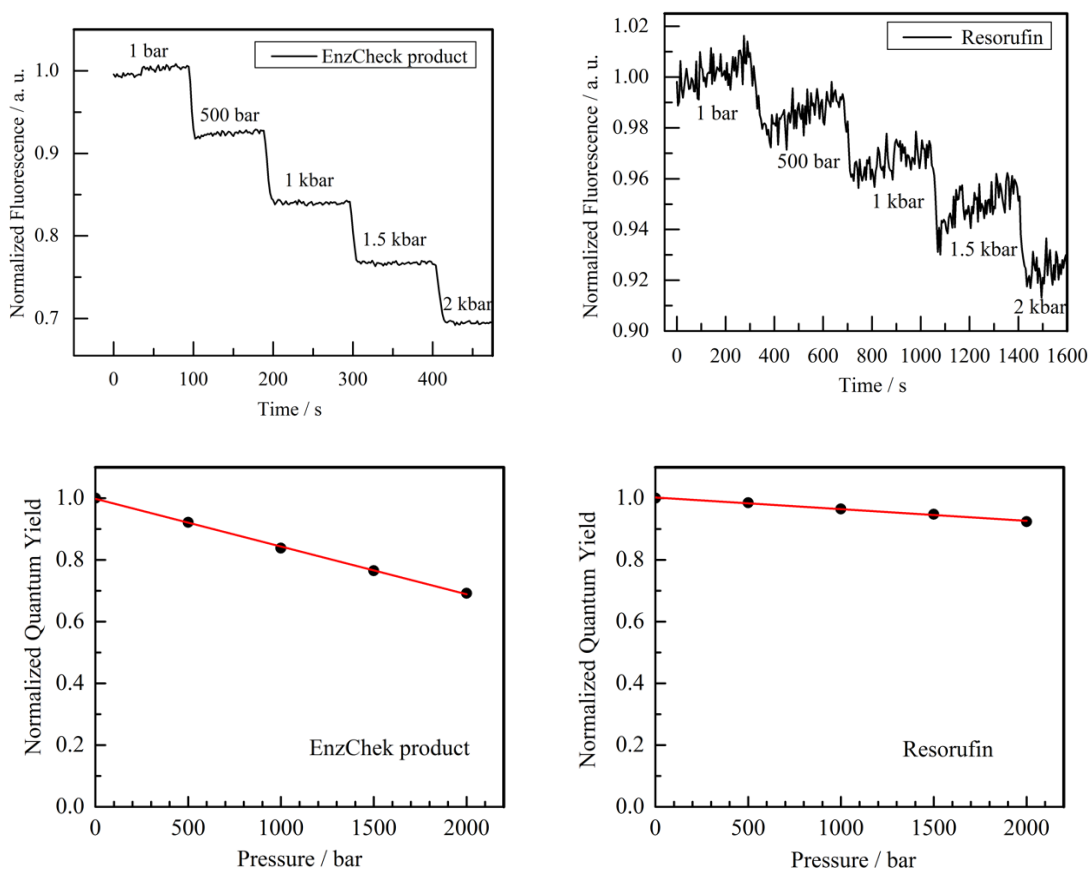


Figure 24. Pressure dependence of fluorescence intensity of the assay product of EnzChek and resorufin.

The pressure dependence of the fluorescence intensity of an enzyme product has been assessed by analyzing the enzyme assay after about five hours, when the fluorescence intensity of the product has reached a constant value. This steady-state fluorescence intensity was measured as a function of pressure and was normalized to 1 bar.

3.2.5. FTIR spectroscopy

Infrared absorption spectra of HRP and α -CT were recorded using a Nicolet 6700 Fourier transform infrared spectrometer from Thermo Fisher Scientific at a spectral resolution of 2 cm^{-1} . Sample solutions were analyzed in a thermostatted diamond anvil cell. Barium sulfate was added to the sample as an internal pressure sensor. All spectra were corrected for background measured with buffer solution, in this case D_2O was used as solvent.

3.3. Results and discussion

3.3.1. Pressure stability of HRP and α -CT

In this study, the enzymatic activities of HRP and α -CT were performed using enzymatic assays under pressures up to 2000 bar at 25 or 20 °C, respectively. It is helpful to separate pressure effects on the enzyme kinetics from pressure effects on the protein conformation. Free HRP and α -CT do not unfold in solution in this pressure range [65-67]. However, in the adsorbed state, the conformational stability of proteins is usually lowered. This means that the temperature and pressure of protein unfolding are significantly lowered after adsorption at an aqueous-solid interface [59, 68, 69]. Thus, we have analyzed the conformation of HRP and α -CT when they are adsorbed on silica particles and, for comparison, free in solution as a function of pressure. Using FTIR spectroscopy in combination with a diamond anvil cell, the amide I' band (in D₂O) has been recorded. This band is known to be sensitive for the secondary structure of a protein. Any change in the secondary structure leads to a change of the band shape, because the amide I' band is a superposition of the infrared absorption bands of the various secondary structure elements, which have all individual wavenumbers [44]. In figure 25, the amide I' bands of HRP and α -CT both in the adsorbed state on silica particles and free in solution are plotted. Apparently, no major change of the band shape of the amide I' bands can be observed, when pressure is increased up to 2 kbar, indicating stable secondary structures of the enzymes. Indeed, the pressure of unfolding has been reported to be 12 kbar in the case of HRP [65] and about 4 kbar in the case of α -CT [66, 67].

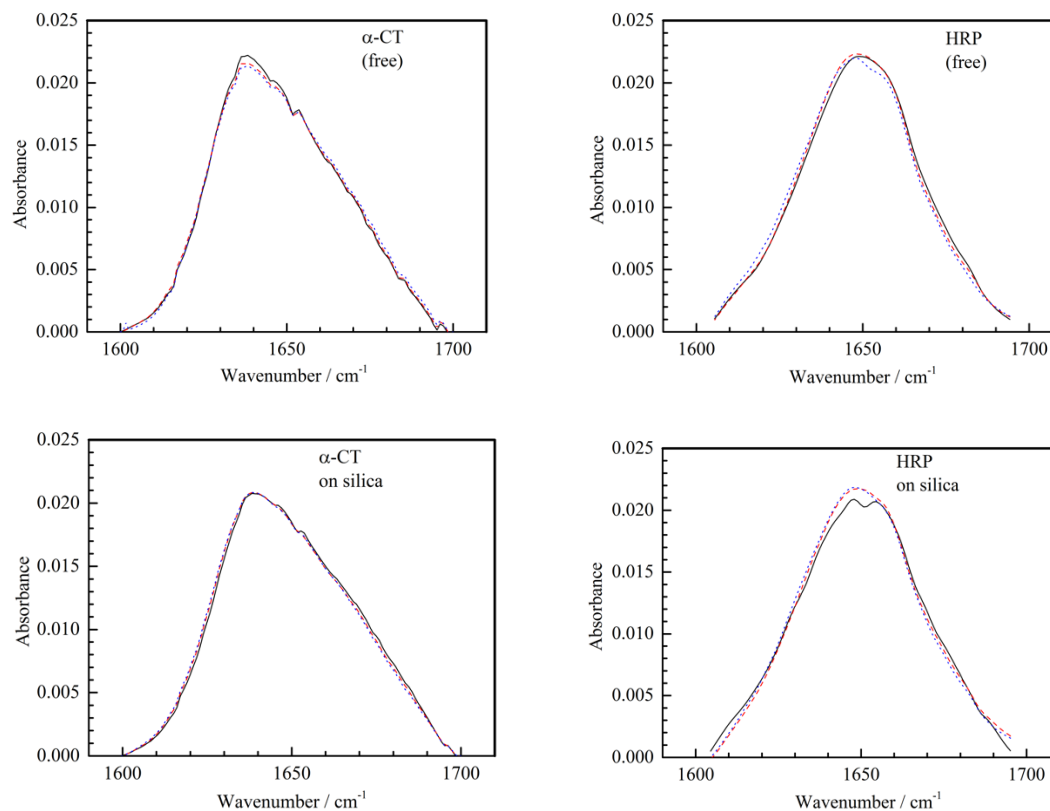


Figure 25. Amide I' band in the FTIR spectra of free and adsorbed α -CT and HRP (selected data). Each diagram contains three overlapping amide I' bands in the pressure range 1–2300 bar indicating the pressure stability of the secondary structures. Data curves refer to 1 bar (solid line), 1000 bar (dashed line), and 2300 bar (dotted line).

In addition, the tertiary structure of α -CT was probed by recording the Trp fluorescence band (unfortunately, the Trp fluorescence of HRP was too weak to observe due to intramolecular Trp heme energy transfer [70]). A red shift of the Trp fluorescence band indicates an exposure of buried Trp residues to water in the course of protein unfolding. These experiments were done using ISS K2 fluorimeters. The spectra cover 300–450 nm. As can be seen in figure 26, the Trp bands of free and adsorbed α -CT do not shift with pressure clearly indicating an intact tertiary structure up to 2000 bar. For comparison, the Trp band of α -CT has also been measured as a function of temperature (Figure 26). Here, a pronounced red-shift of this band is observed upon thermal unfolding. Thus, pressure-induced changes of the enzyme kinetics of HRP and α -CT are not related to any pressure-induced partial unfolding of these enzymes.

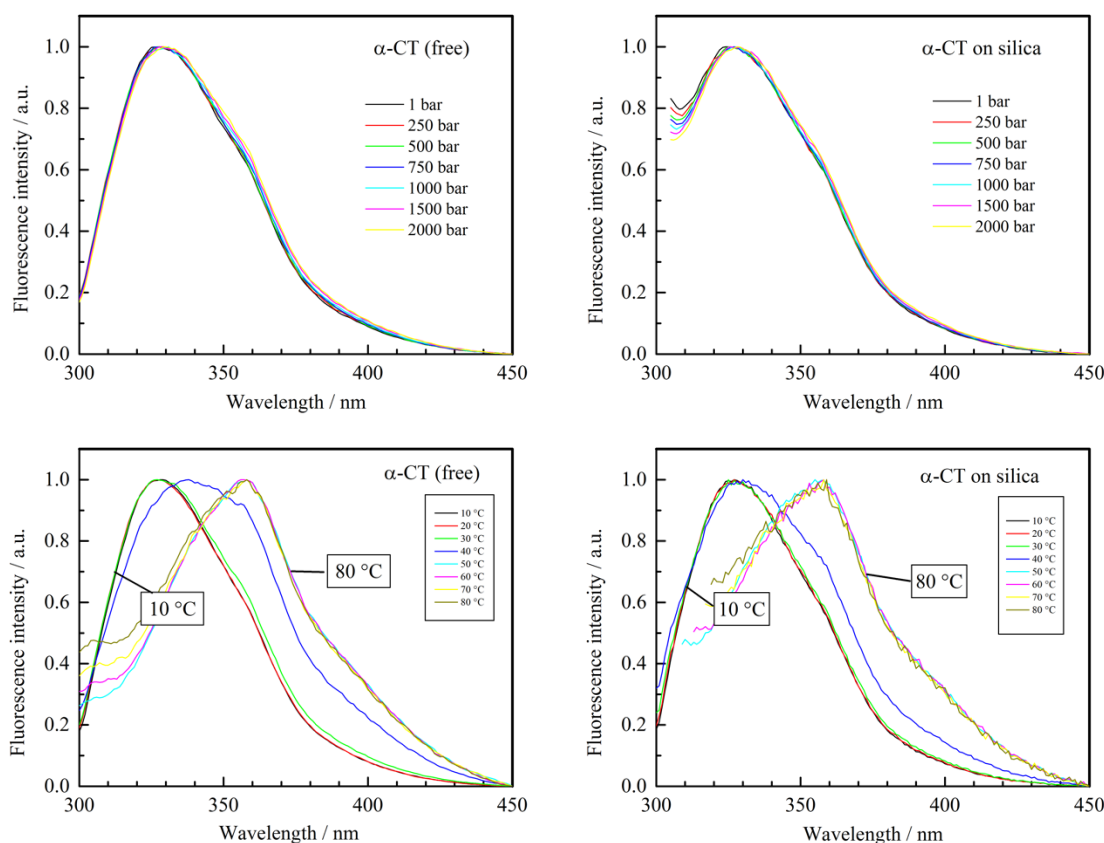
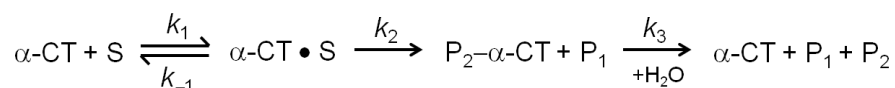


Figure 26. Tryptophan fluorescence of α -CT as a function of pressure and temperature. Effect of pressure on the Trp fluorescence spectrum of α -CT: free in solution and adsorbed on silica particles. Each diagram shows 7 overlapping spectra in the pressure range 1 – 2000 bar. There is no red-shift of the spectra with increasing pressure indicating the pressure stability of the tertiary structure of free and adsorbed α -CT.

3.3.2. Pressure effects on the enzymatic activity of free and adsorbed α -CT

α -CT from bovine pancreas has a molar mass of about $25,000 \text{ g mol}^{-1}$ and an isoelectric point of about 9 giving a positive net charge to the enzyme at neutral pH-values [63,64]. However, α -CT binds to and is active on both negatively and positively charged surfaces of polyelectrolyte layers [11]. α -CT cleaves peptide bonds, preferentially those formed by the aromatic amino acids Trp, Tyr, and Phe [27]. It hydrolyzes a peptide bond via an initial nucleophilic attack of the residue Ser195, which is located in the active site. The mechanism is of Michaelis-Menten type [27]:



Here, S is the substrate, which is hydrolyzed into the products P_1 and P_2 . As described in the Materials and methods section, we have used a large concentration of substrate (a few mg mL^{-1}) that is saturating the enzyme (a few $\mu\text{g mL}^{-1}$). In this case, the rate of the enzymatic reaction is determined by step 2 and step 3 with a rate constant of $k_{\text{cat}} = k_2k_3/(k_2+k_3)$ [54]. It has been proposed that k_2 is small and rate-limiting for a peptide hydrolysis (this study), whereas k_3 is small and rate-limiting for an ester hydrolysis [24, 25, 27]. A back reaction is also avoided by high substrate concentration. Therefore, the ΔV^\ddagger -values of α -CT, as observed in this study, probably refer to step 2 in the reaction scheme, where the enzyme is acylated (P_2 - α -CT) and an amine (P_1) is released.

In figure 27, logarithmic plots of the normalized fluorescence slopes, r/r_0 , are shown for α -CT free in solution. The change of $\ln(r/r_0)$ with pressure, p , is proportional to the negative activation volume, $-\Delta V^\ddagger$. Apparently, the logarithmic plot is not consistent with a constant activation volume over the whole pressure range studied. Indeed, pressure dependent activation volumes are described as the more usual case [71]. The activation volume is the difference of the volumes of the transition state and the E+S mixture, $\Delta V^\ddagger = V_{\text{ES}^\ddagger} - V_{\text{E+S}}$. If these volumes, V_{ES^\ddagger} and $V_{\text{E+S}}$, have different compressibility, a change of ΔV^\ddagger with pressure is the result. In our case, the curved data in figure 27 can be approximated with two linear ranges from 1 to 500 bar and from 500 to 2000 bar. These linear ranges yield activation volumes of -67 mL mol^{-1} (1 – 500 bar) and -15 mL mol^{-1} (500 – 2000 bar).

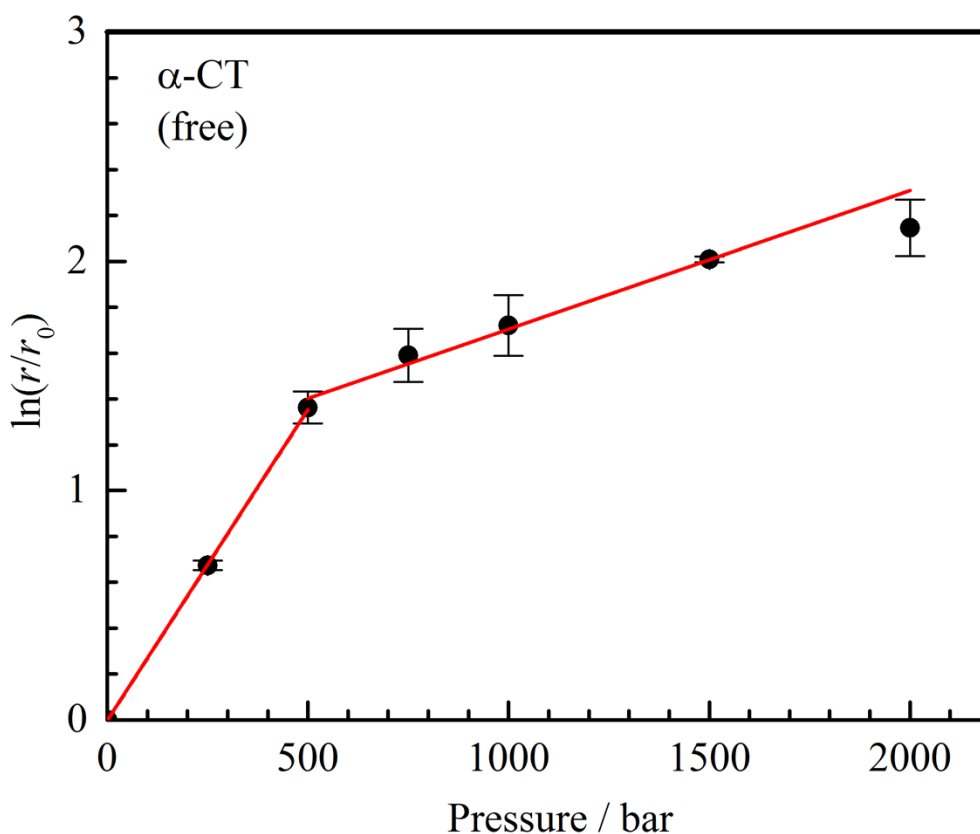


Figure 27. Pressure dependence of the enzymatic activity of free α -CT. The slopes of the plots are determined by linear fits. They are proportional to the negative activation volume. Each error bar covers the results of two independent measurements. r and r_0 are the slopes of the fluorescence intensity as a function of time under high and ambient pressure, respectively.

A negative activation volume indicates that the volume of the transition state is smaller than the volume of the E+S. In this way, high pressure favors the formation of the transition state, because the activation free energy is lowered by $p\Delta V^\ddagger$. The outcome is a faster enzymatic reaction. Negative activation volumes of α -CT have also been found in the literature [24,25]. Taniguchi *et al.* report activation volumes in the range from -4.4 to -35 mL mol⁻¹ for the enzyme deacylation (step 3 in the reaction scheme) [24]. Mozhaev *et al.* have studied the acylation of the enzyme (step 2 in the reaction scheme) and observed an activation volume of about -10 mL mol⁻¹ at 20 °C and -25 mL mol⁻¹ at 50 °C [25]. These values are in good agreement with our value of -15 mL mol⁻¹ above 500 bar at 25 °C. However, the strongly negative activation volume observed in this study below 500 bar has not been resolved so far.

The corresponding data of the α -CT catalysis in the adsorbed state on silica particles are shown in figure 28. Remarkably, as found for free α -CT, adsorbed α -CT has a non-

constant activation volume in the pressure range of 1- 2000 bar. There is a slight increase of the enzymatic rate up to 500 bar reaching a maximum at about 750 bar. At higher pressures, the enzymatic rate is decreasing with increasing pressure. From linear fits, activation volumes of -4 mL mol^{-1} (1 – 500 bar) and $+5 \text{ mL mol}^{-1}$ (1000 – 2000 bar) can be determined (Figure 28). When comparing the data of free α -CT (Figure 27) with those of adsorbed α -CT (Figure 28), similar pressure profiles can be observed except for an overall reduction of the slopes and a corresponding increase of the activation volumes upon adsorption of α -CT on silica particles. Apparently, adsorption adds a positive contribution to the activation volume.

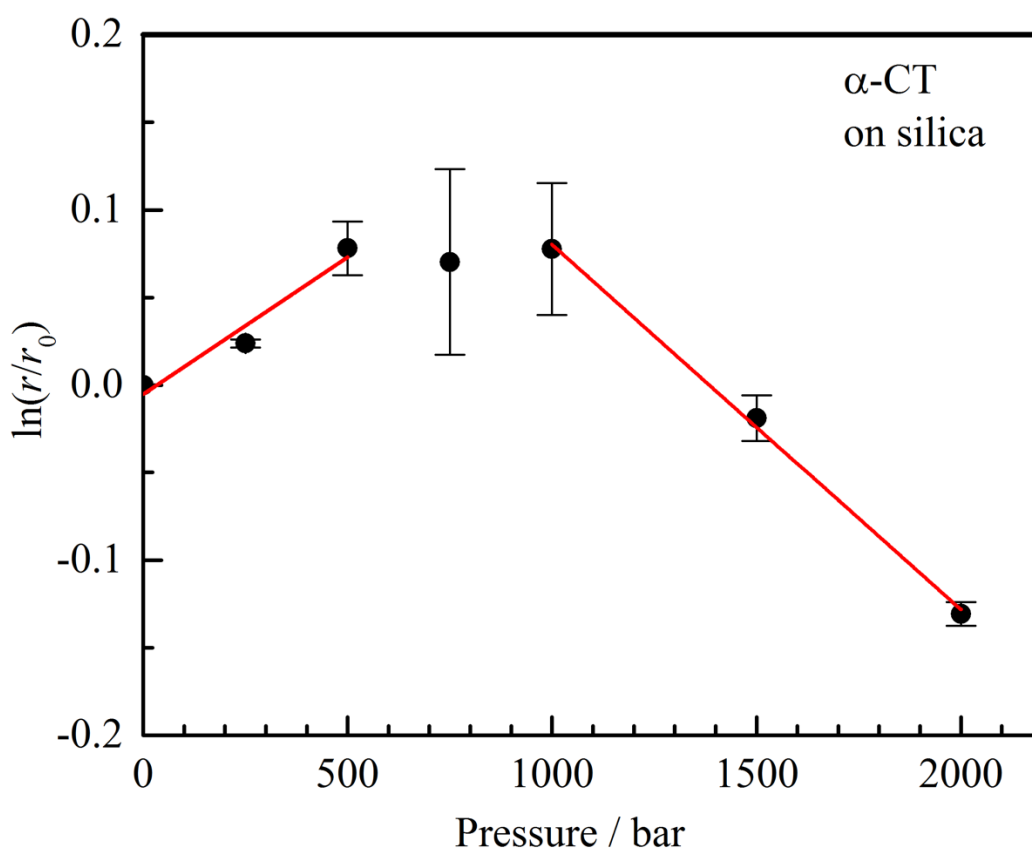


Figure 28. Pressure dependence of the enzymatic activity of adsorbed α -CT. The slopes of the plots are determined by linear fits. They are proportional to the negative activation volume. Each error bar covers the results of two independent measurements. r and r_0 are the slopes of the fluorescence intensity as a function of time under high and ambient pressure, respectively.

A volume diagram of α -CT catalysis is given in figure 29. Activation volumes are illustrated as arrows pointing from the E+S mixture to the transition state (ES*). In the literature, sources of activation volumes are discussed [16, 19, 20, 72]. Exposure of

hydrophobic and charged amino acid residues to water during the formation of the transition state will cause a higher hydration density and a negative activation volume. Indeed, Mozhaev *et al.* have attributed the observed negative activation volume of α -CT to the increased hydration of the transition state dipole [25]. Moreover, conformational changes of the enzyme forming the transition state can be linked to the generation or the filling of void volumes inside the enzyme.

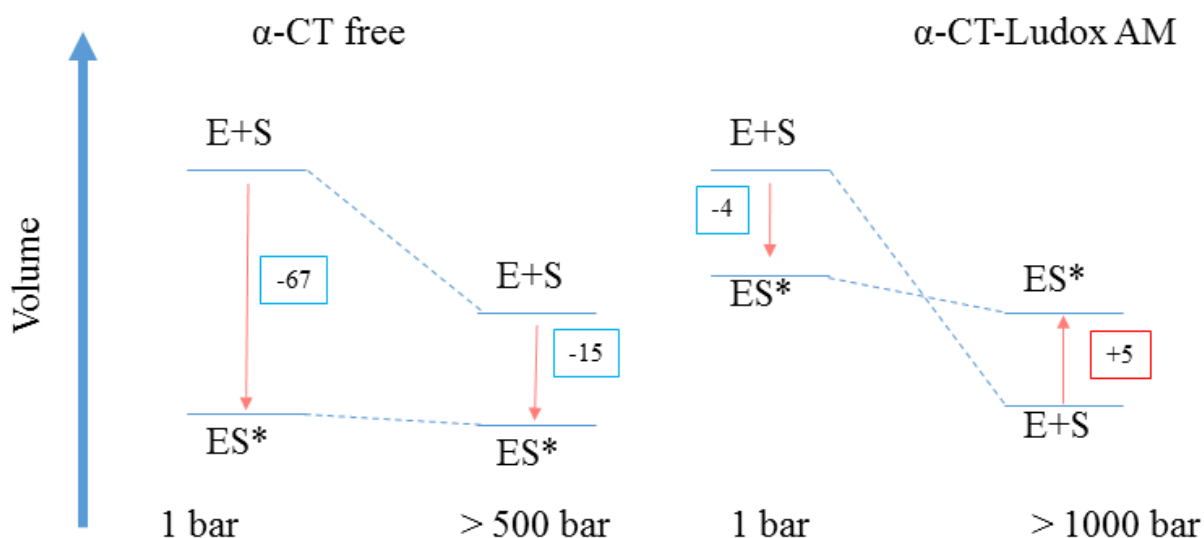


Figure 29. Activation volumes of free and adsorbed α -CT (not to scale, ΔV^\ddagger given in mL mol^{-1}). In both cases, the activation volume depends on the pressure. The E+S mixture is compressed in a stronger way than the transition state (ES^*). The volume levels at low and high pressures are arranged assuming a volume reduction of both E+S and ES^* by pressure.

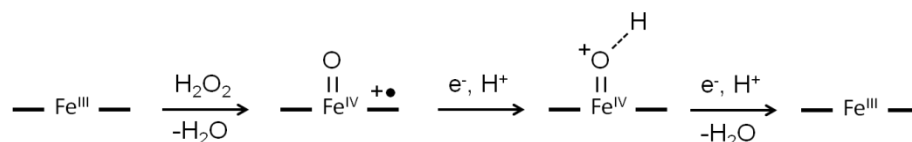
In both cases of free and adsorbed α -CT, more positive activation volumes were observed in the higher pressure range. This may be explained by a stronger compression of the E+S relative to the ES^* , as illustrated in the volume diagram (Figure 29). If $V_{\text{E+S}}$ is compressed in a stronger way than V_{ES^*} , the activation volume, which is the difference $V_{\text{ES}^*} - V_{\text{E+S}}$, becomes larger. From conformational studies, it is clear that α -CT does not undergo significant changes in the secondary and tertiary structure in the pressure range of 1 – 2000 bar (Figure 25, 26). However, we could speculate that the substrate binding leaves some void volume at ambient pressure. At about 500 bar, the substrate molecule might be pushed deeply into the enzyme pocket in a way that the fitting is optimized and V_{ES^*} becomes smaller.

Upon adsorption of α -CT on the silica particles, the activation volumes are increased (Figure 29). It is likely that an increase of the transition state volume, V_{ES^*} , is the reason for this finding. When an enzyme is catalyzing a chemical reaction, conformational flexibility of

the enzyme is mandatory. However, in the adsorbed state, this conformational flexibility will be reduced. As a consequence, the transition state might have a non-perfect, distorted geometry with an increased void volume, which increases V_{ES^*} and ΔV^\ddagger of α -CT in the adsorbed state. Moreover, the location of water molecules in the active site of the enzyme appears to be a crucial factor. There might be gaps in the transition state that are just too small to accommodate a water molecule. However, a clear molecular picture of the immobilization and pressure effects on the α -CT catalysis is not possible at this point.

3.3.3. Pressure effects on the enzymatic activity of free and adsorbed HRP

For comparison, we have also studied the effect of pressure on the catalytic activity of free and adsorbed HRP. HRP has a molar mass of about 44,000 g mol⁻¹, is mainly α -helical, and binds heme as prosthetic group [30, 31]. HRP catalyzes the oxidation of a substrate by H₂O₂. The mechanism is based on the initial binding of an oxygen atom from H₂O₂ to the iron atom of heme. Then, two electrons are transferred successively from the substrate to the heme group, and a water molecule is finally released after uptake of two protons [30, 32]:



This mechanism is much more complex than the peptide cleavage by α -CT. The two intermediates in the above scheme are denoted as compound I and compound II. In this study, HRP catalyzes the oxidation of the Amplex Red® substrate by hydrogen peroxide to the product resorufin. Resorufin is detected by its fluorescence. In the enzymatic assay, a large excess of hydrogen peroxide (1 mM) and Amplex Red (50 μ M) that bind to HRP (0.026 μ M) was used. This excess disfavors the back reaction and ensures the maximum enzymatic rate. The rate-limiting steps will be the successive transfers of two electrons from an Amplex Red molecule to the heme group. Recent single molecule fluorescence experiments are consistent with a two-electron mechanism, where the two electrons originate from a single Amplex Red molecule and fluorescent resorufin is formed while it is still confined in the enzyme [73]. Alternatively, it has been proposed that HRP oxidizes an Amplex Red molecule by a one-electron transfer only. Afterwards, the formed non-fluorescent radical intermediate is released from the enzyme and reacts to resorufin by dismutation [74].

The measured enzymatic activity of HRP using Amplex Red as the substrate is shown in figure 30. The observed slope of the product fluorescence, r , is plotted as a function of pressure, p , on a logarithmic scale. In both cases, free HRP and adsorbed HRP, the slope of the product fluorescence and thus the associated rate constant of product formation decreased as the pressure increased. This indicates positive activation volumes, which increase the activation free energies by the amount $p\Delta V^\ddagger$. As found for α -CT, the plots of $\ln(r/r_0)$ vs. p (Figures 30 and 31) are non-linear suggesting non-constant activation volumes of free and adsorbed HRP in the pressure range 1 – 2000 bar. To estimate activation volumes, we have divided the studied pressure range into a lower and higher pressure range in a similar way as described above for α -CT. From the linear fits (Figure 30), we can derive activation volumes of $+16 \text{ mL mol}^{-1}$ (1 – 500 bar) and $+2 \text{ mL mol}^{-1}$ (500 – 2000 bar) in the case of free HRP.

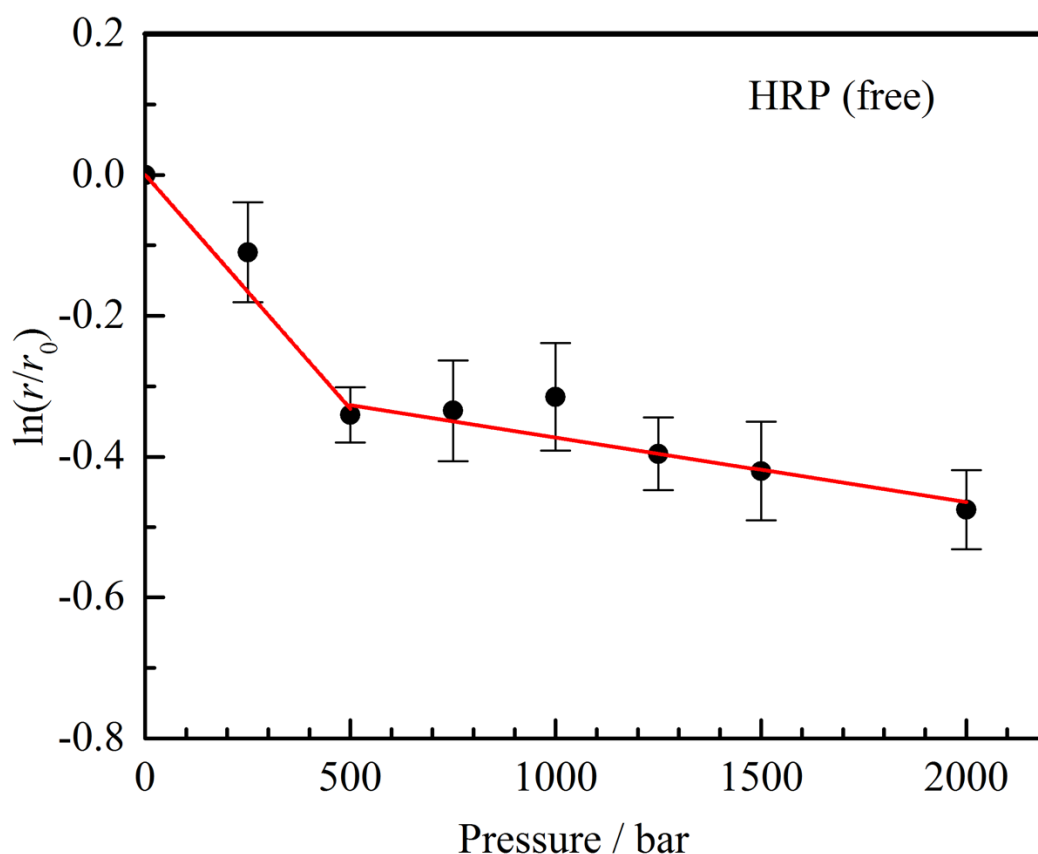


Figure 30. Pressure dependence of the enzymatic activity of free HRP. The slopes of the plot are determined by linear fits. They are proportional to the activation volume. Each error bar covers the results of four independent measurements. r and r_0 are the slopes of the fluorescence intensity as a function of time under high and ambient pressure, respectively.

For adsorbed HRP, corresponding values of +27 mL mol⁻¹ (1 – 250 bar) and +2 mL mol⁻¹ (250 – 1500 bar) are obtained (Figure 31). All activation volumes obtained in this way are summarized in a volume diagram (Figure 32).

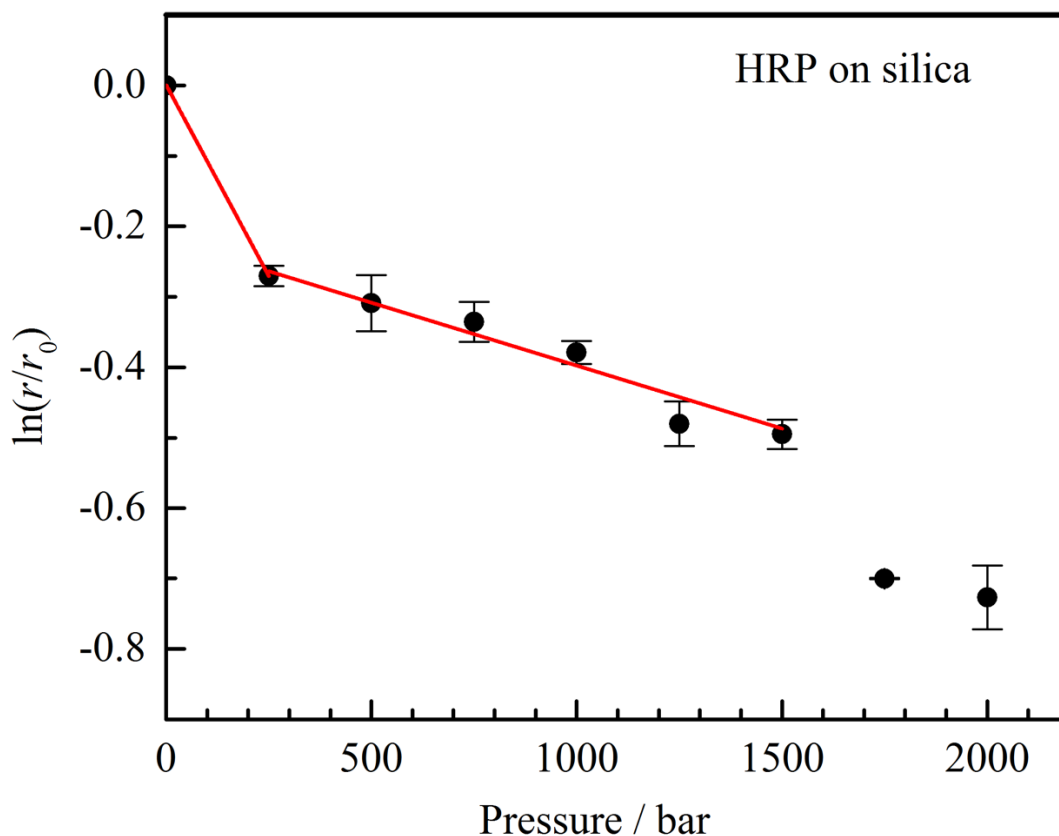


Figure 31. Pressure dependence of the enzymatic activity of adsorbed HRP. The slopes of the plot are determined by linear fits. They are proportional to the activation volume. Each error bar covers the results of four independent measurements. r and r_0 are the slopes of the fluorescence intensity as a function of time under high and ambient pressure, respectively.

Overall, the volume profiles of free and adsorbed HRP appear to be similar (Figure 32). Presumably, the mechanism of the enzymatic reaction does not change upon adsorption, and no large distortion of the active site occurs when HRP interacts with the silica particles. However, in contrast to α -CT, activation volumes of HRP tend to be smaller at higher pressures. Above 500 bar, an activation volume of only +2 mL mol⁻¹ indicates that the volumes of the transition state and E+S are very similar, and pressure has little effect on the enzymatic rate. Apparently, pressure can compress the transition state stronger than the E+S leading to a reduction of the activation volume, $\Delta V^\ddagger = V_{ES^*} - V_{E+S}$.

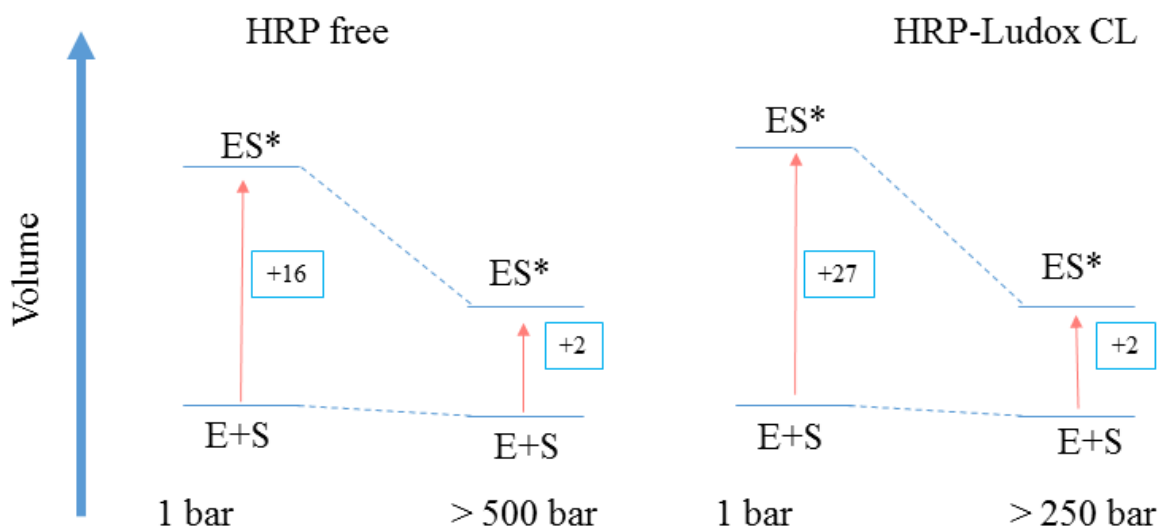


Figure 32. Activation volumes of free and adsorbed HRP (not to scale, ΔV^\ddagger given in mL mol^{-1}). In both cases, the activation volume depends on the pressure. ES^* is compressed in a stronger way than E+S . The volume levels at low and high pressures are arranged assuming a volume reduction of both E+S and ES^* by pressure.

So far, molecular interpretation of the volume diagrams given in figure 32 is difficult. Assuming that the transfers of two electrons from Amplex Red to HRP are rate-limiting, it can be concluded that E+S grows in volume to form the transition state, where the electron transfer can happen, because $V_{\text{ES}^*} > V_{\text{E+S}}$. Probably, electron transfer requires some shift of Amplex Red away from the optimum binding position thereby creating some void volume. However, at pressures above 500 bar, the increased volume of the transition state is suppressed resulting in $V_{\text{ES}^*} \approx V_{\text{E+S}}$. This finding is supported by earlier compressibility measurements of HRP in the low and high pressure range [75]. Below 100 bar, HRP has a large compressibility, whereas HRP is less compressible at higher pressures. It has been concluded that the enzyme has soft domains at ambient conditions, which are compressed and become rigid at higher pressures [75]. Thus, a larger compressibility of HRP at ambient conditions is linked to a larger density fluctuation, which could be the reason for the larger activation volumes of free and adsorbed HRP that are observed below 500 bar (Figure 32). At higher pressures, a rigid compressed structure of HRP is consistent with little volume change during the oxidation of Amplex Red®.

3.4. Conclusions

The effect of pressure on the enzymatic activity of free and adsorbed α -CT and HRP has been studied.

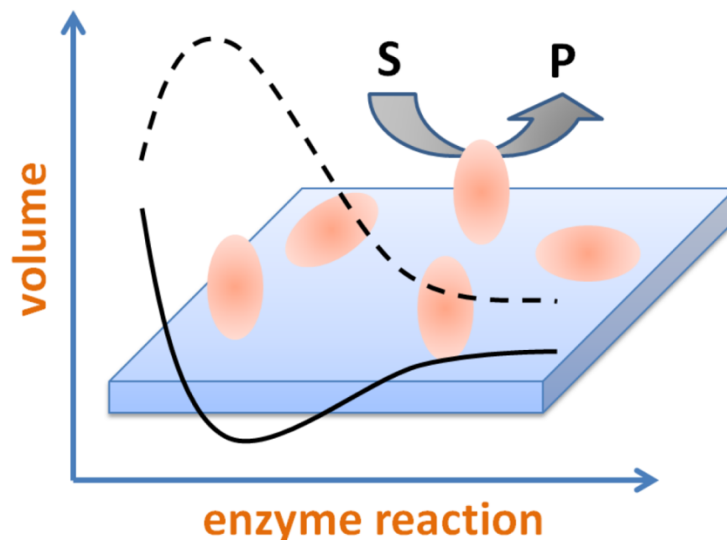
In the case of free α -CT, it is known that the enzymatic rate increases with increasing pressure. This effect could be confirmed by the present study, but a more pronounced pressure activation of free α -CT at lower pressures up to 500 bar was observed. Upon adsorption on silica particles, a positive contribution is added to the activation volume of α -CT. However, up to 500 bar, the activation volume of adsorbed α -CT is still negative and the enzymatic activity can still be enhanced by the application of pressure. These findings demonstrate a new potential strategy to optimize enzymatic reactions on carrier particles.

On the other hand, the observed activation volumes of HRP are generally positive and similar in the free and the adsorbed state. However, above about 500 bar, very small activation volumes are observed, only. Although molecular interpretations of the activation volumes determined in this study are difficult, the obtained volume profiles provide some framework for mechanistic discussions.

The observed pressure-dependence of the activation volumes of α -CT and HRP suggest that the transition state of HRP is more compressed under pressure than E+S, whereas the E+S of α -CT is more compressed under pressure than the ES*. Apparently, the transition state of α -CT is rather rigid and cannot easily be compressed, whereas the transition state of HRP exhibits some void volume.

4. Effect of interfacial properties on the activation volume of adsorbed enzymes

The work of the present study has been published and subsequently reprinted from Colloids and Surfaces B: Biointerfaces 140 (2016) 497–504, Schuabb, V., Cinar, S. and Czeslik, C., “Effect of interfacial properties on the activation volume of adsorbed enzymes” with permission from Elsevier. Copyright (2016) Elsevier B. V.



4.1. Background

Enzymes can be immobilized on solid surfaces [2,3], and enzymatic reactions on surfaces can be studied by surface-sensitive methods. In applied biotechnology, enzymes immobilized on particles can be recovered from the reaction mixture by centrifugation, sedimentation, filtration or magnetic forces [76] and can be reused, which is very relevant regarding expensive enzymes. However, any immobilized protein might have some degree of conformational change and/or denaturation by interaction with any given artificial surface [6,77]. One good alternative to create a native-like chemical environment for immobilized enzymes are hydrophilic and soft surfaces, such as PEG and polysaccharides [78-80]. However, even in the folded state, an immobilized enzyme can lose part of its activity, especially if the active site is blocked by the interface or the conformational dynamics are slowed down.

As written in chapter 3, enzymatic activities depend on temperature and pressure. Higher temperatures lead to faster chemical reactions. In the case of enzymes, this chemical principle is limited by the temperature of unfolding of the enzyme, where any activity is lost. Applying pressure, on the other hand, will slow down or accelerate enzymatic reactions depending on the sign of the activation volume, ΔV^\ddagger .

Many factors could affect the catalytic rate of adsorbed enzymes. Beside temperature and pressure, the nature of the interface will play a key role. There are several studies in the literature where enzymatic activities have been determined at various aqueous-solid interfaces under ambient pressure [2,3]. For example, a higher activity of subtilisin BPN' was observed on hydrophilic surfaces as compared to hydrophobic surfaces [81]. In addition, enzymes have also been embedded in polymer layers, such as polyelectrolyte multilayers and brushes, where a high degree of activity can be preserved [82-84]. In contrast, adsorption of α -CT on titania particles leads to a substantial loss of enzyme activity [85]. Thus, it is very interesting to understand the effect of pressure on adsorbed enzymes by changing the nature of the interface in a systematic way.

This is the first study that comprises the pressure effect on α -CT and HRP adsorbed on hydrophilic, hydrophobic, positively and negatively charged surfaces. The enzymatic rates of both enzymes have been determined by UV absorption spectroscopy at 1 bar and by total internal reflection fluorescence (TIRF) spectroscopy from 1-2000 bar, where a quartz prism was used as the adsorbent material. TIRF spectroscopy is a surface-sensitive method that will not detect molecules free in solution [46]. Besides that, the surface of a quartz prism can be

easily modified with any sort of polymer films and polyelectrolyte multilayers applying spin-coating or the layer-by-layer deposition technique [48]. The TIRF experiments up to 2000 bar have been carried out using a home-built high pressure cell described recently [47]. In addition, all modified surfaces have been characterized and verified by X-ray reflectometry (XRR), which probes the electron density profile of an interface [86]. Also, the secondary structures of the adsorbed enzymes were monitored by attenuated total reflection Fourier transform infrared (ATR-FTIR) spectroscopy [87]. The shape of the amide I band in a protein FTIR spectrum is sensitive to its secondary structure [44].

4.2. Experimental details

4.2.1. Proteins and chemicals

HRP was purchased from Thermo Fisher Scientific (cat. No. 01-2001), and bovine pancreas α -CT was purchased from Sigma-Aldrich (cat. No. C7762). The substrates, Amplex Red® (10-acetyl-3,7-dihydroxyphenoxazine) and Ala-Ala-Phe-7-amido-4-methylcoumarin, were obtained from Thermo Fisher Scientific (cat. No. A12222) and Sigma-Aldrich (cat. No. A3401), respectively. Aqueous NH_3 solution, aqueous H_2O_2 solution, NaN_3 , N-p-tosyl-L-phenylalanine chloromethyl ketone, poly(styrene) (PS), poly(ethyleneimine) (PEI), poly(allylamine hydrochloride) (PAH), and poly(styrene sulfonate) (PSS) were all purchased from Sigma-Aldrich.

4.2.2. Enzymatic assays

The enzymes were dissolved in 20 mM Tris base buffer solution, which is known to have a low reaction volume and low pressure sensitivity [88]. A solution of $1.25 \mu\text{g mL}^{-1}$ HRP at $\text{pH} = 7.4$ was deposited on the adsorbent surfaces for three hours at 4°C . Then, the surface was washed with buffer solution. Only irreversibly adsorbed enzyme molecules should remain. The reaction mixture contained $150 \mu\text{M}$ Amplex Red and 1 mM H_2O_2 in buffer solution at $\text{pH} = 7.4$. HRP catalyzes the oxidation of the substrate Amplex Red into the product resorufin by H_2O_2 . Because resorufin absorbs UV light and is fluorescent, it can be quantified easily. Enzyme kinetics were recorded by TIRF emission at 585 nm (excitation at 530 nm) and UV absorption at 530 nm at 25°C .

Alternatively, a solution of 0.5 mg mL^{-1} α -CT at $\text{pH} = 7.8$ was deposited on the adsorbent surfaces for three hours at $4 \text{ }^\circ\text{C}$. After washing the surface with buffer solution, the reaction mixture containing $500 \text{ }\mu\text{M}$ Ala-Ala-Phe-7-amido-4-methylcoumarin at $\text{pH} = 7.8$ was added. α -CT hydrolyzes this substrate molecule into the product 7-amino-4-methylcoumarin (7-AMC). The rate of 7-AMC formation was measured at $20 \text{ }^\circ\text{C}$ by TIRF (exc. at 380 nm , em. at 480 nm) and UV absorption at 380 nm .

4.2.3. Interfaces

The quartz prisms used for TIRF spectroscopy and XRR are made of fused silica (Corning 7980) and were obtained from Micros Präzisionsoptik (Schmiedefeld, Germany). They were cleaned in concentrated nitric acid overnight. The internal reflection elements used for ATR-FTIR spectroscopy consist of Si and have been purchased from Resultec (Illerkirchberg, Germany). They were cleaned in a 1:1:5 mixture of NH_3 (30 %), H_2O_2 (30 %) and H_2O at $70 \text{ }^\circ\text{C}$ for 15 min before modification. The bare silica surfaces of both materials were used for enzyme adsorption. Using the spin-coating technique, a thin film of PS was made on one side of the prism by simply spin-coating a 15 mg mL^{-1} PS solution in toluene at 2000 rpm . The polyelectrolyte multilayers were prepared by successive incubation with aqueous solutions (layer-by-layer) of PEI (0.01 M monomer concentration), PSS (0.01 M monomer concentration with 1 M NaCl), and PAH (0.01 M monomer concentration with 1 M NaCl). Each layer deposition was carried out for 20 min followed by intensive rinsing with pure water [48].

4.2.4. Instrumental techniques

TIRF spectroscopy was applied to determine enzymatic rates over time under different pressures and for all modified surfaces. It was carried out using the K2 fluorometer from ISS (Champaign, Illinois, USA). It was operated in photon-counting mode with a Xe arc lamp as light source. The setup of the high-pressure TIRF sample cell has already been described in detail [47] and the description can be found in section 2.2.4.. The temperature was kept constant using an external water bath.

The intensity of the fluorophores was corrected for the pressure dependence of the fluorescence quantum yield of the product (Figure 33). It was measured using an enzymatic assay with HRP or α -CT (adsorbed on quartz surface). The assay was allowed to run for about

five hours until the fluorescence intensity of the product reached a constant value, and no additional product was formed. Then, the fluorescence intensity of this assay was measured as a function of pressure. After normalization to 1 bar (Figure 33), the fluorescence intensity, $I(p)$, was used to correct the raw slope, $r_{\text{raw}}(p)$, by calculating $r(p) = r_{\text{raw}}(p)/I(p)$.

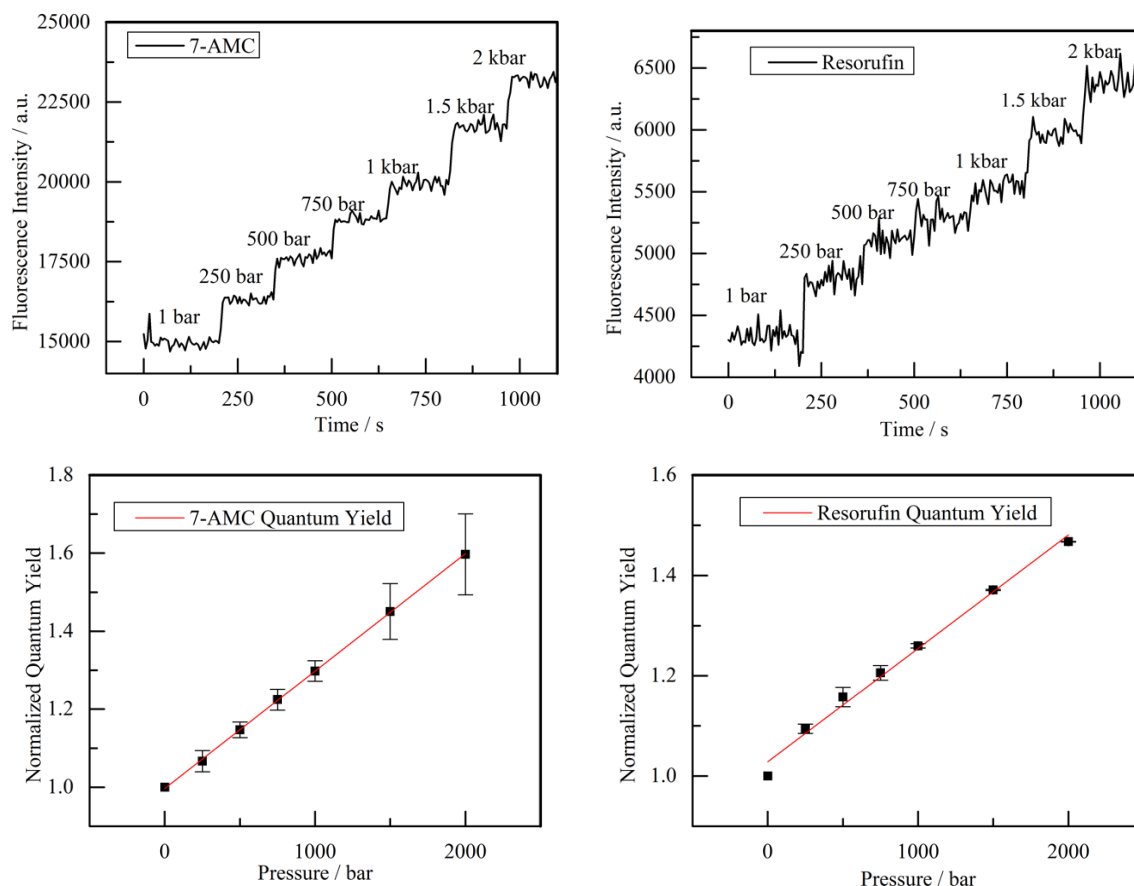


Figure 33. Pressure dependence of total internal reflection fluorescence intensity of the assay products.

The pressure dependence of the fluorescence intensity of an enzyme product has been assessed by analyzing the enzyme assay after about five hours, when the fluorescence intensity of the product has reached a constant value. This steady-state fluorescence intensity was measured as a function of pressure and was normalized to 1 bar. The error bars cover the scattering of three independent measurements.

UV-VIS absorption measurements were carried out to determine absolute enzyme activities, observing changes the concentration of the product over a given time period. The UV-1800 spectrometer from Shimadzu (Duisburg, Germany) was used.

The thickness of a polymer layer prepared on a quartz prism surface (PS film, polyelectrolyte multilayer) was estimated by XRR. The same quartz prisms used for TIRF experiments were deployed for XRR, and the surface modifications were prepared in identical

ways. The Seifert XRD 3000 TT reflectometer from GE Inspection Technologies (Ahrensburg, Germany) was used, which was operated with the Mo-K α wavelength (0.71 Å). The raw data were then converted into reflectivity curves by normalization of the reflected X-ray intensity to the incident intensity. They are scaled as a function of wavevector transfer, $Q = (4\pi/\lambda) \sin \theta$, where λ is the wavelength and θ is the angle of incidence.

ATR-FTIR spectroscopy was used to estimate potential changes of the secondary structure content of an enzyme induced by adsorption on the different chemically modified surfaces. The ATR accessory includes a water-jacketed sample cell from Pike Technologies (Madison, Wisconsin, USA), which was placed in the sample compartment of a Nicolet 6700 FTIR spectrometer from Thermo Fisher Scientific. Constant temperature of the sample is maintained by a water flow circulating through the water jacket. During all measurements, the sample was kept under D₂O solution. The measurements were performed at a spectral resolution of 2 cm⁻¹. Before enzyme immobilization on the ATR Si crystal, a background spectrum was recorded that was subtracted from the following sample spectrum. In the case of a polymer layer on the crystal, the background spectrum includes any contribution from the polymer.

4.3. Results and discussion

4.3.1. Sample characterization

The enzyme activity measurements were performed at four different aqueous-solid interfaces. The adsorbent materials were bare quartz, quartz covered with a PS film, quartz covered with a PEI-(PSS-PAH)₂-PSS multilayer, and quartz covered with a PEI-(PSS-PAH)₂-PSS-PAH multilayer. In this way, a polar (bare quartz), a hydrophobic (PS film), a negatively charged (PSS ending multilayer), and a positively charged (PAH ending multilayer) surface have been prepared. HRP has a net charge of about 0 at neutral pH-values [62,88], whereas α -CT has a small positive net charge at neutral pH-values due to an isoelectric point at pH = 9 [63,64].

The successful preparation of the polymer layers on the quartz prisms was checked at the air by XRR (Figure 34). Kiessig fringes can be observed in all cases, which result from the interference of the X-ray beams reflected at the air-polymer interface and the polymer-quartz interface. There is a simple relation between the width of the Kiessig fringes, ΔQ , and the total thickness of the polymer layer, d , given as [86]:

$$\Delta Q = \frac{2\pi}{d}$$

In the case of a PS film, a thickness of about 590 Å has been determined using equation above. The PSS ending multilayer has about 140 Å of thickness (23 Å per layer), and the PAH ending multilayer has about 170 Å of thickness (24 Å per layer), as measured in the dry state at the air (Figure 34). These values were reproduced within ± 10 Å from 4 independent measurements and are similar to literature values [90]. Therefore, the surface modifications appear to be successful.

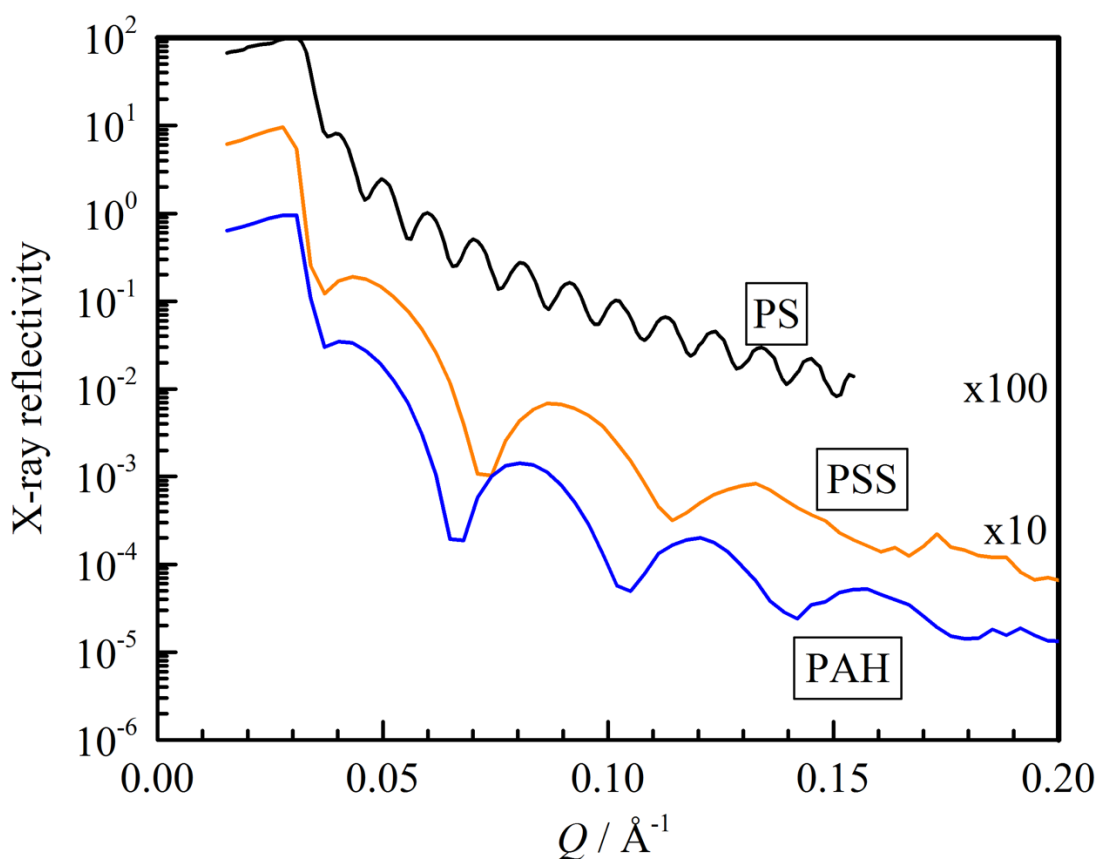


Figure 34. X-ray reflectivity of quartz surfaces modified with a PS film and polyelectrolyte multilayers ending with PSS and PAH. The data were recorded at the air.

Furthermore, the secondary structure of α -CT and HRP, adsorbed at the aqueous-solid interfaces mentioned above, was investigated by following changes of the amide I' band collected using the ATR-FTIR technique (*performed by Süleyman Cinar*). The amide I' band (the prime indicates D₂O as the solvent) of proteins in the infrared spectrum between 1700 –

1600 cm^{-1} is mainly related to the C=O stretching mode of the peptide bonds. The exact wavenumber of this mode depends on the type of secondary structure the peptide bonds are involved in [44]. Thus, the shape of the amide I' band is sensitive to the overall secondary structure content of protein molecules under a specific condition.

As seen in figure 35, both α -CT and HRP essentially retain their secondary structures at all aqueous-solid interfaces studied here, as judged from the maximum wavenumber and the shape of the amide I' band of these enzymes. The FTIR spectra shown in figure 35 were obtained in transmission mode in the case of the free enzymes and in ATR mode in the case of the adsorbed enzymes. The aqueous-solid interfaces were incubated with the enzyme solutions for 20 min followed by rinsing with Tris buffer solution. Thus, only irreversibly adsorbed enzyme molecules are detected. Unfortunately, in the case of HRP, the degree of adsorption is rather low leading to a low signal-to-noise ratio. However, the preservation of native secondary structure of proteins upon adsorption at aqueous-solid interfaces has already been reported before. For example, it has been observed that α -CT, HRP, lysozyme and ribonuclease A do not change their secondary structures upon adsorption on silica particles [91,92]. It is interesting to note that even the hydrophobic PS surface does not induce major changes on the secondary structures of α -CT and HRP (Figure 35), whereas polyelectrolyte multilayers are known to maintain the structure and activity of adsorbed and embedded protein molecules in many cases [50,82,83,93].

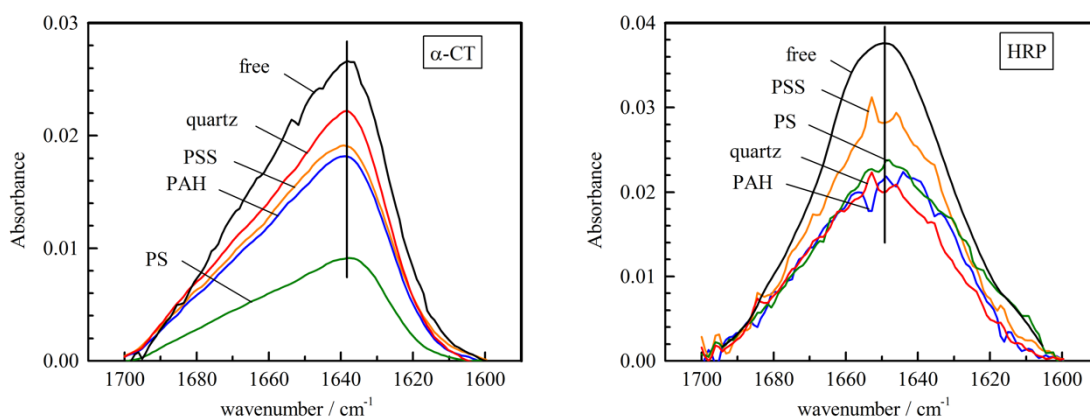


Figure 35. Amide I' bands of α -CT and HRP, recorded both free in solution and irreversibly adsorbed at various aqueous-solid interfaces (performed by Süleyman Cinar). Samples were analyzed in D_2O pD = 7, at 1 bar and 25°C. The vertical lines indicate the maximum wavenumbers of the free enzymes in solution.

4.3.2. Enzyme activities at different interfaces

Absolute activities of α -CT and HRP irreversibly adsorbed on quartz, a PS film, a PSS and a PAH ending multilayer were determined by incubation of these surfaces with 600 μ L enzyme-free reaction mixture containing the substrate. After 250 s at 1 bar and 25 °C, the inhibitor NaN₃ for HRP or N-p-tosyl-L-phenylalanine chloromethyl ketone for α -CT was added to stop the enzymatic reaction, and the concentration of the formed product was measured by UV spectroscopy. All observed UV absorbance are listed in table 1.

	Quartz	PS	PSS	PAH
α -CT ^a	1.00 \pm 0.07	0.61 \pm 0.08	0.92 \pm 0.08	0.57 \pm 0.07
HRP ^b	1.00 \pm 0.15	1.40 \pm 0.22	0.89 \pm 0.25	0.95 \pm 0.17

^a Wavelength used to detect AMC was 380 nm.

^b Wavelength used to detect resorufin was 530 nm.

Table 1. Activities of α -CT and HRP adsorbed on quartz, a PS film, a PSS and a PAH ending multilayers.

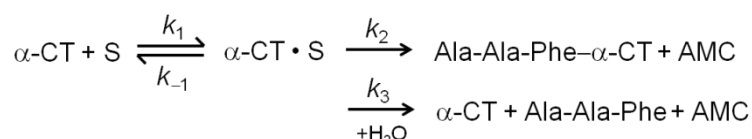
Each data represents the concentration of product formed in a 600 μ L enzyme-free reaction mixture that is in contact with the interface over 250 s at 1 bar and 25 °C. The data were obtained by UV absorption measurements and normalized to the value of the water–quartz interface. Each error is calculated from four independent measurements.

As seen in table 1, α -CT activity is highest on quartz and a PSS ending multilayer, which are both hydrophilic and negatively charged. In contrast, maximum HRP activity is found on a hydrophobic PS film. Generally, the values listed in table 1 depend on a series of issues. High values are expected, if there is a high degree of enzyme adsorption, a low degree of denaturation, little dynamic restrictions and little blocking of the active site by neighboring enzyme molecules or the interface. From the ATR-FTIR spectra shown in figure 35, it is suggested that the reduced activity of α -CT on a PS surface could be explained by the reduced degree of adsorption. Furthermore, it has been observed that α -CT can be activated by polyelectrolytes that are oppositely charged to the substrate [57]. Here, we use a positively charged substrate molecule, Ala-Ala-Phe-7-amido-4-methylcoumarin, which is partially protonated at the NH₂ and NH groups. In agreement with that study [57], the enzymatic activity is smaller on positively charged PAH as compared to negatively charged PSS (Table 1). Moreover, it has also been reported that α -CT activity is four times higher on a negatively

charged polyelectrolyte multilayer than on a positively charged polyelectrolyte multilayer [94], which is also in good agreement with our results (Table 1). In the case of HRP, the degree of adsorption on the various surfaces seems to be similar, as can be estimated from the ATR-FTIR spectra in figure 35. Thus, the enhanced activity of HRP on a PS surface is probably related to lowered activation energy due to interactions with the PS surface.

4.3.3. Activation volume of α -CT

α -CT hydrolyzes peptide bonds, preferentially those formed by aromatic amino acids [27]. After the binding of the substrate molecule, which is Ala-Ala-Phe-7-amido-4-methylcoumarin in this study, the cleavage of the peptide bond and the product release, which is the fluorescent 7-AMC, can be described by Michaelis-Menten mechanism [54]:



Assuming that the adsorbed α -CT molecules are saturated by the substrate molecules, S, which are present in a relatively high concentration (500 μM), the rate of the enzymatic reaction is determined by step 2 and step 3. The turnover number can be expressed by the equation $k_{\text{cat}} = k_2 k_3 / (k_2 + k_3)$ [54]. It has been proposed that k_2 is small and rate-limiting ($k_{\text{cat}} \approx k_2$) for a peptide hydrolysis, as studied here, whereas k_3 is small and rate-limiting for an ester hydrolysis [27]. Therefore, the ΔV^\ddagger -values of α -CT, as reported in this study, can refer to step 2 in the reaction scheme, where the enzyme is acylated (Ala-Ala-Phe- α -CT) and 7-AMC is released. In the case of $[\text{S}] < K_M$, ΔV^\ddagger is the difference between the volumes of the transition state, V_{ES^\ddagger} , and the reagents, $V_{\text{E+S}}$.

The formation of 7-AMC was recorded by TIRF spectroscopy here. The analysis of the fluorescence signal to extract an activation volume followed the procedure described recently [91]. Briefly, any fluorescence intensity is proportional to the fluorophore concentration, c . Thus, the rate of product formation, dc/dt , is proportional (not equal) to the slope of the fluorescence intensity that is plotted as a function of time (Figure 36).

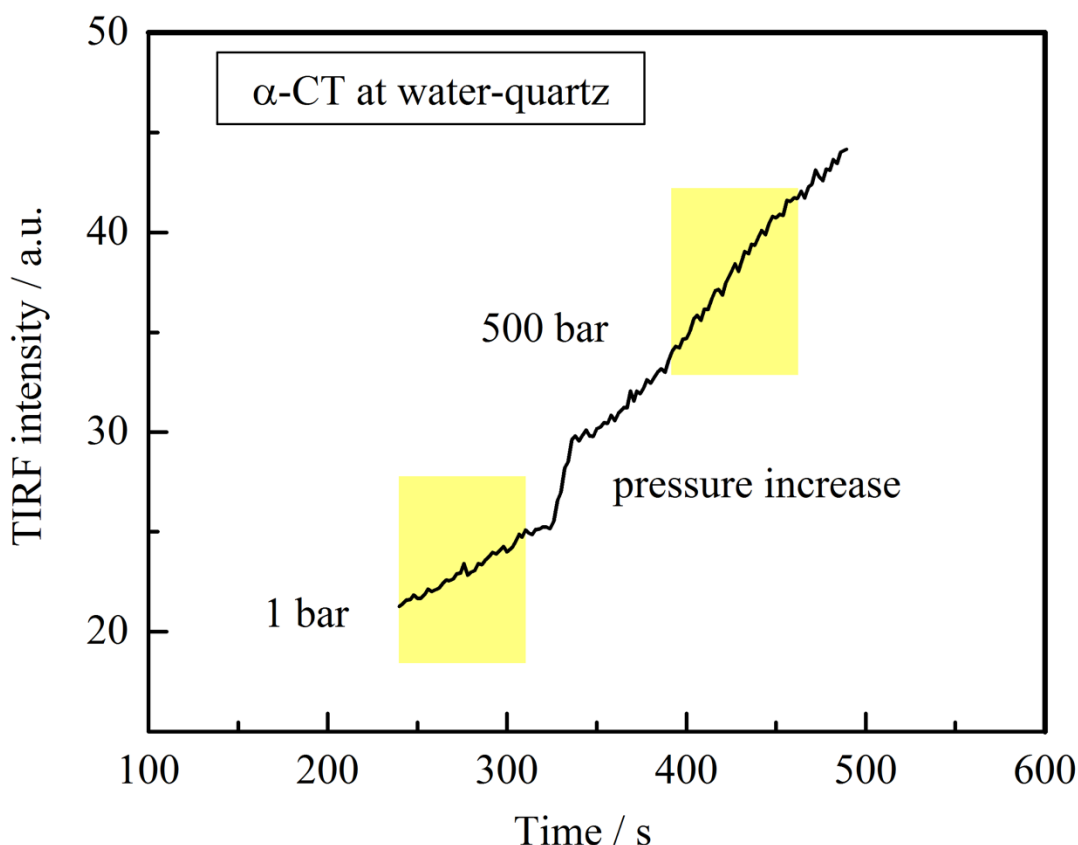


Figure 36. Total internal reflection fluorescence intensity as a function of time showing enzymatic activity of α -CT at water-quartz interface (typical data). The fluorescence intensity has been measured at 1 bar and after pressure increase. The slope of the data is proportional to the rate of the enzymatic reaction. The slopes before and after the pressure increase have been determined by fits over the highlighted time intervals.

To remove all instrumental factors affecting the fluorescence intensity, the slope observed under pressure, r , has been normalized to the slope observed under ambient pressure, r_0 . Each enzymatic assay started with a few minutes of data collection at 1 bar followed by a 1–2 min period, during which the pressure has been increased, and a further time period under high pressure. The slope at 1 bar, r_0 , was always constant and has been determined by a linear fit. The slope under high pressure, r , has often been observed to be unstable immediately after the pressure increase, which might indicate a structural relaxation of the enzyme. Thus, we left a time interval of 1 min after pressure increase before evaluating the slope, r . The ratio of the slopes measured before and after the pressure change can be related to the ratio of the corresponding rate constants:

$$\frac{r}{r_0} = \frac{k}{k_0}$$

So, the activation volume can be calculated by,

$$\left(\frac{\partial \ln(r/r_0)}{\partial p}\right)_T = -\frac{\Delta V^\ddagger}{RT}$$

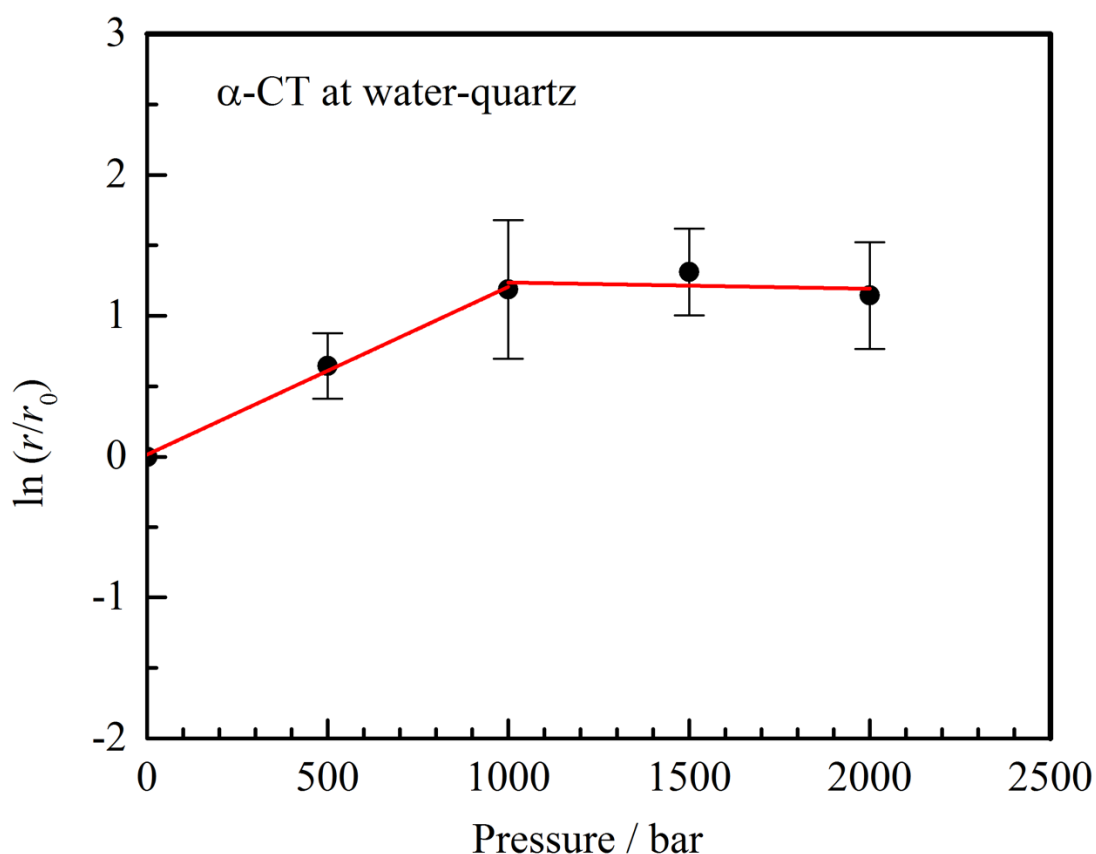


Figure 37. α -CT pressure dependent enzymatic activity when adsorbed on quartz. r is the rate of product formation under pressure, and r_0 is the rate at 1 bar. The data were obtained by high-pressure TIRF spectroscopy. Error bars cover the scattering of two measurements at 500 bar, three at 1000 bar, four at 1500 bar.

In figures 37-40, plots of $\ln(r/r_0)$ as a function of pressure, p , are given for α -CT adsorbed on bare quartz, a PS film, a PSS ending multilayer and a PAH ending multilayer under aqueous solution. Apparently, in the case of the water-quartz interface (Figure 37), the pressure dependence of adsorbed α -CT enzymatic activity was not constant. This finding is in favorable agreement with previous studies of α -CT free in solution and adsorbed on negatively charged silica particles [91]. Below 1000 bar, pressure strongly activates α -CT on planar quartz (Figure 37). A negative activation volume of $\Delta V^\ddagger = -29 \text{ mL mol}^{-1}$ was obtained from a linear fit in this lower pressure range. In contrast, no pressure dependence of α -CT enzymatic activity on planar quartz was detected at 1000 – 2000 bar (Figure 37). Generally,

there is no reason to assume that the activation volume of an enzyme is constant and thus independent of pressure. As mentioned above, the activation volume is the difference of the volumes of the transition state and the enzyme-substrate mixture, $\Delta V^\ddagger = V_{ES^\ddagger} - V_{E+S}$. If these two states have different compressibility, then ΔV^\ddagger is pressure dependent. As concluded before, the enzyme-substrate mixture seems to be more compressible than the transition state of α -CT in solution and adsorbed on silica [91]. It was observed that the reduced pressure dependence of α -CT activity at the water-quartz interface above 1000 bar (Figure 37) could not be explained by a reduced degree of α -CT adsorption, because a reduced pressure dependence was also observed for non-adsorbed α -CT [91]. Furthermore, the degree of protein adsorption at the silica-water interface has been found to increase with pressure [95].

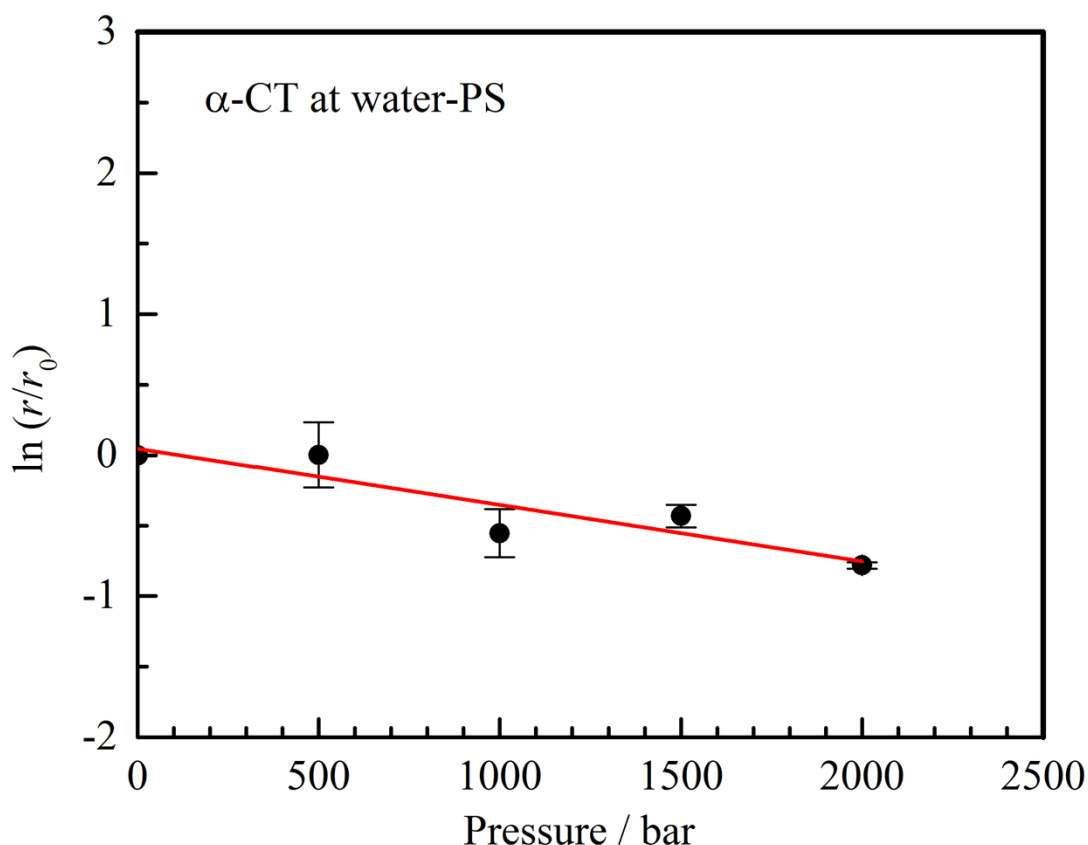


Figure 38. α -CT pressure dependent enzymatic activity when adsorbed on PS film. r is the rate of product formation under pressure, and r_0 is the rate at 1 bar. The data were obtained by high-pressure TIRF spectroscopy. Error bars cover the scattering of at least two independent measurements.

The effect of pressure on the enzymatic activity of α -CT adsorbed on water-PS interface is very different from α -CT activity when adsorbed at the water-quartz interface (Figure 38). Within the experimental errors, a linear fit over the whole studied pressure range

yields a positive activation volume of $+10 \text{ mL mol}^{-1}$, indicating that pressure inactivates α -CT when adsorbed on hydrophobic PS.

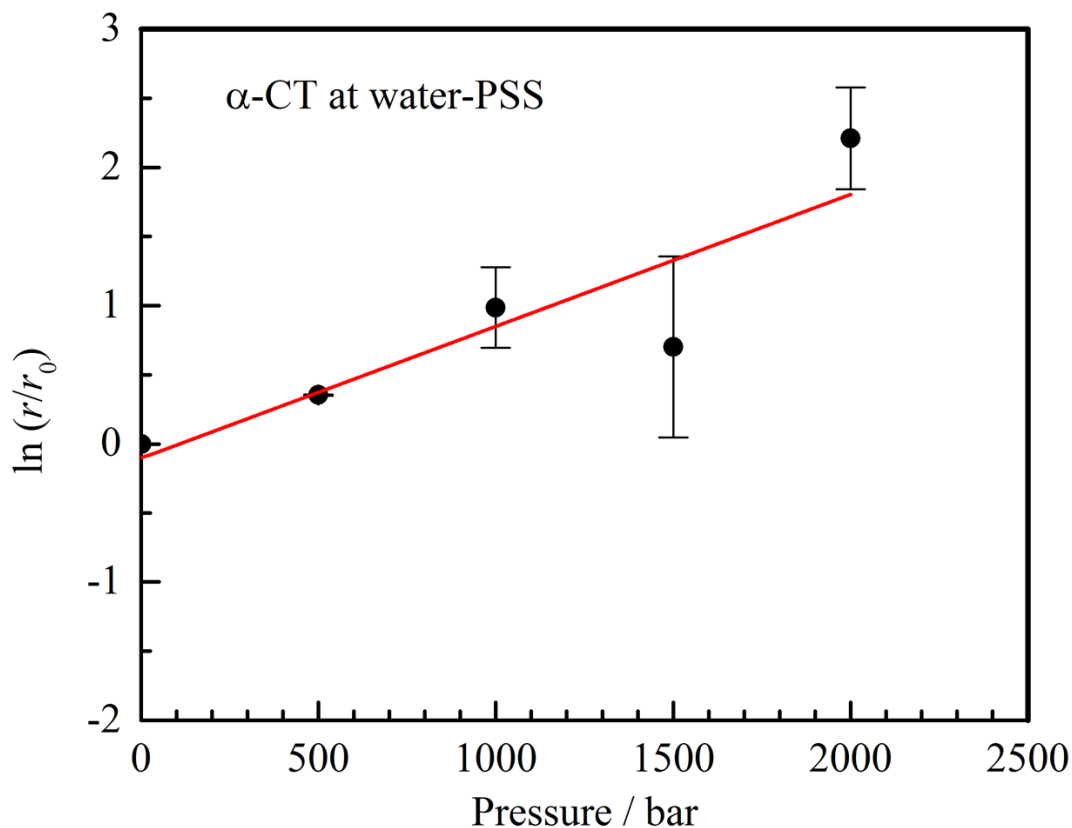


Figure 39. α -CT pressure dependent enzymatic activity when adsorbed on PSS ending multilayers. r is the rate of product formation under pressure, and r_0 is the rate at 1 bar. The data were obtained by high-pressure TIRF spectroscopy. Error bars cover the scattering of at least two independent measurements.

It is also interesting to compare the pressure effects on the activity of α -CT, when adsorbed on the negatively charged water-PSS interface (Figure 39) or the positively charged water-PAH interface (Figure 40). Whereas a positive slope of $\ln(r/r_0)$ vs. pressure could be observed in the case of the water-PSS interface, virtually no pressure effect was found in the case of the water-PAH interface (Figure 40). Again, within the experimental errors, constant activation volumes are consistent with both plots. The activation volume of α -CT on PSS is -23 mL mol^{-1} , very similar to that found on quartz (Figure 37).

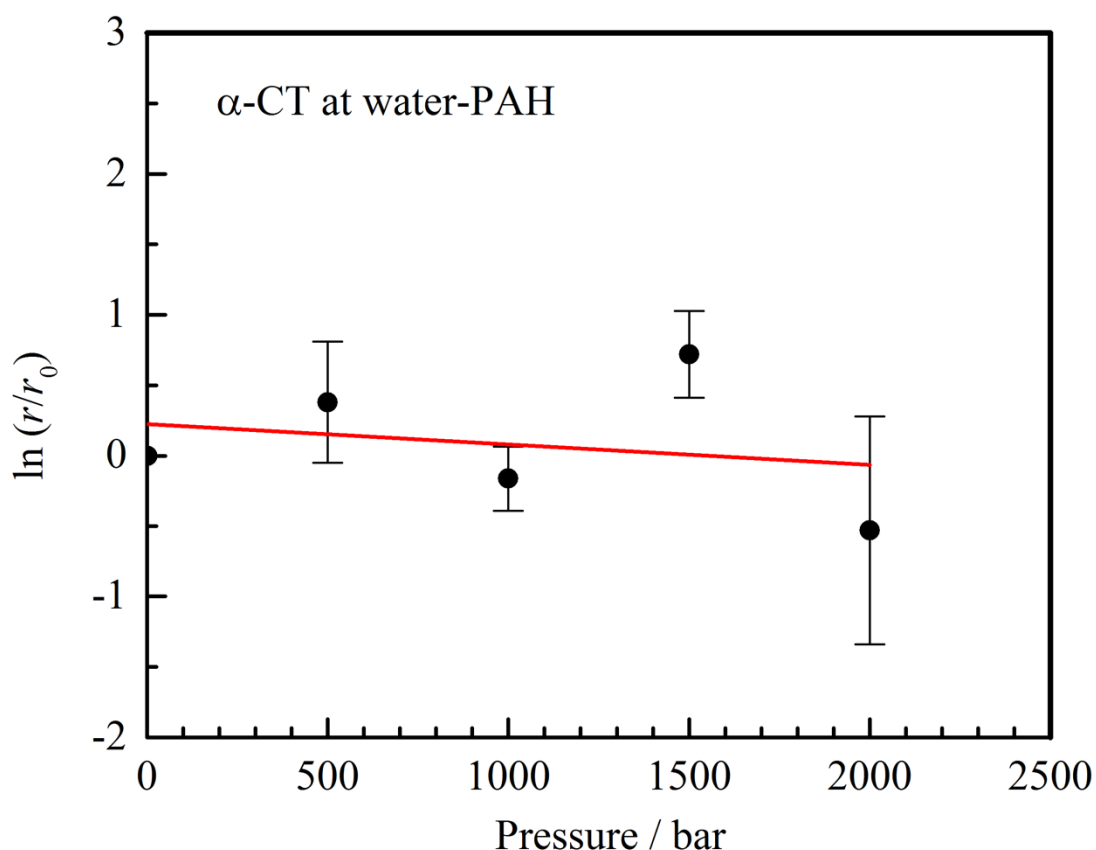


Figure 40. α -CT pressure dependent enzymatic activity when adsorbed on PAH ending multilayers. r is the rate of product formation under pressure, and r_0 is the rate at 1 bar. The data were obtained by high-pressure TIRF spectroscopy. Error bars cover the scattering of at least two independent measurements.

All data in figures 37-40 suggest that α -CT can be activated by pressure, when it is adsorbed on a negatively charged surface like quartz and PSS. However, α -CT was also activated by pressure, when it was free in aqueous solution, where negative activation volumes of -67 mL mol^{-1} below 500 bar and -15 mL mol^{-1} at 500 – 2000 bar were reported [91]. Similarly, Mozhaev *et al.* have found values of about -10 mL mol^{-1} at 20 °C and -25 mL mol^{-1} at 50 °C for free α -CT [25]. Thus, a negatively charged adsorbent surface seems to have less impact on the stereochemistry of the transition state of step 2 in the mechanism of α -CT catalysis than a positively charged or a hydrophobic adsorbent surface.

In general, an increase of the activation volume can easily be explained by a small distortion of the active site due to adsorption of the enzyme. When small void volumes in the transition state are generated that cannot accommodate a water molecule (18 mL mol^{-1}), then V_{ES^*} and ΔV^\ddagger will increase. Another reason for an increased activation volume could be restricted dynamics of the active site due to immobilization of the enzyme at the interface.

When 7-AMC leaves the active site, water molecules must enter. This replacement requires some intermediate void volume, when the active site is rather rigid. Indeed, strong hydrophobic interactions between a PS surface and α -CT could induce a small distortion and restricted dynamics of the active site, which is consistent with the most positive activation volume of α -CT observed in this study.

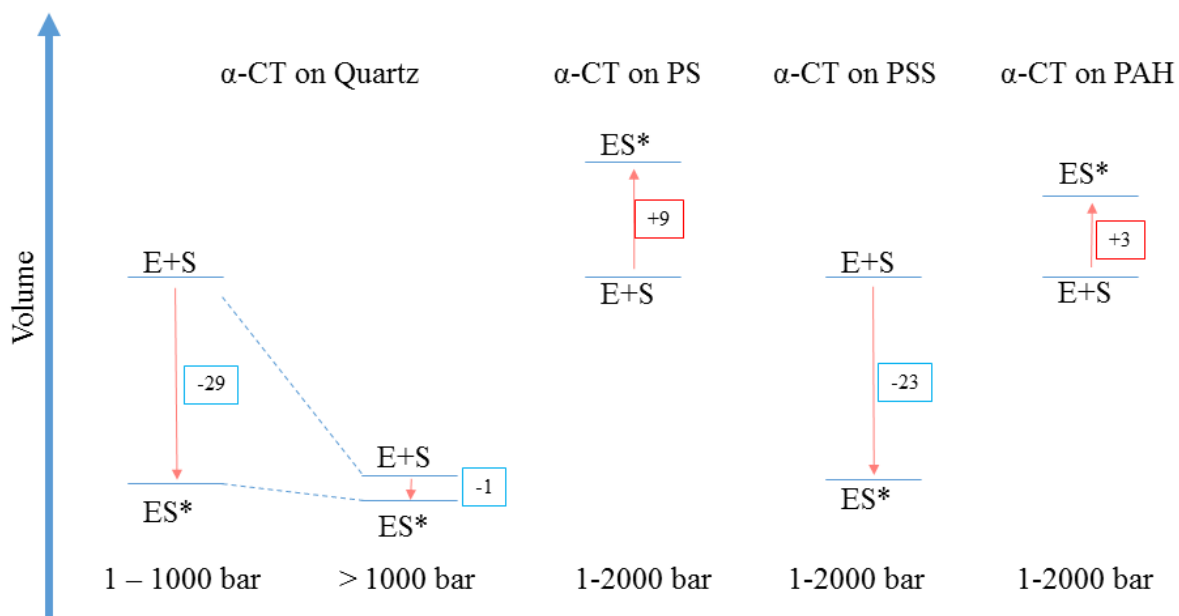


Figure 41. Activation volumes of α -CT adsorbed on quartz, a PS film, a PSS ending and a PAH ending multilayer (not to scale, ΔV^\ddagger given in mL mol^{-1}). The activation volume depends on the pressure and on the surface chemistry.

4.3.4. Activation volume of HRP

Besides α -CT, we have also studied horseradish peroxidase (HRP). A peroxidase is an enzyme that catalyzes the oxidation of a substrate by H_2O_2 . HRP binds heme as prosthetic group. The mechanism of catalysis is rather complex and can be summarized in the scheme of section 3.3.3 in this present work [30,32]. In the enzymatic assay, relatively high concentrations of H_2O_2 (1 mM) and Amplex Red® (150 μM) and a very low concentration of HRP (1.25 $\mu\text{g mL}^{-1}$) were used to incubate the adsorbent surface. The rate-limiting steps are probably the successive transfers of two electrons from the Amplex Red molecule to the heme. There is some evidence from single molecule fluorescence experiments that there is a distribution of conformations and a breathing motion of the active site of HRP, when the bonded substrate is converted into product [73].

HRP has been adsorbed on bare quartz, a PS film, a PSS and a PAH ending multilayer. After rinsing with buffer solution and adding reaction mixture, the product formation, resorufin, was detected by TIRF spectroscopy at 1 bar and under high pressures. The analysis of the time-dependent fluorescence intensity in terms of the slopes at 1 bar, r_0 , and at elevated pressure, r , has been carried out in the same way as described above for α -CT.

In figures 42-45, plots of $\ln(r/r_0)$ as a function of pressure, p , are given for HRP adsorbed at these four different interfaces.

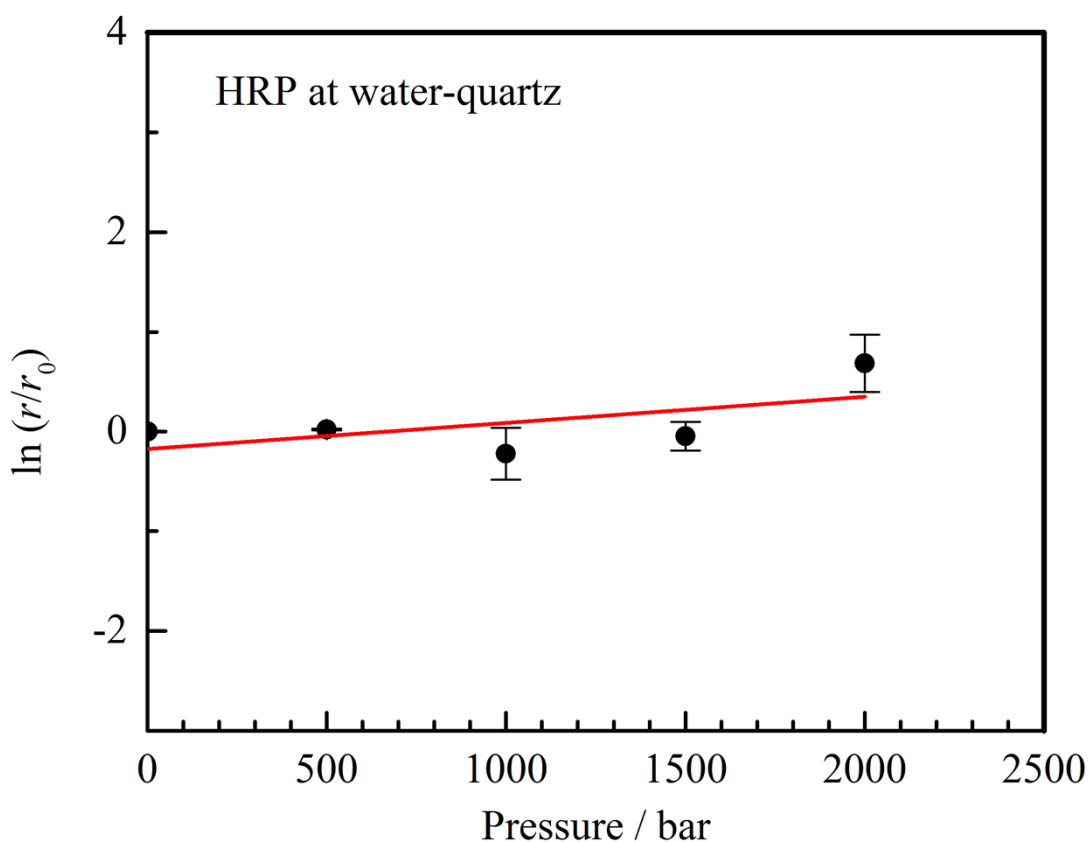


Figure 42. HRP pressure dependent enzymatic activity when adsorbed on quartz. r is the rate of product formation under pressure, and r_0 is the rate at 1 bar. The data were obtained by high-pressure TIRF spectroscopy. Error bars cover the scattering of two independent measurements.

In the case of HRP at the water-quartz interface, there is no significant pressure dependence of the rate of product formation up to 1500 bar (Figure 42). This observation is very similar to the behavior found earlier for HRP adsorbed on silica particles, where a very small activation volume of about $+2 \text{ mL mol}^{-1}$ has been found in the pressure range of 250 – 1500 bar [91].

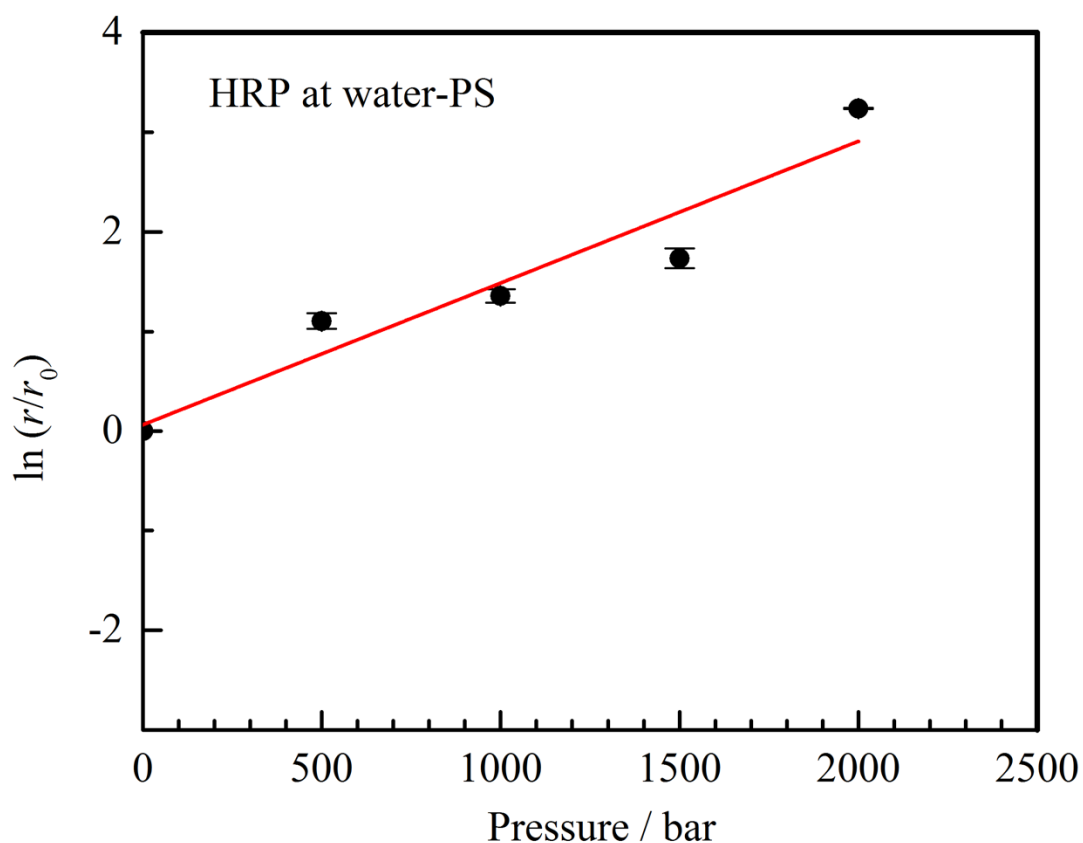


Figure 43. HRP pressure dependent enzymatic activity when adsorbed on PS film. r is the rate of product formation under pressure, and r_0 is the rate at 1 bar. The data were obtained by high-pressure TIRF spectroscopy. Error bars cover the scattering of two independent measurements.

Remarkably, when HRP is adsorbed on a hydrophobic PS film, application of pressure leads to a strong activation of this enzyme (Figure 43). From a linear fit in the pressure range of 1 – 2000 bar, a negative activation volume of -35 mL mol^{-1} was determined. So far, pressure inactivation has been reported for HRP in solution. Thus, immobilization of HRP on PS can reverse this pressure effect.

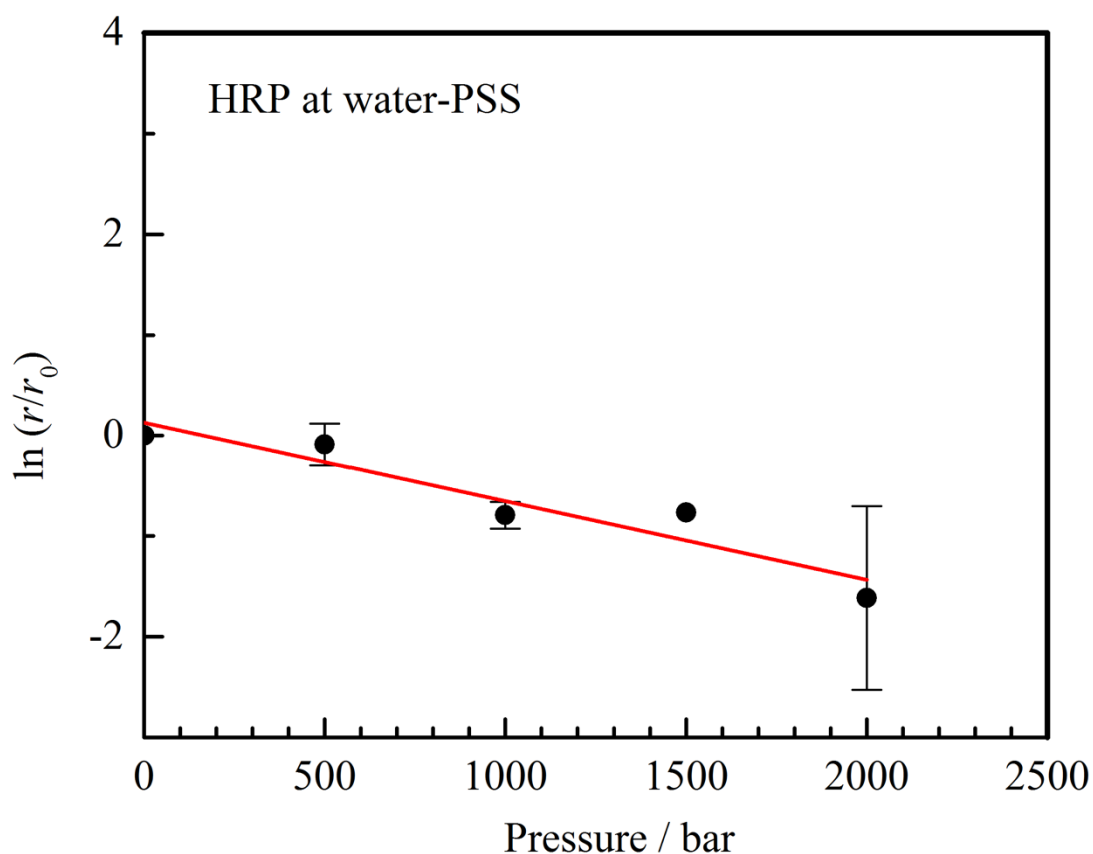


Figure 44. HRP pressure dependent enzymatic activity when adsorbed on PSS ending multilayers. r is the rate of product formation under pressure, and r_0 is the rate at 1 bar. The data were obtained by high-pressure TIRF spectroscopy. Error bars cover the scattering of two independent measurements.

In contrast, when HRP is adsorbed on charged hydrophilic polyelectrolyte multilayers, pressure always inhibits the enzymatic activity, regardless of the sign of the charges. Positive activation volumes of $+19 \text{ mL mol}^{-1}$ on PSS (Figure 44) and $+16 \text{ mL mol}^{-1}$ on PAH (Figure 45) ending multilayers were deduced from linear fits.

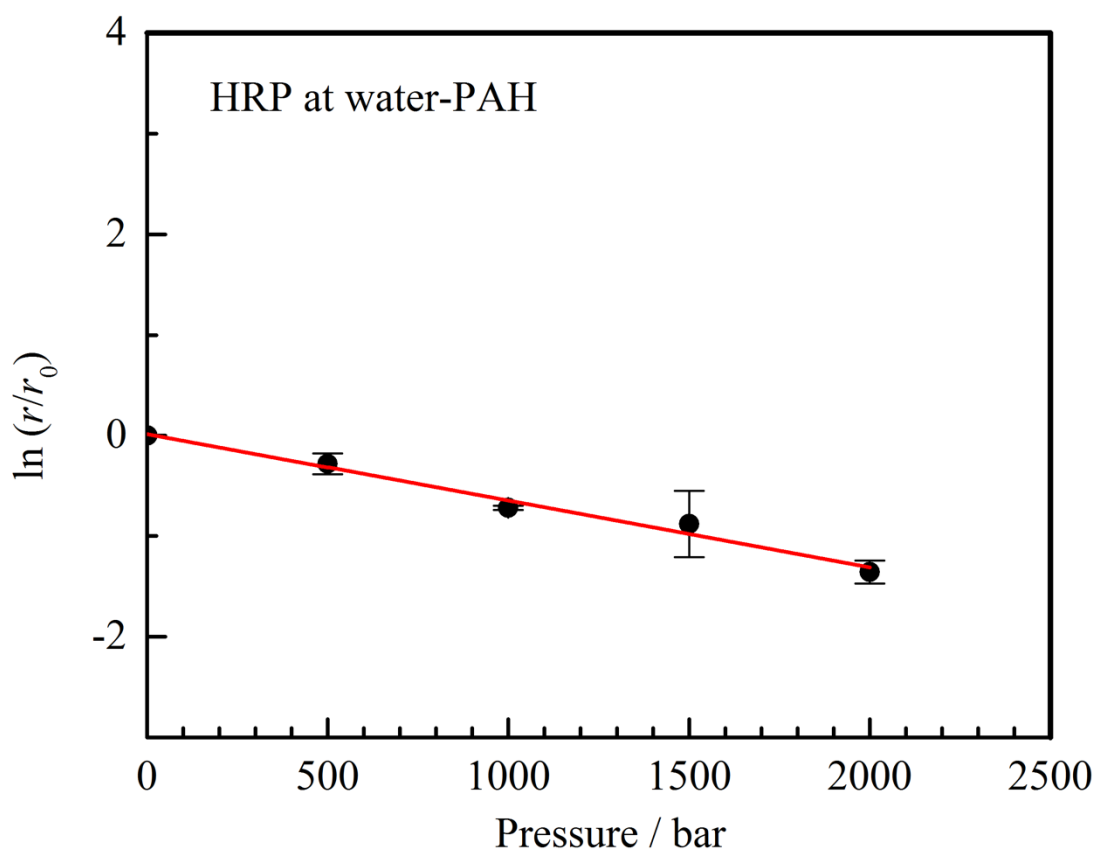


Figure 45. HRP pressure dependent enzymatic activity when adsorbed PAH ending multilayers. r is the rate of product formation under pressure, and r_0 is the rate at 1 bar. The data were obtained by high-pressure TIRF spectroscopy. Error bars cover the scattering of two independent measurements.

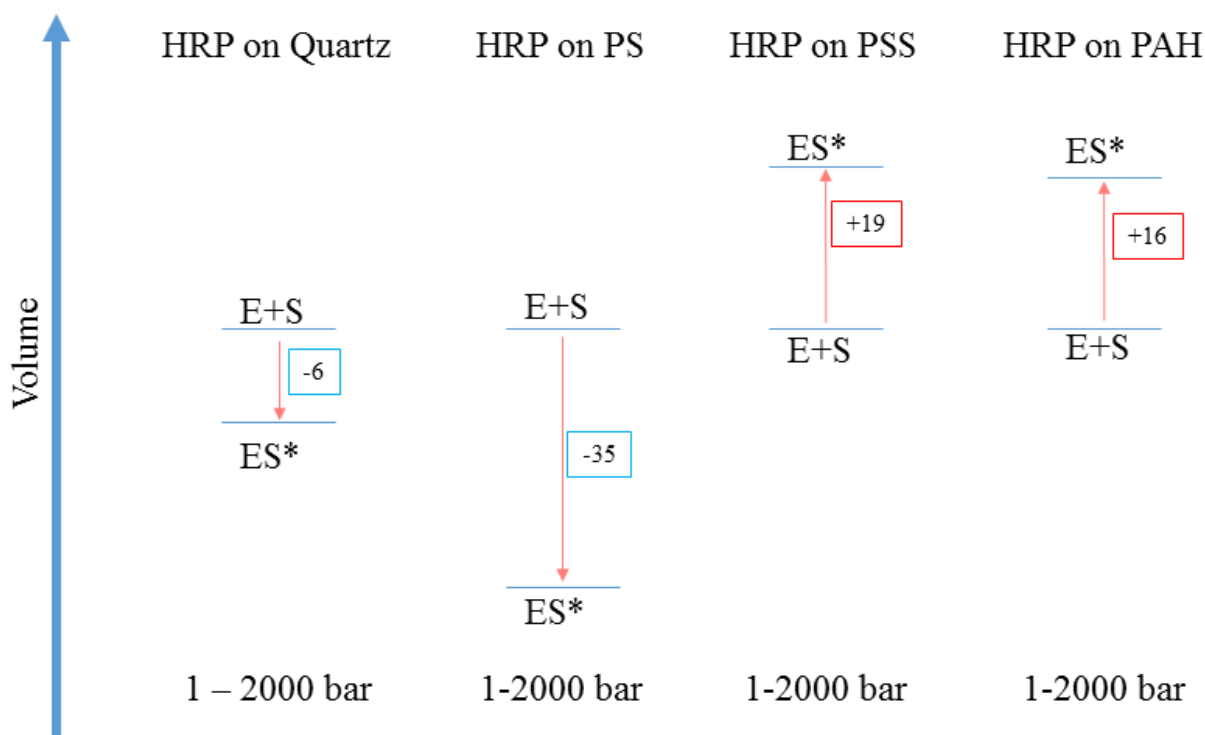


Figure 46. Activation volumes of HRP adsorbed on quartz, a PS film, a PSS ending and a PAH ending multilayer (not to scale, ΔV^\ddagger given in mL mol^{-1}). The activation volume depends on the surface chemistry.

Remarkably, the activation volume of both enzymes, α -CT and HRP, strongly depends on the kind of interface used for immobilization (Figure 41 and 46). In contrast to α -CT, where a hydrophilic negatively charged environment enables pressure-induced enzyme activation, HRP activity is enhanced by pressure at a hydrophobic surface. At this point, we cannot give any molecular details about the origin of these findings. However, in the case of α -CT, a more positive activation volume at all interfaces studied can be observed as compared to that found in solution, which can be explained by a distortion or restricted dynamics of the active site at an interface, as outlined above. In the case of HRP, the activation volume decreases upon adsorption at the water-PS interface. This opposite behavior could be explained by an increased volume of the enzyme relative to that of the transition state, V_{ES^*} , thereby making the activation volume $\Delta V^\ddagger = V_{\text{ES}^*} - V_{\text{E+S}}$ more negative.

It is interesting to see that negative activation volumes of α -CT and HRP were observed at the same interfaces that showed larger activities at 1 bar (Table 1, Figure 41 and 46). It is not straightforward to explain this observation. The activation free energy, ΔG^\ddagger , can be decomposed into the activation energy, ΔU^\ddagger , the activation volume, ΔV^\ddagger , and the activation entropy, ΔS^\ddagger :

$$\Delta G^\# = \Delta U^\# + p\Delta V^\# - T\Delta S$$

If $\Delta V^\#$ is small or even negative, then $\Delta G^\#$ is reduced. At 1 bar, a negative activation volume of -18 mL mol^{-1} (size of a water molecule) contributes $p\Delta V^\# = -1.8 \text{ J mol}^{-1}$ to $\Delta G^\#$, which can be neglected. Only at high pressures, $p\Delta V^\#$ becomes significant. For example, at 1000 bar and 298 K, the rate constant increases by a factor of two due to a small negative activation volume of -18 mL mol^{-1} . Thus, there are no simple thermodynamic arguments relating a negative activation volume to fast enzyme kinetics at 1 bar. However, a negative activation volume indicates a tight packing of the reaction components in the transition state. This allows for strong favorable interactions that might be responsible in part for small activation energies, i.e. fast enzymatic reactions at 1 bar.

4.4. Conclusions

The enzymatic activities and activation volumes of α -CT and HRP were successfully measured at four different aqueous-solid interfaces (polar, non-polar, negatively and positively charged). For both enzymes, the activation volume is strongly dependent on the kind of interface used for immobilization.

In the case of HRP, even a negative activation volume and a corresponding pressure activation of the enzyme has been found on a hydrophobic PS surface, in contrast to free HRP, which is deactivated by pressure [91].

α -CT, when adsorbed on planar quartz, shows a similar pressure-dependence of its activity as α -CT on silica particles [91]. According to the results of this study, a negative activation volume of α -CT seems to be associated with negatively charged hydrophilic surfaces, as those of silica particles, quartz and PSS. Moreover, large enzymatic activities were measured at interfaces where negative activation volumes were observed.

At this point, mechanistic details of the enzymatic reactions at the various interfaces cannot be given on the molecular level. However, pressure could be a useful tool to enhance enzymatic activity by choosing the right interfacial properties for enzyme immobilization.

**5. Advantages of adsorbing
 α -CT on silica nanoparticles
- A high-pressure stopped-
flow study**

5.1. Background

As seen in chapter 3 and 4, pressure can enhance the activity of adsorbed enzymes due to negative activation volumes [91]. Also, the chemistry of the adsorbent surface plays an important role in the activation volume profile [40]. Taking the example of α -CT on quartz and on PSS-ending polyelectrolyte multilayers, both are negatively charged surfaces, it was demonstrated that the activation volume is negative [40], as found on silica nanoparticles Ludox AM [91]. All these measurements were done with fluorescence spectroscopy techniques, such as high pressure fluorescence, used in chapter 3, and high pressure TIRF, used in chapter 4. Both fluorescence techniques have a dead time of 4-5 minutes, due to the high pressure cell assembling. In order to follow the enzymatic activity from its very beginning, the stopped-flow technique was used in this work.

Stopped-flow experiments have proven to be a very powerful method to follow enzymatic reactions over the very first seconds [96]. As explained in section 2.2.7., the stopped-flow equipment can mix the enzyme and substrate solutions in the observation chamber and record the data immediately, with very few seconds of delay and a resolution on the order of ms. In this chapter, the stopped-flow technique was used as a different approach to monitor the activity of free and adsorbed enzymes. The activity of α -CT, free and adsorbed on Ludox AM, was analyzed using the same Ala-Ala-Phe-7-AMC substrate mentioned in chapter 4. However, the release of the product, 7-AMC, was followed using UV-VIS absorbance at 370 nm as a function of time.

The stopped-flow equipment used in this work was a high pressure stopped-flow instrument (HP-SF). The entire stopped-flow system is built inside a high-pressure autoclave and it allows kinetics up to 2000 bar. The HP-SF system brought additional and important information to this study. It pressurizes the samples before mixing, in contrast to the experiments in chapters 3 and 4, where samples ran for some time at 1 bar and were then pressurized while already mixed. When pressurizing the enzyme and substrate solutions before mixing, the molecules adopt new thermodynamic and conformational states, and later they are mixed in the observation chamber. Besides that, this equipment recorded the α -CT kinetics using the UV-VIS absorbance, and for the first time the activation volume was calculated from an absolute scale method.

It has been shown in the literature, that trypsin is adsorbed on mesoporous silica. After 20 days 70% of initial native state retained in contrast to the solution where 45% retained due to autolysis [97]. These findings strongly suggest that α -CT, as well as other proteases, could be

protected from autolysis by simply adsorbing the proteases on a surface, and this would also create conditions for recycling this enzyme for several reaction cycles. Therefore, the autolysis activity of free vs adsorbed α -CT as a function of time was also analyzed in this work by polyacrylamide gel electrophoresis (PAGE).

5.2. Experimental details

5.2.1. Proteins and chemicals

Bovine pancreas α -CT (cat. No. C7762), the substrate Ala-Ala-Phe-7-amido-4-methylcoumarin (cat. No. A3401), and Ludox AM colloidal silica particles (cat. No. 420875) were purchased from Sigma-Aldrich. The SDS-PAGE silver staining kit, PlusOne™ Silver Staining kit for proteins, was purchased from GE Healthcare (cat. No. 17-1150-01).

5.2.2. Enzymatic assays

The calculus of the surface area coverage of the silica particles followed the description in chapter 3 and was adapted for this work as can be seen below:

Ludox AM: 100 μL of a 1.31 g mL^{-1} solution. From the density of 1.31 g mL^{-1} and the surface area of 220 $\text{m}^2 \text{g}^{-1}$, a surface area of 28,8 m^2 in 100 μL solution of silica particles can be calculated (1:11).

α -CT: molar mass of 25000 g mol^{-1} that corresponds to a mean radius of $r = 1.9 \text{ nm}$ using a specific volume of 0.7 $\text{cm}^3 \text{g}^{-1}$. From this radius, a footprint area of $\pi r^2 = 1.1 \cdot 10^{-17} \text{ m}^2$ per molecule can be estimated. Covering 1% of Ludox AM area, 1100 μL solution (1:11 Ludox AM:Buffer) will permit the use of 0.73 mg of protein, which is 26,5 μM , in a volume of 1100 μL .

UV-VIS absorption measurements of α -CT were carried out to determine absolute enzyme activities as a function of substrate concentration. This was done to estimate the kinetic parameters of α -CT free and adsorbed on Ludox AM. A UV-1800 spectrometer from Shimadzu (Duisburg, Germany) was used.

To determine the Michaelis-Menten constant, K_M , of α -CT for Ala-Ala-Phe-7-AMC, stock solutions of 123.75 mM Ala-Ala-Phe-7-AMC and 1 mg mL^{-1} α -CT were prepared. The concentrations of Ala-Ala-Phe-7-AMC tested were 5 μM , 25 μM , 50 μM , 75 μM , 100 μM ,

300 μ M, 500 μ M, 1000 μ M and 1500 μ M with a final enzyme concentration of 0.05 mg mL⁻¹. The reaction buffer used was 20 mM TRIS-HCl (pH 7.8). The UV absorbance was recorded at 370 nm during 100 s, at 20°C. All samples had their background corrected before the addition of α -CT. The reaction dead time was 15 s.

To determine the K_M of α -CT-Ludox AM for Ala-Ala-Phe-7-AMC, stock solutions of 123.75 mM Ala-Ala-Phe-7-AMC and 0.031 mg mL⁻¹ α -CT adsorbed on Ludox AM were prepared. The concentrations of Ala-Ala-Phe-7-AMC tested were 0 μ M, 50 μ M, 100 μ M, 250 μ M, 500 μ M, 1000 μ M and 1500 μ M with a final enzyme concentration of 0.015 mg mL⁻¹. The reaction buffer was 20 mM TRIS-HCl pH 7.8, and the absorbance at 370 nm was recorded at 20°C for 100 s. Ludox-AM particles increase the light scattering, therefore background solutions were recorded using a quartz cuvette, buffer and Ludox-AM without enzyme for each substrate concentration. This background absorption was then subtracted from the respective kinetic signal. The reaction dead time was 15 s.

The calculations of the kinetic parameters were done by converting the absorbance signal into molar concentration. The molar extinction coefficient of 7- AMC is $\epsilon = 15000$, according to the molecule data sheet given by Sigma-Aldrich [99,100]. The kinetic velocity, v , was then calculated during the time interval in which all measurements were linear. The 7-AMC absorbance was converted into μ M, and divided by the time in second, then normalized to the enzyme concentration in μ M. This gives $v/[E]_{total}$ in s⁻¹ (μ M μ M⁻¹ s⁻¹). All data were fitted with the Michaelis-Menten model in Origin 9.0 software, and K_M and k_{cat} were estimated.

For the HP-SF, 0.4 mg of α -CT is dissolved in 4 mL of 20 mM TRIS-HCl buffer (pH 7,8) or in 4 mL of 20 mM TRIS-HCl buffer (pH 7,8) with Ludox-AM (1:11). This dilution creates a 0.1 mg mL⁻¹ or 1.25 μ M enzyme solution. The protein is left to adsorb on Ludox AM in 20 mM TRIS-HCl buffer (pH 7.8) during 3 hours at 4 °C. After this period, the adsorbed enzyme is ready to be used in the kinetic assays. The substrate solutions of 1 mM or 3 mM Ala-Ala-Phe-7-amido-4-methylcoumarin were also prepared in 4 mL of 20 mM TRIS-HCl buffer (pH 7,8). The TRIS base buffer is known for a low reaction volume and low pressure sensitivity [88].

In the high pressure stopped-flow system, there are two syringes. One syringe was filled up with enzyme solution (α -CT free or adsorbed on Ludox AM) and the other syringe was filled with substrate solution (1 mM or 3 mM Ala-Ala-Phe-7-AMC). After a 1:1 mixing in the observation chamber, the final concentrations were half of what it is in the syringes. The reactions were recorded at 20°C, during 100 s and in the pressure range from 1 to 2000

bar, in 500 bar steps. The absorbance was collected with the monochromator set at 370 nm, and the instrumental offset was corrected to force all samples to start at 0 absorbance at time 0 s. The equipment used was a High Pressure Stopped Flow System HPSF-56 from HiTech Scientific.

After offset correction, the curves were all fitted in the initial time interval when the increase of the signal was linear, and the slopes for each condition were determined. The ratio of the rates measured at 1 bar and higher pressures can be related to the ratio of the corresponding rate constants:

$$\frac{r}{r_0} = \frac{k}{k_0}$$

The meaning of the rate constants is discussed below. A plot of $\ln(r/r_0)$ as a function of pressure, p , yields a curve whose slope contains the activation volume, as seen in chapters 3 and 4:

$$\left(\frac{\partial \ln(r/r_0)}{\partial p} \right)_T = -\frac{\Delta V^\ddagger}{RT}$$

This equation can be applied to all measured pressures, p , and does not require a constant activation volume. When the activation volume is pressure dependent, a change in the slope of $\ln(r/r_0)$ vs. p is observed.

Reversibility tests of the enzyme activity were done after the complete pressure dependent reaction set at 1, 500, 1000, 1500, 2000 bar. After the 2000 bar-kinetics, the pressure was slowly reduced to 1 bar, which was about 1 hour after the first reaction started, and again 1 bar-reactions were recorded. The slope of these kinetics curves were then compared to the first 1 bar kinetics of the experiment set.

5.2.3. Autolysis and SDS-PAGE

Sodium dodecyl sulfate polyacrylamide gel electrophoresis (SDS-PAGE) was used to monitor the autolysis of free and adsorbed α -CT. 0.15 mg mL^{-1} ($6 \text{ }\mu\text{M}$) α -CT was diluted in 20 mM TRIS-HCl (pH 7.8) or 20 mM TRIS-HCl (pH 7.8) with Ludox AM (1:11). α -CT, free and adsorbed on Ludox-AM, was incubated over 24 hours at room temperature, and samples were analyzed at different times: 0 minute, 10 minutes, 30 minutes, 60 minutes, 120 minutes,

240 minutes, and one last sample after 24 hours. Then, the denaturant sample buffer, Laemmli buffer, was added to each sample and stored at $-80\text{ }^{\circ}\text{C}$. 30 μL of these samples were analyzed by 18% SDS-PAGE using a Bio-Rad Mini-Protean™ Kit. The protein bands were stained using the GE silver staining kit, following the manufacturer's protocol. Gel images were captured with the AlphaImager Mini equipment from ProteinSimple. The images were analyzed by the image processing software ImageJ from NIH-USA. In this software, the intensity of each band is quantified [98]. The intensities were normalized to the time 0 sample and plotted as a function of time.

5.3. Results and discussion

5.3.1. Determination of K_M and k_{cat}

The activities of free and adsorbed α -CT were successfully measured at different substrate concentrations. In figure 47, the enzymatic activity shows a substrate concentration dependence from 0 to 1500 μM . It indicates that the enzyme is not completely saturated by Ala-Ala-Phe-7-AMC below 1500 μM .

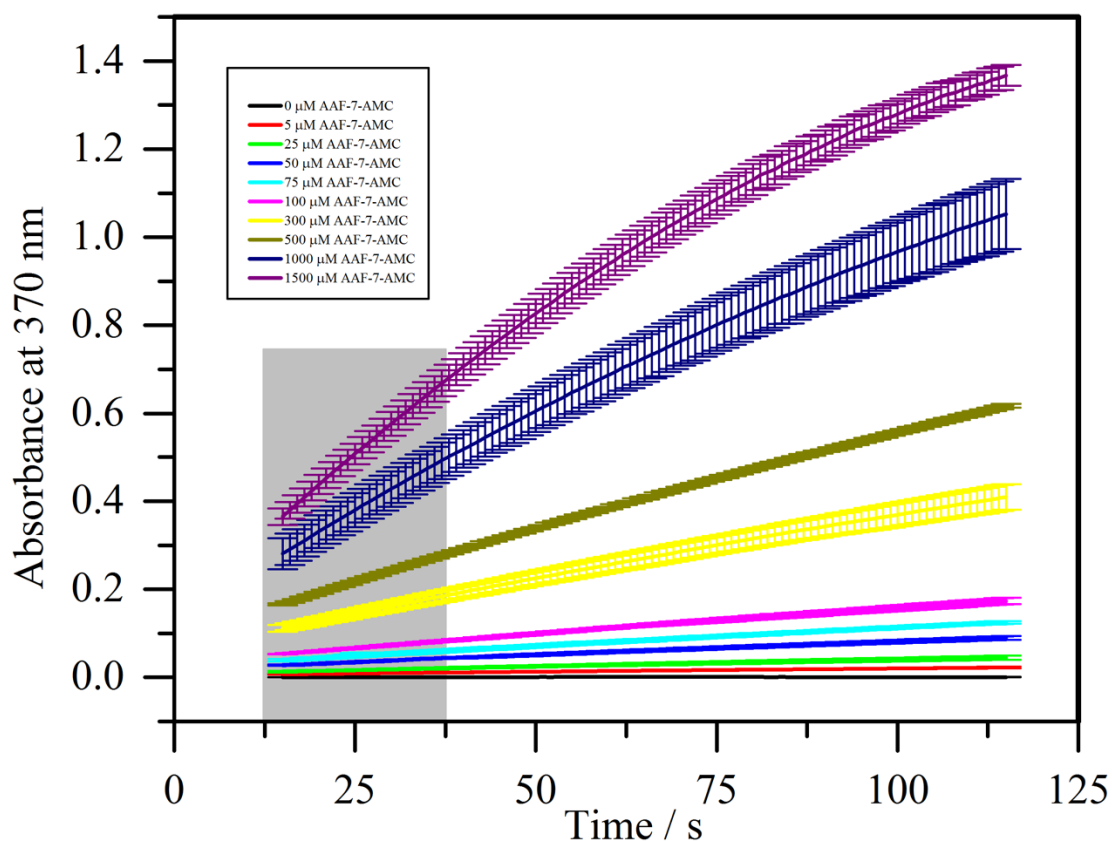


Figure 47. Enzymatic activity of α -CT measured with different Ala-Ala-Phe-7-AMC concentrations. The analyzed data is indicated by the grey rectangle. The absorbance increase is substrate concentration dependent, which indicates that free α -CT was not completely saturated below 1500 μ M at 20 $^{\circ}$ C, during 100 s. The reaction mixture contained 0.05 mg mL $^{-1}$ of enzyme, the substrate concentration varied from 5 to 1500 μ M. The dead time is 15 s. The error bars cover the scattering of two independent measurements.

On the other hand, adsorbed α -CT (Figure 48) increased its activity up to 500 μ M of substrate. At higher concentrations, the enzymatic rates did not show significant enhancement. It is important to notice that any concentration above 1500 μ M was excluded due to the lack of solubility of the substrate Ala-Ala-Phe-7-AMC in water.

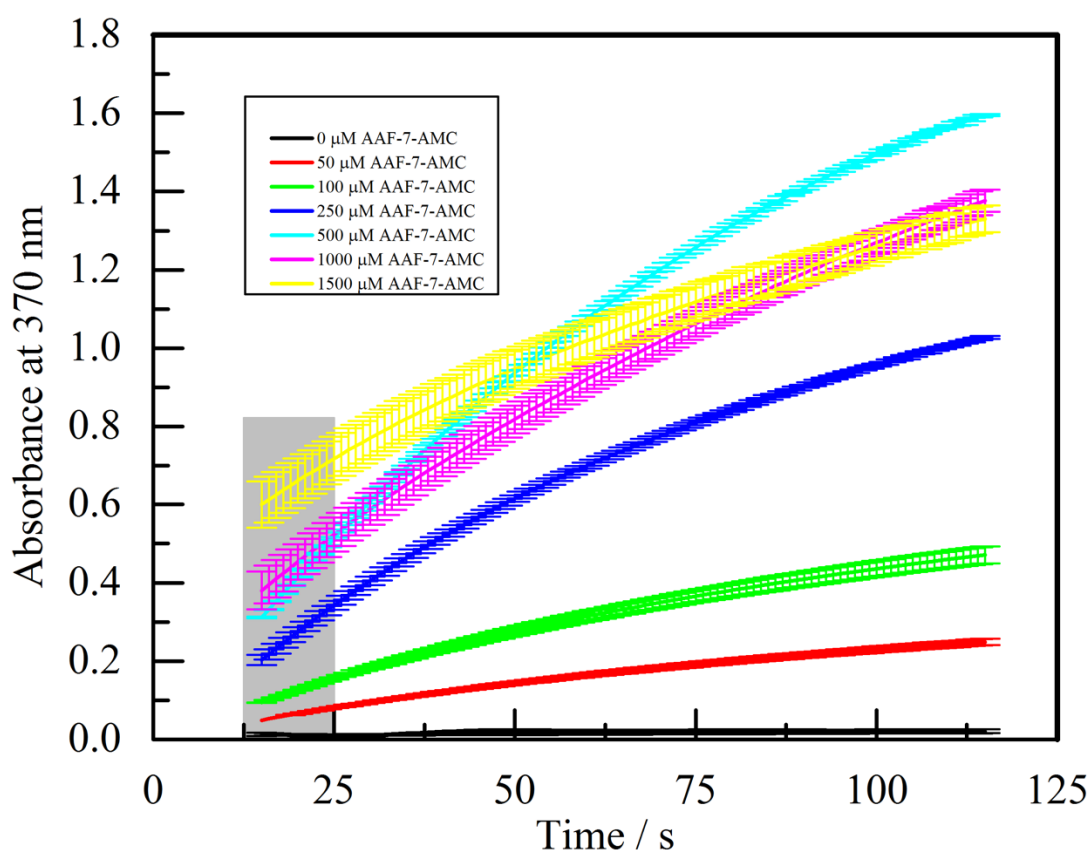


Figure 48. Enzymatic activity of α -CT adsorbed on Ludox AM® measured with different Ala-Ala-Phe-7-AMC concentrations. The analyzed data is indicated by the grey rectangle. The absorbance increase is dependent on the substrate concentration, which indicates that adsorbed α -CT is not completely saturated below 1500 μM at 20 $^{\circ}\text{C}$, during 100 s. The reaction mixture contained 0.015 mg mL^{-1} of enzyme, the substrate concentration varied from 5 to 1500 μM . The dead time is 15 s. The error bars cover the scattering of two independent measurements.

The data points highlighted in gray, at figures 47 and 48, were used to calculate the enzyme kinetic rates. Through a non-linear fit, using the Michaelis-Menten equation [100], K_M and k_{cat} could be determined. In figure 49, the Michaelis-Menten plots of free and adsorbed α -CT related to the substrate Ala-Ala-Phe-7-AMC are shown. The plots clearly show that the adsorbed enzyme has a higher velocity. According to the fit parameters, adsorbed α -CT has a K_M equal to $704 \pm 46 \mu\text{M}$, and the free α -CT has a K_M of $779 \pm 140 \mu\text{M}$. However, k_{cat} , was significantly increased due to adsorption. k_{cat} of adsorbed α -CT is $5,27 \pm 0,24 \text{ s}^{-1}$, in contrast to k_{cat} of free α -CT, which is $0,75 \pm 0,10 \text{ s}^{-1}$. If the enzyme efficiency (k_{cat}/K_M) is calculated [100], then it is possible to say that the adsorbed state is approximately 8 times more efficient than the free enzyme. It has been shown in literature that the efficiency

of enzymes can be increased after interacting with surfaces. Trypsin encapsulated in liposomes had greater activity than in solution, and it was 2 orders of magnitude higher [101]. Similar results for trypsin were found using fluorescence microscopy [102]. Horseradish peroxidase activity was found to have hundred-fold higher activity when encapsulated in polymersomes [103]. Also, α -CT trapped inside vesicles has a catalytic turnover 14 times higher than in solution [100]. Our findings are in good agreement with these reports in literature. The increase of activity of adsorbed α -CT has nothing to do with major structural changes. The adsorption of α -CT on Ludox AM nanoparticles does not affect its secondary and tertiary structures [91]. Therefore, the more pronounced activity in the adsorbed state could only be related to a small conformation arrangement during the adsorption process, and this new conformational state could achieve higher enzymatic rates.

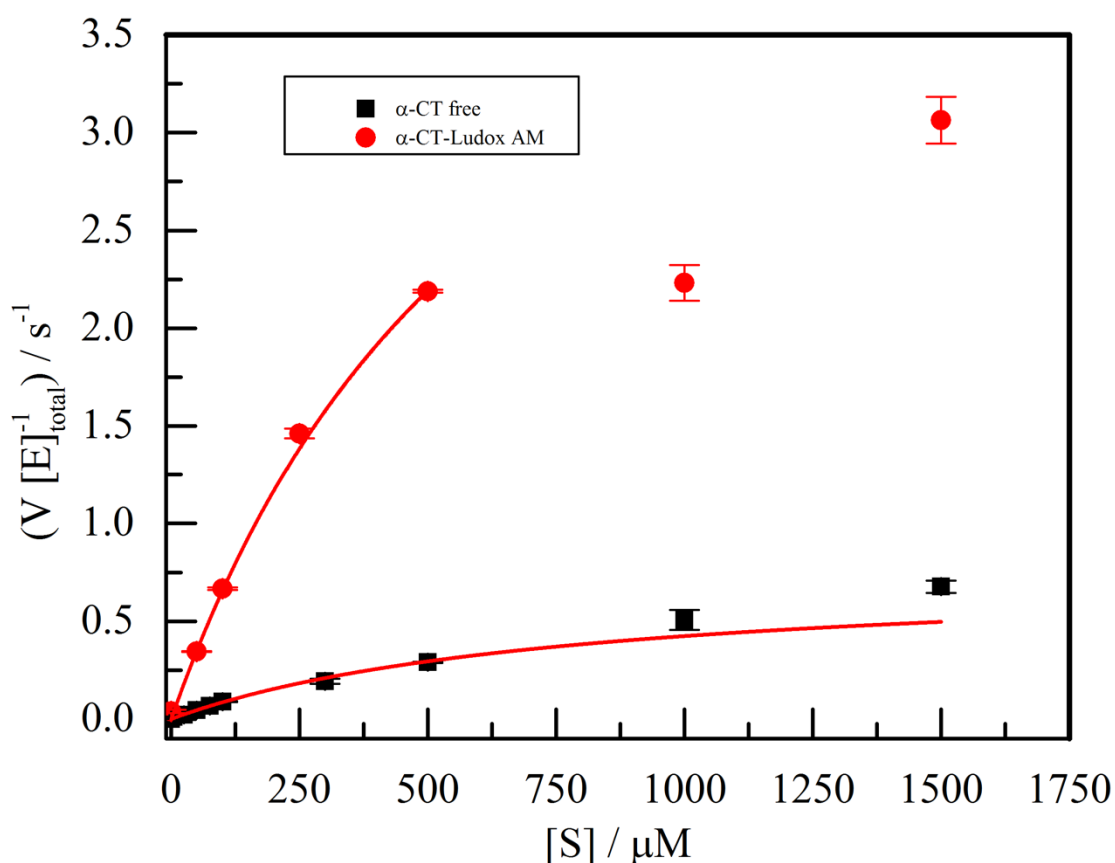


Figure 49. Michaelis-Menten plot of α -CT free and adsorbed on Ludox AM® for Ala-Ala-Phe-7-AMC. The calculated parameters for free α -CT are $K_M = 779 \pm 140 \mu\text{M}$ and $k_{\text{cat}} = 0,75 \pm 0,10 \text{ s}^{-1}$. The parameters for adsorbed α -CT are $K_M = 704 \pm 46 \mu\text{M}$ and $k_{\text{cat}} = 5,27 \pm 0,24 \text{ s}^{-1}$. The error bars cover the scattering of two independent measurements. In the case of α -CT on Ludox AM data at $[S] > 500 \mu\text{M}$ do not follow Michaelis-Menten kinetics, probably due to light scattering at aggregated particles.

5.3.2. High-pressure stopped-flow experiments

The activity of α -CT was successfully measured in the HP-SF system when free in solution and adsorbed on silica nanoparticles with two different substrate concentrations of 500 μ M and 1500 μ M.

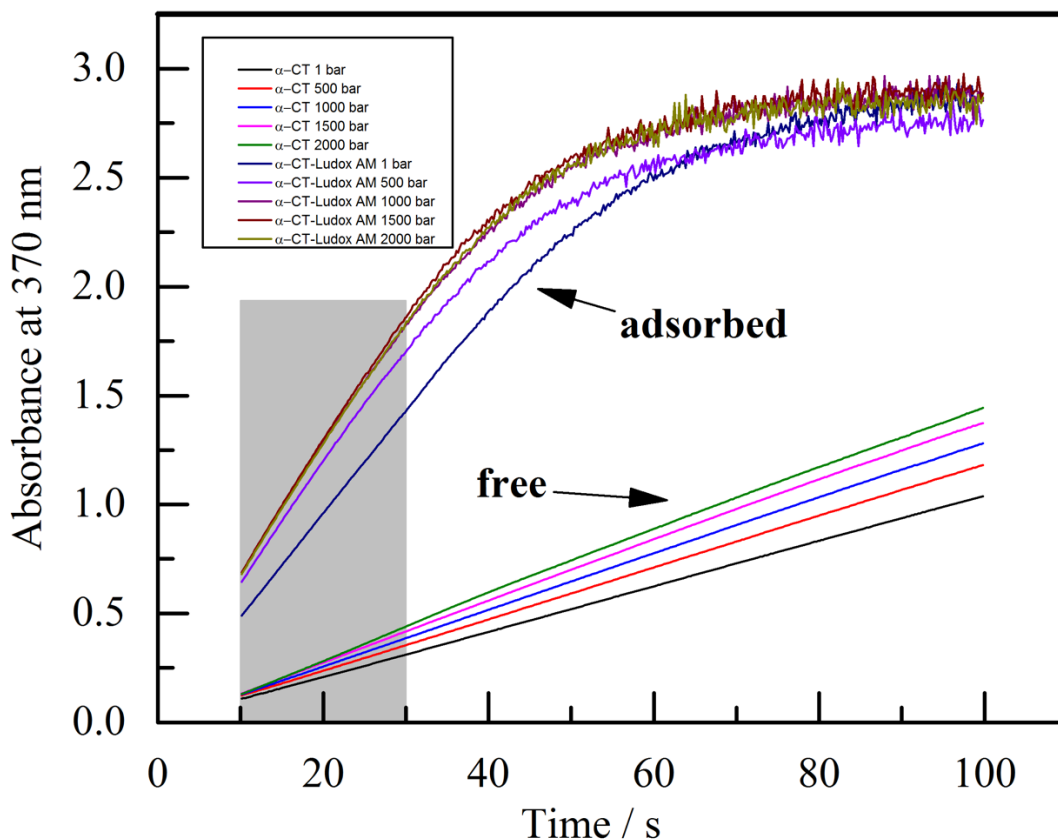


Figure 50. High pressure stopped-flow kinetics of α -CT free and adsorbed on Ludox AM® with 500 μ M of Ala-Ala-Phe-7-AMC (selected data). The analyzed data is indicated by the grey rectangle.

As can be seen in figures 50 and 51, at 500 μ M and 1500 μ M substrate concentrations, the total activity at 1 bar of α -CT in solution was linear during the first 100 s of reaction. On the other hand, adsorbed α -CT shows a very fast signal increase during the first 30 seconds, reaching the detection limit after 50 seconds. This suggests that there is a strong reaction acceleration due to adsorption at 1 bar, in agreement with the results found with the UV-VIS measurements described in the section above (Figures 47-48). When pressure increases, both free and adsorbed α -CT respond positively, increasing their enzymatic rates. This is in agreement with previous pressure studies on this enzyme [40,91]. The effect of pressure on

adsorbed α -CT seems to be more prominent in the first 500 bar range, and less effective after 1000 bar. This result is in good agreement with the results found by Schuabb & Czeslik in 2014, using the same system. On the other hand, free α -CT was sensitive to pressures up to 2000 bar.

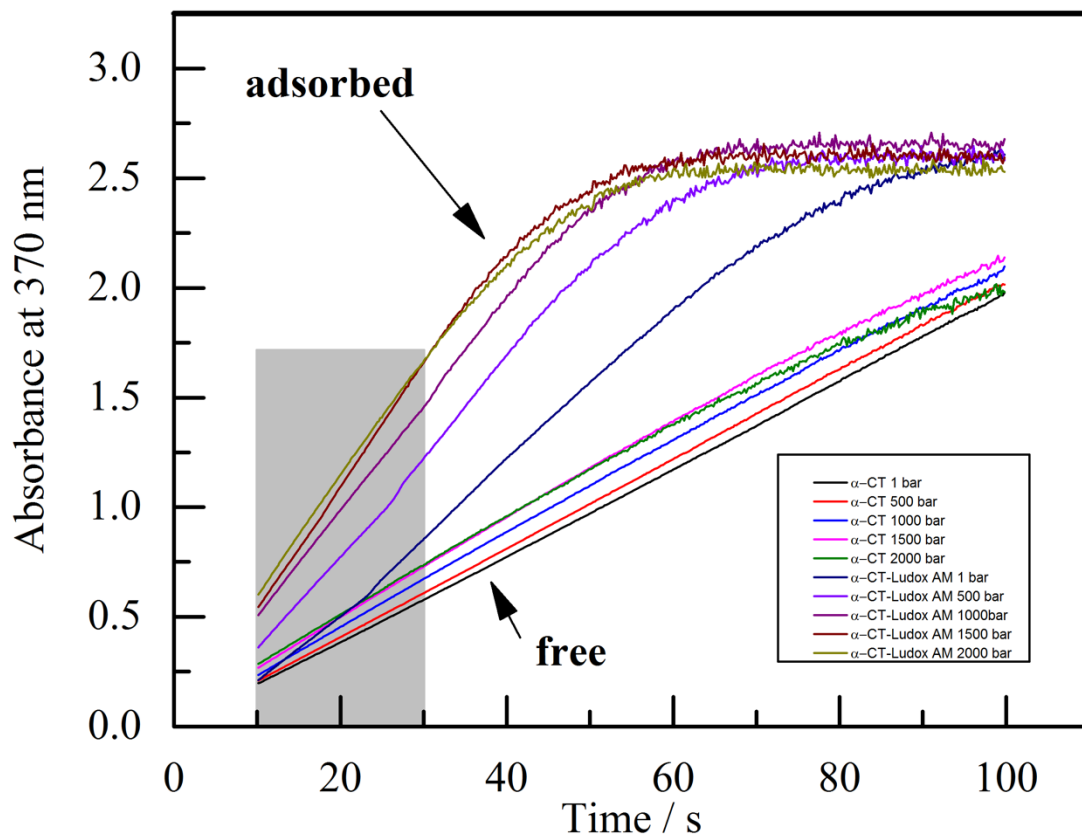


Figure 51. High pressure stopped-flow kinetics of α -CT free and adsorbed on Ludox AM® with 1500 μ M of Ala-Ala-Phe-7-AMC (selected data). The analyzed data is indicated by the gray rectangle.

As compared to 500 μ M of substrate (Figure 50), at 1500 μ M of substrate (Figure 51), the free and adsorbed α -CT enzymatic rates are similar to each other. As shown in the figure 49, at 1500 μ M, both adsorbed and free α -CT are almost saturated by substrate. However, they have different pressure responses. The adsorption is the major factor in the difference between these two catalytic states of α -CT.

5.3.3. Activation volumes

Since the kinetics of free and adsorbed α -CT are sensitive to pressure, the activation volumes of these reactions were calculated.

Free α -CT, with 500 μ M of substrate, shows a two-step pressure activation. Activity increases with pressure up to 2000 bar, and there is no leveling off, as shown in figure 52.

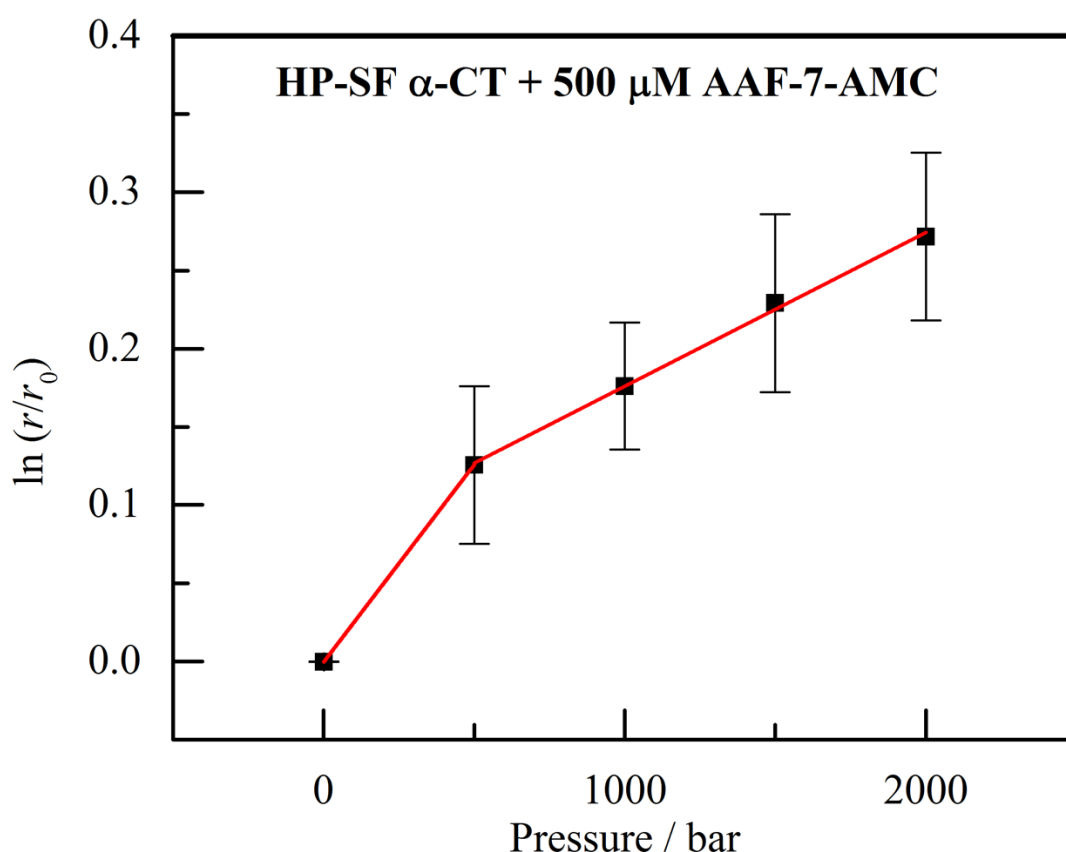


Figure 52. Pressure dependence of free α -CT enzymatic activity with 500 μ M of Ala-Ala-Phe-7-AMC. The error bars cover the scattering of three independent measurements.

In contrast, the adsorbed α -CT displays a more significant pressure effects below 1000 bar and very little response after this pressure point (Figure 53). These two results are in very good accordance with Schuabb & Czeslik (2014), when the same profile was observed for free and adsorbed α -CT, using fluorescence spectroscopy. The activation volume of each case was calculated. With 500 μ M, ΔV^\ddagger for free α -CT is about -6 mL mol^{-1} up to 500 bar, and from 500-2000 bar, ΔV^\ddagger is $-2.4 \pm 0.1 \text{ mL mol}^{-1}$.

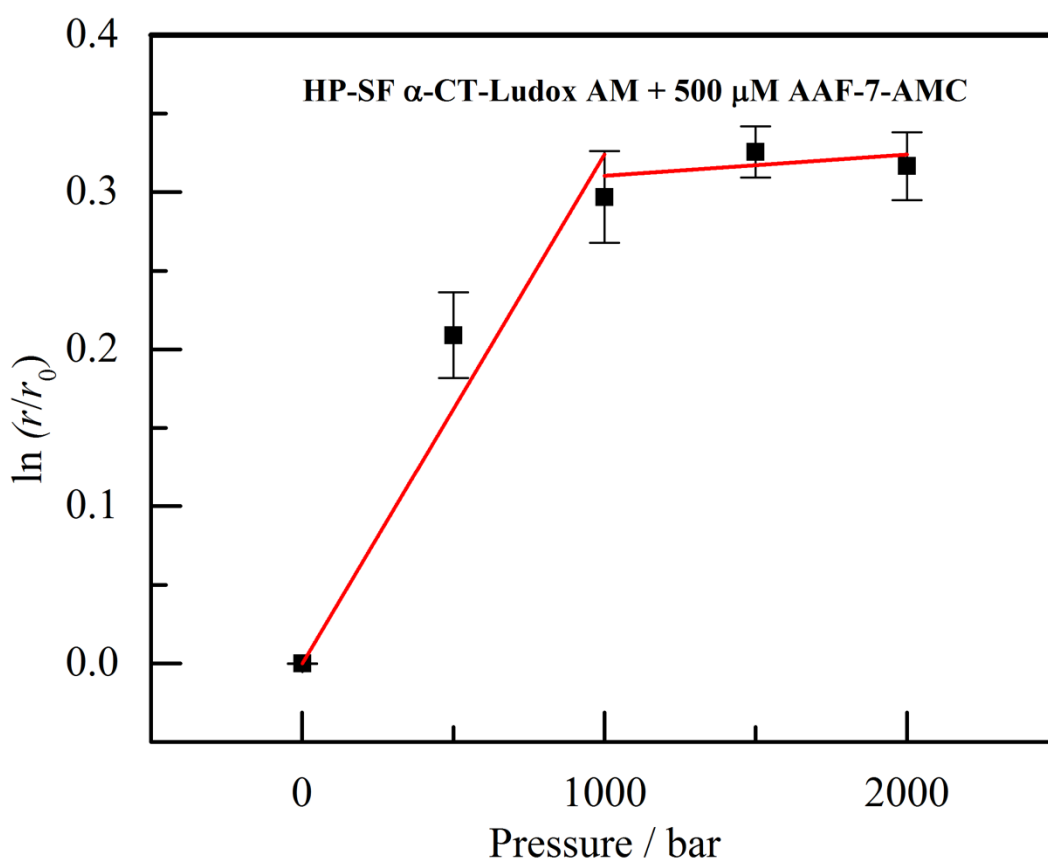


Figure 53. Pressure dependence of α -CT enzymatic activity when adsorbed on Ludox AM® with 500 μ M of Ala-Ala-Phe-7-AMC. The error bars cover the scattering of three independent measurements.

Adsorbed α -CT has a ΔV^\ddagger about $-8 \pm 1 \text{ mL mol}^{-1}$ up to 1000 bar, and from 1000-2000 bar ΔV^\ddagger is $0.3 \pm 0.6 \text{ mL mol}^{-1}$. This result is in agreement with data published in 2014 by Schuabb & Czeslik. The profiles are similar, showing in solution a progressive increase of activity as pressure increases (negative activation volume) and, with the adsorbed enzyme, an increase from 1 to 1000 bar (negative activation volume) and a reduced pressure activation from 1000 to 2000 bar (more positive activation volume). The most significant difference between the current results and those published in 2014 are the ΔV^\ddagger values. The data published in 2014 showed larger activation volumes, around -60 mL mol^{-1} for free α -CT. In figure 52, an activation volume of -6 mL mol^{-1} for free α -CT is found. One possible reason for this deviation could be that, different protease substrates were used. In the study of by Schuabb and Czeslik (2014) a peptide from the EnzChek protease kit, whose sequence and structure are protected and not available, was used. The substrate used here was the Ala-Ala-Phe-7-AMC. The structural difference between these two substrates might be responsible for the difference in the activation volume values. At small [S], the activation volume is the

difference between E+S and ES*. The volume of the substrate and how it interacts with the enzyme can also contribute to this difference in volume. The simple fact that one substrate could attract one more water molecule than the other substrate into the active site, could cause a distortion of 18 ml mol⁻¹ [40]. On the other hand, in the HP-SF system both molecules are pre-pressurized before being mixed. This can also be responsible for lower volumes of the reactants, since some void volumes might have been filled before the reaction. Furthermore, in the literature, small values of the activation volume of α -CT were also found using UV absorbance spectroscopy and the HP-SF technique [104]. This also reinforces the idea that a pre-pressurization of the reactants could in fact play a role in reducing activation volume values. In contrast, in the study published in 2014, the molecules were mixed at 1 bar, left to react for a small period of time, and were then pressurized. Another possible reason for the different ΔV^\ddagger values could be a difference between the methods. Any comparison between the results from a relative scale method, such as fluorescence, with a quantitative method as the UV absorbance, can lead to some deviations. Furthermore, the HP fluorescence data are corrected for the pressure dependence of the quantum yield, which might be a source of error.

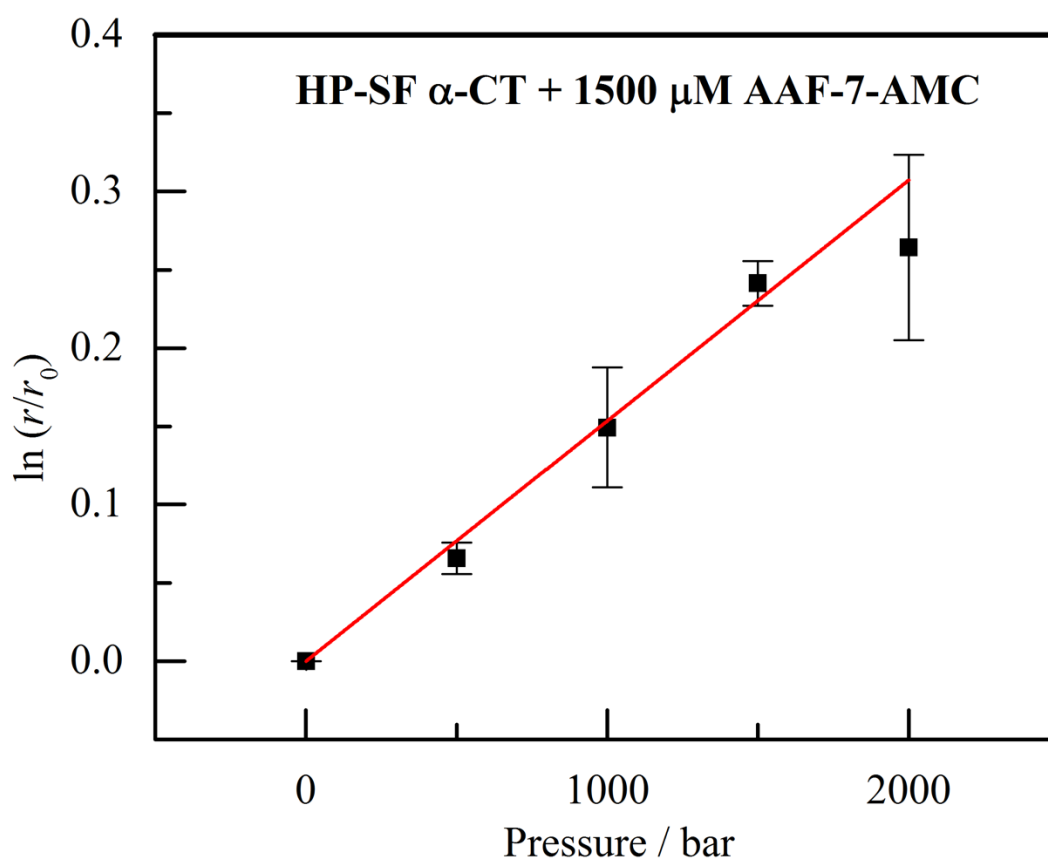


Figure 54. Pressure dependence of the enzymatic activity of free α -CT with 1500 μM of Ala-Ala-Phe-7-AMC. The error bars cover the scattering of three independent measurements.

When the substrate concentration is increased up to 1500 μM , ΔV^\ddagger for free α -CT is $-3.7 \pm 0.2 \text{ mL mol}^{-1}$ from 1-2000 bar. ΔV^\ddagger for adsorbed α -CT is $-14 \pm 1.0 \text{ mL mol}^{-1}$ from 1-1000 bar, and ΔV^\ddagger from 1000-2000 bar is $-2.5 \pm 1.0 \text{ mL mol}^{-1}$ (Figure 54 and 55).

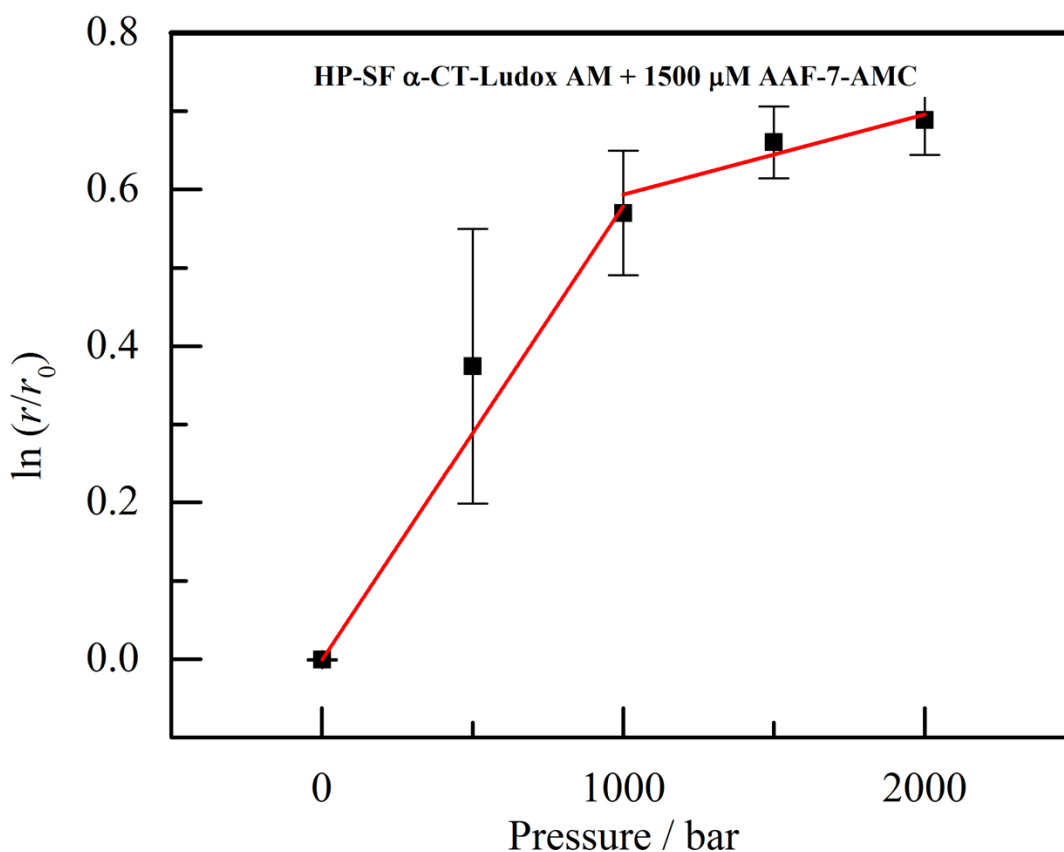


Figure 55. Pressure dependence of the enzymatic activity of α -CT when adsorbed on Ludox AM® with 1500 μM of Ala-Ala-Phe-7-AMC. The error bars cover the scattering of three independent measurements.

The activation volume plot of adsorbed α -CT with 1500 μM of substrate is very similar to the plot with 500 μM of substrate. But different ΔV^\ddagger values are encountered. The higher substrate concentration almost doubles the negative activation volume value for the adsorbed α -CT, going from -8 ml mol^{-1} with 500 μM to -14 mL mol^{-1} with 1500 μM up to 1000 bar. On the other hand, from 1000 to 2000 bar similar activation volumes for both substrate concentrations were found, as seen in figure 56.

Activation volumes for free and adsorbed α -CT are in the same order as found with 500 μM of substrate. Alternatively, with 1500 μM of substrate, free α -CT is lacking the strong pressure activation in the lower pressure range. Only in this case, we can surely say that the enzyme is saturated by the substrate and the activation volume refers to the step ES-complex \rightarrow ES* transition state.

Apparently, in all other cases, higher pressures lead to smaller (less negative) activation volumes. This finding suggests that the E+S mixture or the ES-complex is more compressible than the ES* transition state. α -CT has the so-called ping-pong type of kinetic mechanism.

This mechanism requires a new substrate to bind to the enzyme, and this promotes the release of the second product [105]. This step could be faster with higher substrate concentrations, and adsorbed enzymes could have a better interaction with the substrate. At this point, there is no molecular explanation for these findings, and more specific methods would be necessary to help understanding these events.

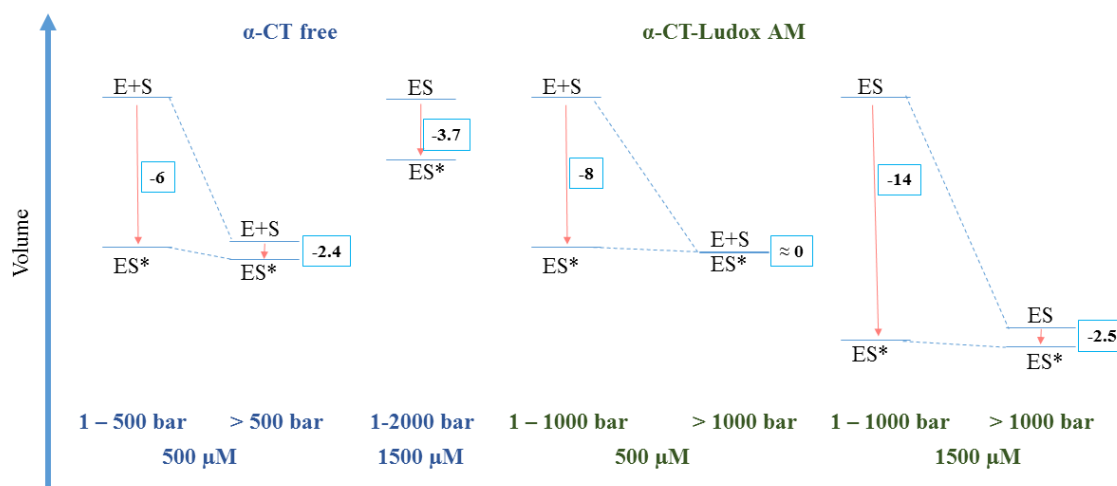


Figure 56. Activation volumes of α -CT free and adsorbed on Ludox AM® with 500 and 1500 μ M of Ala-Ala-Phe-7-AMC (not to scale).

5.3.4. Reversibility

Additional information can be easily extracted from HP-SF experiments, such as the reversibility of the pressure response. In figure 57, free and adsorbed α -CT shows the same enzymatic rate at 1 bar before and after 2000 bar pressurization. The slopes of each activity are overlaid before and after pressure treatment, proving that there is no irreversible pressure induced effect on free neither on adsorbed α -CT. This is desirable, when an enzymatic system is projected to run several reaction cycles under pressure.

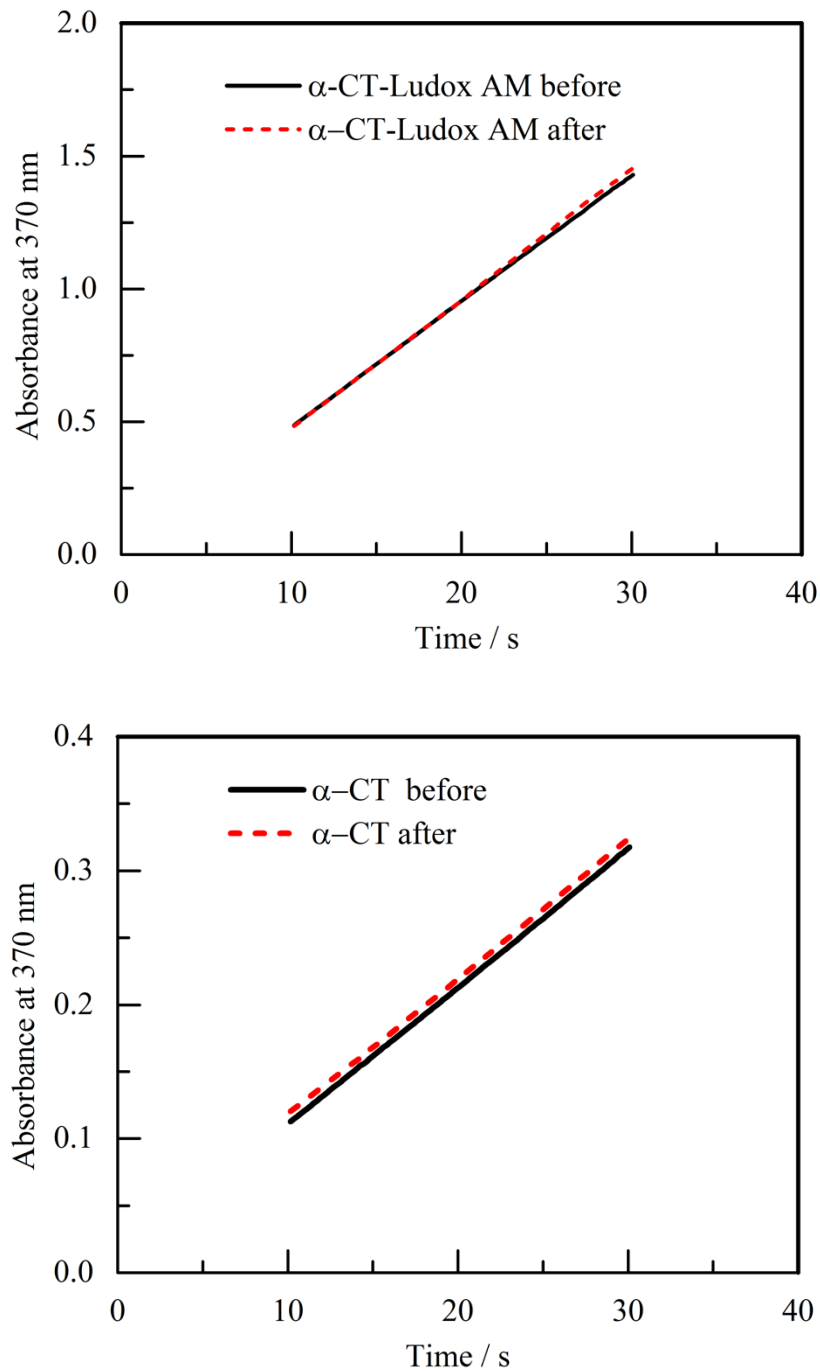

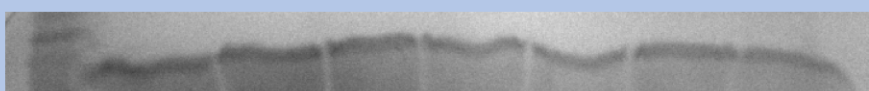


Figure 57. Reversibility test of α -CT free and adsorbed on Ludox AM® before and after pressurization up to 2000 bar (selected data).

5.3.5. Autolysis

The autolysis activity of free and adsorbed α -CT was successfully measured using the SDS-PAGE method. As seen in figure 58, after 24 hours, almost 80% of adsorbed enzyme is still in the uncleaved state, whereas around 20% of free α -CT. In the literature, this is also reported for trypsin adsorbed on mesoporous silica, when after 20 days the immobilized

trypsin shows 70% of initial state in contrast to the dissolved trypsin that shows only 45% [97]. These findings strongly suggest the idea that immobilization of α -CT, as well as other proteases, could be a tool in order to protect proteases against autolysis, and this could create conditions for recycling these enzymes.

Time / min	M.W.	0	10	30	60	120	240	1440	
α -CT									
α -CT-Ludox AM									

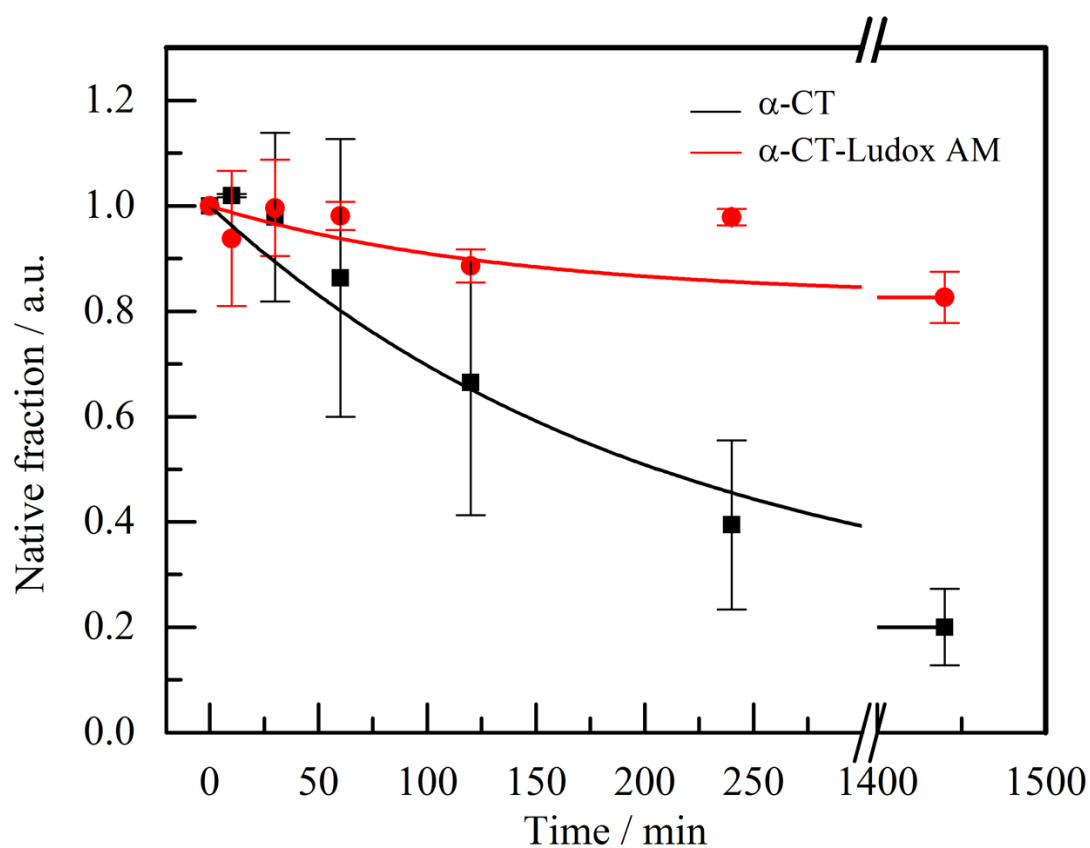


Figure 58. Autolysis test of α -CT free and adsorbed on Ludox AM®. Top: the 25 kDa band of free and adsorbed α -CT as a function of time (selected data). Bottom: the intensity of the 25 kDa band as a function of time. The error bars cover the scattering of two independent measurements.

5.4. Conclusions

The enzyme activity of free and adsorbed α -CT was successfully measured with Ala-Ala-Phe-7-AMC as the substrate using UV-VIS spectroscopy and the HP-SF technique. Through UV-VIS spectroscopy, K_M and k_{cat} of both free and adsorbed α -CT were determined. Free α -CT has a K_M of approximately 780 μ M, whereas adsorbed α -CT has a K_M of approximately 705 μ M. The kinetic rate constant k_{cat} for free α -CT is 0.75 s^{-1} and for adsorbed α -CT 5.27 s^{-1} .

Activation volumes of free and adsorbed α -CT were determined for the first time using the HP-SF technique in UV-VIS mode. Two substrate concentrations were tested giving an insight of substrate concentration dependence of the activation volume. ΔV^\ddagger of free α -CT with 500 μ M of substrate is -6 $mL mol^{-1}$ from 1 to 500 bar and from 500 to 2000 bar ΔV^\ddagger is -2.4 $mL mol^{-1}$. ΔV^\ddagger of adsorbed α -CT with 500 μ M of substrate is -8 $mL mol^{-1}$ from 1 to 1000 bar and from 1000-2000 bar ΔV^\ddagger is $0.3 \pm 0.6 mL mol^{-1}$. Increasing the substrate concentration up to 1500 μ M, ΔV^\ddagger for free α -CT is -3,7 $mL mol^{-1}$ from 1-2000 bar. ΔV^\ddagger for adsorbed α -CT is -14 $mL mol^{-1}$ from 1 to 1000 bar and from 1000 to 2000 bar it is -2,5 $mL mol^{-1}$ (Figures 54 and 55).

It is important to highlight that the increase of the substrate concentration from 500 to 1500 μ M almost doubled the negative activation volume of adsorbed α -CT, from 1 to 1000 bar. The pressure acceleration is reversible in the free and adsorbed state, as the enzyme had the same activity before and after 2000 bar treatment.

The autolysis of free and adsorbed α -CT was also monitored, and the results clearly show that the adsorption of α -CT strongly protects the enzyme, keeping higher amount of native conformation for longer periods.

Overall, these results explored some advantages of adsorbing enzymes on nanoparticles. The adsorption of α -CT promotes higher kinetic rates, reversible activation by pressure due to negative activation volumes, and drastic reduction of the autolysis of α -CT.

6. Global summary

An enzyme is a special type of protein with a catalytic property. This specialty has been improved in order to catalyze biochemical reactions, usually under mild conditions, such as neutral pH-values, ambient pressure and ambient temperatures. Usually they are very specific for a particular reaction pathway enabling yields with high enantiomeric excess [1]. Therefore, enzymes are very attractive for use in biotechnological, pharmaceutical, and biomedical processes. The greatest disadvantage of using enzymes, compared to chemical catalysts, is their relatively low stability and their relatively high cost. There are many examples of expensive enzymes that are worth being recovered from the reaction media to be reused in many cycles. Using filtration or centrifugation, enzymes are easily removed from a reaction mixture, when the enzymes are immobilized on carrier particles large enough to be retained or sedimented [2-3].

Making contact with an aqueous-solid interface represents a major perturbation of the environment of a given protein, because this surface can replace water molecules at the protein surface, especially when it is a hydrophobic surface. In addition, an aqueous-solid interface may provide a different pH-value, when dissociating chemical groups are present, and a different ionic strength, when it is carrying charged groups. Thus, any adsorption of proteins and immobilization of enzymes at aqueous-solid interfaces may lead to some changes in the conformation of the protein [6-8]. The interactions with a surface can also slow down the dynamics of a protein, and the overall enzymatic activity at interfaces may be decreased by an unfavorable orientation of the enzyme molecules too, when the active site is blocked either by the material surface or by neighboring enzyme molecules [9].

As detailed in this work, the application of pressure is a new complementary, synergistic or even compensating tool to increase the activity of enzymes immobilized at aqueous-solid interfaces. Pressure can have two major effects on enzymes, since enzymes are proteins with a folded conformation and are reaction catalysts. There is a negative volume-change, ΔV , related to the unfolding of proteins, leading to a pressure-induced unfolding. On the other hand, the catalytic properties of enzymes have been shown to sensitively depend on pressure, below the pressure of unfolding. There are several examples, where pressure accelerates or decelerates enzymatic reactions [19,20]. Under pressure, low volume states are preferred over higher volume. A transition state is favored under pressure, when it has a smaller volume than the reactants. This is expressed as negative activation volume, ΔV^\ddagger . Pressure experiments on the enzymatic activity of the strawberry peroxidase have shown that there is an increased rate of oxidation after pressure treatment at 4000 bar for five minutes [22]. In a similar way, pressurization caused an impressive activation of carrot peroxidase after a one-minute

treatment at 4000-5000 bar [23]. The enzymatic activity of α -chymotrypsin at high pressures has also been studied. In the temperature range of 10-65 °C, a maximum rate constant of hydrolysis by α -chymotrypsin has been found at 45 °C and 2000 bar [24]. Moreover, an increase in pressure at 20 °C results in an acceleration of the hydrolysis catalyzed by α -chymotrypsin, reaching a 6.5-fold increase in activity at 4700 bar. At 50 °C and a pressure of 3600 bar, the activity is higher more than 30 times [25].

In the present work, we explored the effects of pressure on enzymes immobilized at aqueous-solid interfaces such as silica nanoparticles and planar surfaces with different chemical modifications. Using well-chosen models, horseradish peroxidase and alpha-chymotrypsin, we show the way pressure influences enzymatic reactions at interfaces and explore the question how pressure can be used to compensate limitations in enzyme activity at interfaces by favoring low-volume transition states and reaction pathways. Another target of this study is the role of surface chemistry in the activation of a given reaction.

Activation volumes of enzymes adsorbed on silica particles

In the first part of the thesis, enzymes were immobilized on silica nanoparticles. The activation volumes of two enzymes, α -chymotrypsin (α -CT) and horseradish peroxidase (HRP), when they are adsorbed on silica particles and free in solution, have been determined.

The secondary structures of these enzymes were monitored by FTIR spectroscopy. The results show no major change due to adsorption up to 2000 bar. The tertiary structure of α -CT was measured by tryptophan fluorescence spectroscopy, and it was revealed that it remains the same from 1 up to 2000 bar. So, the adsorption on silica nanoparticles did not create any change in the structure of α -CT and HRP, and therefore, any pressure effect will be related to the enzyme kinetics.

The kinetic experiments have been carried out using fluorescence assays under pressures up to 2000 bar. In all cases, activation volumes were found to depend on the applied pressure, suggesting different compressibilities of the enzyme-substrate mixture and the transition state.

The volume profiles of free and adsorbed HRP are similar. Free HRP has an activation volume of +16 mL mol⁻¹ from 1 to 500 bar and +2 mL mol⁻¹ from 500 to 2000 bar. Adsorbed HRP has +27 mL mol⁻¹ from 1-250 bar and +2 mL mol⁻¹ from 250 to 2000 bar. Presumably, the mechanism of the enzymatic reaction does not change upon adsorption, and no large distortion occurs, when HRP interacts with the silica nanoparticles. Above 500 bar, an

activation volume of $+2 \text{ mL mol}^{-1}$ indicates that the volumes of ES^* and E+S are very similar, and pressure has little effect on the enzymatic rate.

For α -CT, larger activation volumes (more positive values) are found in the adsorbed state. However, up to about 500 bar, the enzymatic reaction of α -CT, which is adsorbed on silica particles, is characterized by a negative activation volume. Free α -CT has an activation volume of -67 mL mol^{-1} from 1 to 500 bar and -15 mL mol^{-1} from 500 to 2000 bar. Adsorbed α -CT has an activation volume of -4 mL mol^{-1} from 1 to 500 bar and $+5 \text{ mL mol}^{-1}$ from 500 to 2000 bar. This is the first report in the literature that shows an activation of an adsorbed enzyme by pressure. This finding demonstrates that pressure is new strategy to optimize enzymatic reactions on carrier particles.

Effects of interfacial properties on the activation volume of adsorbed enzymes

We saw previously that pressure can have a positive influence on adsorbed enzymes kinetics. In this second part, the enzymatic activities of α -CT and HRP that are adsorbed on various chemically modified planar surfaces have been studied, and the combined effects of surface chemistry and pressure on the kinetics of adsorbed enzymes have been evaluated. The enzymes were adsorbed on bare quartz, hydrophobic poly(styrene) (PS), positively charged poly(allylamine hydrochloride) (PAH), and negatively charged poly(styrene sulfonate) (PSS).

The secondary structures of these enzymes were monitored by Fourier transform infrared (FTIR) spectra collected in attenuated total reflection (ATR) mode. The results do not indicate major adsorption induced conformational changes of the enzymes at any interface studied.

The activity measurements of the enzymes at the aqueous-solid interfaces were determined by using high-pressure total internal reflection fluorescence (TIRF) spectroscopy.

Apparently, the pressure response of the adsorbed enzymes strongly depends on the interfacial chemistry. α -CT can be activated by pressure on negatively charged surfaces like quartz and PSS. The activation volume of α -CT found on quartz is -29 mL mol^{-1} from 1 to 1000 bar and -1 mL mol^{-1} from 1000 to 2000bar, on a PS film $+9 \text{ mL mol}^{-1}$, on a PSS-ending multilayer -23 mL mol^{-1} and on a PAH-ending multilayer $+3 \text{ mL mol}^{-1}$.

On the other hand, HRP is activated by pressure on the hydrophobic PS film. The activation volume of HRP found on quartz is -6 mL mol^{-1} from 1 to 2000 bar, on a PS film -35 mL mol^{-1} , on a PSS-ending multilayer $+19 \text{ mL mol}^{-1}$ and on a PAH-ending multilayer $+16 \text{ mL mol}^{-1}$.

In addition, the absolute activities of α -CT and HRP on quartz, PS, PAH and PSS were determined by UV absorption at ambient pressure. Remarkably, large activities are found on those surfaces that are associated with negative activation volumes.

Overall, the results of this study show that pressure is again a useful tool to enhance enzymatic activity especially in combination with the right adsorbent material.

Advantages of adsorbing α -CT on silica nanoparticles – A high-pressure stopped-flow study

In this last chapter, a different approach to track the activity of adsorbed enzymes on surfaces was used. The stopped-flow technique was used to monitor the activity of α -CT free and adsorbed on Ludox-AM. By monitoring the UV-VIS absorbance of the reaction product as a function of time. Furthermore, another important aspect of using adsorbed enzymes, especially in the case of proteases, was tested as a function of time, the autolysis activity.

First K_M and k_{cat} were determined with UV-VIS spectroscopy. The activity of α -CT is strongly accelerated due to adsorption. The adsorption seems to induce a higher affinity for the substrate, as K_M for adsorbed state was 704 μ M, whereas for the free enzyme it was 779 μ M. The kinetic rate constant k_{cat} , was 5.27 s^{-1} and 0.75 s^{-1} , in the adsorbed and free state, respectively.

By increasing the substrate concentration, from 500 to 1500 μ M, the negative activation volume of the adsorbed α -CT almost doubled, from -8 to -14 $mL mol^{-1}$ from 1 to 1000 bar, followed by a pressure insensitive range from 1000-2000 bar. In the case of free α -CT, the increase of the substrate concentration did not change the ΔV^\ddagger values in a major way. This pressure acceleration is reversible in both cases, having the same enzymatic activity before and after 2000 bar treatment.

The autolysis of the enzyme was also followed, in the adsorbed and free states. The adsorption of α -CT strongly protects the enzyme, increasing the amount of uncleaved enzyme for longer periods.

All these results together brought to light some of the advantages of adsorbing an enzyme, especially, if the intention is to recycle this system for several times. This work has shown that, in the case of α -CT, the adsorption brought higher kinetic rates. Adsorbed α -CT is also activated by pressure, and this pressure activation appears to be reversible. Also due to adsorption, the rate of autolysis was drastically reduced. In fact, this work has proven that the adsorption of a protein, especially in the case of proteases, could be interesting for a more efficient and reusable system.

7. Zusammenfassung

Enzyme sind Proteine mit katalytischer Eigenschaft. Sie können biochemische Reaktionen bei Umgebungsbedingungen beschleunigen, die in der Regel neutrale pH-Werte, Umgebungsdruck und –Temperatur sind. Dabei sind Enzyme gewöhnlich hoch wirkungs- sowie substratspezifisch und können somit Ausbeuten mit hohem Enantiomerenüberschuss erzielen [1]. Deshalb sind sie sehr attraktiv und nützlich für vielerlei biotechnologische Anwendungen sowie in pharmazeutischen und biomedizinischen Prozessen. Ein großer Nachteil der Verwendung von Enzymen im Vergleich zu chemischen Katalysatoren stellt ihre relativ geringe Stabilität und ihre relativ hohen Herstellungskosten dar. Es gibt viele Beispiele von teuren Enzymen, die aus den Reaktionsmedien aufwendig zurückgewonnen werden, um sie in weiteren Zyklen wiederzuverwenden. Sie können z.B. unter Verwendung von Filtration oder Zentrifugation problemlos aus einer Reaktionsmischung isoliert werden, wenn sie auf Trägerpartikeln immobilisiert sind und das Trägermaterial groß genug für die Separationsmethode ist [2-3].

Der Kontakt eines Proteins in wässriger Lösung mit einer Feststoffoberfläche stellt eine große Störung der Proteinumgebung dar. Adsorptive Wechselwirkungen des Proteins mit einer wässrig-festen Grenzfläche können zu einer Verdrängung von Oberflächenwasser führen; dies gilt insbesondere, wenn die Feststoffoberfläche hydrophob ist. Zusätzlich kann eine wässrig-feste Grenzfläche abweichende pH-Werte besitzen, wenn dissoziierte chemische Gruppen vorhanden sind, sowie eine unterschiedliche Ionenstärke, wenn sie geladene Gruppen aufweist. Auf diese Weise können Adsorption von Proteinen und Immobilisierung von Enzymen an wässrig-festen Grenzflächen Konformationsänderungen im Biomolekül verursachen und die Proteindynamik verlangsamen [6-8]. Ferner kann die Wechselwirkung mit einer festen Oberfläche die gesamte enzymatische Aktivität durch eine ungünstige Orientierung der Enzymmoleküle verringern; denn die aktive Stelle kann entweder von der Materialoberfläche oder durch benachbarte Enzymmoleküle blockiert sein [9].

Die Anwendung hydrostatischen Drucks, wie in der vorliegenden Arbeit gezeigt, ist ein neues, komplementäres, synergistisches oder gar kompensierendes Werkzeug, um die Aktivität von Enzymen, die an wässrig-festen Grenzflächen immobilisiert sind, zu erhöhen. Enzyme sind Proteine mit einer gefalteten nativen Konformation und stellen Reaktionskatalysatoren dar. Die Anwendung hydrostatischen Drucks kann im Wesentlichen auf zwei verschiedene Art und Weisen die Enzymaktivität modulieren. Die Proteinentfaltung geht zumeist mit einer negativen Volumenänderung, ΔV , einher, die bei Druckerhöhung begünstigt wird, was zur druckinduzierten Entfaltung führt. Auf der anderen Seite wurde gezeigt, dass die katalytischen Eigenschaften von Enzymen druckempfindlich sind: Unterhalb

des Entfaltungdruckes können enzymatische Reaktionen sowohl beschleunigt als auch verlangsamt werden [19,20]. Beim erhöhten Druck werden Zustände mit geringen Volumen gegenüber Zuständen, die größere Volumina aufweisen, bevorzugt. Übergangszustände, die ein kompakteres Volumen als ihre Reaktanten besitzen, werden unter Druck begünstigt, so dass enzymatische Reaktionen mit negativen Aktivierungsvolumina ΔV^\ddagger beschleunigt werden. Für die enzymatische Aktivität der Peroxidase aus der Erdbeere wurde gezeigt, dass ihre Oxidationsgeschwindigkeit nach einer Druckbehandlung bei 4000 bar für 5 min erhöht wurde [22]. In ähnlicher Weise wurde eine signifikante Aktivierung der Peroxidase aus Karotten durch eine einminütige Druckbehandlung bei 4000-5000 bar beobachtet [23]. Die Druckuntersuchung an α -Chymotrypsin im Temperaturbereich von 10-65 °C zeigte ebenfalls, dass ihre enzymatische Aktivität für die Hydrolysereaktion eine maximale Geschwindigkeitskonstante bei 45 °C und 2000 bar aufwies [24]. Weiterhin konnte gezeigt werden, dass eine Druckerhöhung bis zu 4700 bar bei 20 °C zu einer 6,5-fachen Beschleunigung der Hydrolyse-Aktivität von α -Chymotrypsin führte, und die Aktivität wurde bei 50 °C und 3600 bar um das 30-fache gesteigert [25].

In der vorliegenden Arbeit wurde die Auswirkung von hohen hydrostatischen Drücken auf adsorbierte Enzyme an wässrig-festen Grenzflächen wie Silica-Nanopartikeln und chemisch modifizierten planaren Oberflächen untersucht. An den Modellenzymen Meerrettich-Peroxidase und α -Chymotrypsin wurden die Druckeinflüsse auf enzymatische Reaktionen an Grenzflächen studiert. Bei Enzymreaktionen mit *low volume*-Übergangszuständen kann die Anwendung von hohen hydrostatischen Drücken die durch Enzymadsorption verursachte Aktivitätshemmung kompensiert werden. Ferner zeigt diese Arbeit den Einfluss der Oberflächenchemie auf das Aktivierungsvolumen einer gegebenen Reaktion auf.

“Activation volumes of enzymes adsorbed on silica particles”

Im ersten Teil dieser Arbeit wurden die ausgewählten Enzyme auf Silica-Nanopartikel immobilisiert. Die Aktivierungsvolumina der beiden Enzyme α -Chymotrypsin (α -CT) und Meerrettich-Peroxidase (HRP), adsorbiert an Silica-Nanopartikeln und frei in Lösung, wurden bestimmt. Die Sekundärstrukturen dieser Enzyme wurden durch Fourier-Transformations-Infrarot-Spektroskopie (FTIR) überwacht, und die Ergebnisse zeigten, dass die adsorbierten Proteine keine wesentliche Änderung in ihren Sekundärstrukturen bis zu 2000 bar aufwiesen. Komplementär wurde die Stabilität der Tertiärstruktur von α -CT mithilfe der Tryptophan-

Fluoreszenz-Spektroskopie bestimmt, und es ergab, dass diese bis 2000 bar stabil blieb. Auf diese Weise wurde zunächst sichergestellt, dass eine Adsorption an Silica-Nanopartikel keine Strukturveränderung dieser Proteine induzierte, und dass der Druckeinfluss sich ausschließlich auf die Enzymkinetik auswirken sollte. Die Reaktionskinetik wurde mithilfe der Fluoreszenzspektroskopie verfolgt und bis zu einem Druck von 2000 bar gemessen. Unter allen Bedingungen wurde eine Abhängigkeit der Aktivierungsvolumina von dem angewandten Druck gefunden, was auf verschiedene Kompressibilitäten der Enzym-Substrat-Mischung und des Übergangszustandes hindeutet.

Für das Enzym HRP waren die Profile der Aktivierungsvolumina für die freie und adsorbierte Form ähnlich. Freie HRP besaß ein Aktivierungsvolumen von $+16 \text{ mL mol}^{-1}$ von 1 bis 500 bar und $+2 \text{ mL mol}^{-1}$ von 500 bis 2000 bar. Das Aktivierungsvolumen der adsorbierten HRP wurde auf $+27 \text{ mL mol}^{-1}$ für 1-250 bar und auf $+2 \text{ mL mol}^{-1}$ für 250-2000 bar bestimmt. Dieser Vergleich zeigt, dass der Mechanismus der enzymatischen Reaktion vermutlich durch die adsorptive Wechselwirkung mit den Silica-Nanopartikeln nicht verändert wird. Bei Drücken oberhalb von 500 bar deutet das geringe Aktivierungsvolumen von $+2 \text{ mL mol}^{-1}$ daraufhin, dass die Volumina von ES^* und E+S sehr ähnlich sind, so dass sich die Druckanwendung nur geringfügig auf die Enzymaktivität auswirkt.

Für das Enzym α -CT wurden größere Aktivierungsvolumina (mehr positive Werte) im adsorbierten Zustand gefunden. Freies α -CT wies ein Aktivierungsvolumen von -67 mL mol^{-1} im Druckbereich von 1 bis 500 bar und eins von -15 mL mol^{-1} von 500 bis 2000 bar auf. Adsorbiert an Silica-Nanopartikeln ging die enzymatische Umsetzung bis zu etwa 500 bar mit einem negativen Aktivierungsvolumen einher, während bei weiterer Druckerhöhung ein positives Aktivierungsvolumen beobachtet wurde. Adsorbiertes α -CT hatte ein Aktivierungsvolumen von -4 mL mol^{-1} von 1 bis 500 bar und $+5 \text{ mL mol}^{-1}$ von 500 bis 2000 bar. Mit diesen Ergebnissen wurde zum ersten Mal in der Literatur gezeigt, dass Enzymreaktionen an wässrig-festen Grenzflächen durch Druckanwendung aktiviert werden können. Somit könnte Druckanwendung eine neue Strategie darstellen, um enzymatische Reaktionen auf Trägerpartikeln zu optimieren.

“Effects of interfacial properties on the activation volume of adsorbed enzymes”

In der ersten Studie konnte gezeigt werden, dass sich der Druckeffekt positiv auf die Aktivität von adsorbierten Enzymen auswirken kann. Im zweiten Teil dieser Arbeit wurde der kombinierte Effekt von Druck und verschiedenen chemisch modifizierten planaren

Oberflächen auf die enzymatische Aktivität von α -CT und HRP untersucht. Die Enzyme wurden an eine blanke Quarzoberfläche, eine hydrophobe Polystyrol- (PS), eine positiv geladene Polyallylamin-Hydrochlorid (PAH)- und eine negativ geladene Polystyrolsulfonat (PSS)-Schicht adsorbiert.

Die Sekundärstrukturen der adsorbierten Enzyme wurden durch FTIR im abgeschwächten Totalreflexion (ATR)-Modus überprüft. Eine Adsorption an die untersuchten Grenzflächen verursachte keine signifikanten Konformationsänderungen der Enzyme. Die Enzymaktivität an der wässrig-festen Grenzfläche wurde mithilfe der Hochdruck-Totalreflexionsfluoreszenzspektroskopie (TIRF) charakterisiert. Die Drucksensitivität der adsorbierten Enzyme hing stark von den chemischen Eigenschaften der Grenzfläche ab. Auf negativ geladenen Oberflächen wie Quarz und PSS konnte z.B. α -CT durch Druckapplikation aktiviert werden. Dabei wurden Aktivierungsvolumina von -29 mL mol^{-1} für 1-1000 bar und -1 mL mol^{-1} für 1000-2000 bar für die Quarz-immobilisierte Variante gefunden. Auf PS-Film zeigte α -CT ein Aktivierungsvolumen von $+9 \text{ mL mol}^{-1}$, auf Multischichten mit einer PSS-Endung -23 mL mol^{-1} und mit einer PAH-Endung $+3 \text{ mL mol}^{-1}$. Dagegen wurde HRP auf dem hydrophoben PS-Film durch Druckapplikation aktiviert. Das Aktivierungsvolumen betrug dabei -35 mL mol^{-1} . Für Quarz und Multischichten mit PSS- oder PAH-Endung waren die Aktivierungsvolumina -6 mL mol^{-1} , $+19 \text{ mL mol}^{-1}$ und $+16 \text{ mL mol}^{-1}$ von 1 bis 2000 bar. Ferner wurden die absoluten Aktivitäten von α -CT und HRP auf Quarz, PS, PAH und PSS durch UV-Absorption bei Umgebungsdruck bestimmt. Dabei wurden große Aktivitäten auf den Oberflächen gefunden, die mit negativen Aktivierungsvolumina verbunden sind.

Insgesamt zeigen die Ergebnisse dieser Studie wieder, dass die Druckapplikation ein nützliches Werkzeug darstellt, um enzymatische Aktivität zu erhöhen, vor allem in Kombination mit der richtigen Adsorptionsoberfläche.

“Advantages of adsorbing α -CT on silica nanoparticles – A high-pressure stopped-flow study “

In diesem letzten Kapitel wurde die Enzymaktivität von α -CT adsorbiert auf Ludox AM mithilfe der Hochdruck-*Stopped-Flow* Technik charakterisiert. Dabei wurden freies und immobilisiertes α -CT im UV-VIS Absorptionsmodus bis 2000 bar vermessen. Ferner wurde ebenfalls die Autolyse-Aktivität der adsorbierten Protease, frei in Lösung und immobilisiert an Ludox AM, analysiert. Die Ergebnisse zeigten, dass die Enzymaktivität des α -CT durch die Adsorption stark beschleunigt wurde. Die K_M - und k_{cat} -Werte der beiden Bedingungen

wurden unter Verwendung von herkömmlicher UV-VIS-Spektroskopie bestimmt. Adsorbiertes α -CT hat einen K_M -Wert von 704 μM , während das freie Enzym einen K_M -Wert von 779 μM aufwies. Weiterhin wurde der k_{cat} -Wert durch die Adsorption um das 8-fache erhöht, mit 0.75 s^{-1} für freies und 5.27 s^{-1} für adsorbiertes α -CT.

Weiterhin wurden zwei Substratkonzentration, 500 μM und 1500 μM , verwendet. Adsorbiertes α -CT zeigte bei der Substratkonzentration von 500 μM ein Aktivierungsvolumen von -8 mL mol^{-1} für 1-1000 bar, gefolgt von einem druckunempfindlichen Bereich von 1000 bis 2000 bar. Die Erhöhung der Substratkonzentration auf 1500 μM verursachte eine Verringerung des Aktivierungsvolumens auf -14 mL mol^{-1} für 1-1000 bar und -2.5 mL mol^{-1} für 1000 bis 2000 bar. Der Druckeffekt war in allen Fällen reversibel. Nach einer Dekompression zurück auf Umgebungsdruck zeigte das Enzym die gleiche Aktivitätsrate wie vor der Druckkompression.

Die Rate der Autolyse von freiem und adsorbiertem α -CT wurde mithilfe der SDS-PAGE quantifiziert. Die Ergebnisse deuteten darauf hin, dass die Adsorption das Enzym stark vor der Autolyse schützt, sodass die Menge des ungeschnittenen Proteins für eine längere Zeit unverändert blieb.

Insgesamt zeigt diese Studie, dass im Falle von α -CT, durch die Adsorption eine höhere Affinität für das Substrat und höhere kinetische Raten erzielt werden konnten. Ferner wurde adsorbiertes α -CT durch Druckanwendung aktiviert. Dieser Effekt war vollständig reversibel. Auch wurde aufgrund der Adsorption die Rate der Autolyse des Enzyms drastisch reduziert.

Zusammenfassend hat diese Arbeit gezeigt, dass Adsorption von Enzymen, insbesondere von Proteasen, an wässrig-festen Grenzflächen eine gute Strategie für einen effizienten Mehrwegeinsatz darstellt.

8. Bibliography

-
- [1] A. Kessel, N. Ben-Tal, Introduction to Proteins, CRC Press, **2011**
- [2] J. N. Talbert, J. M. Goddard, *Colloids Surf. B* **2012**, 93, 8-19
- [3] C. Mateo, J. M. Palomo, G. Fernandez-Lorente, J. M. Guisan, R. Fernandez-Lafuente, *Enzyme Microb. Technol.* **2007**, 40, 1451-1463
- [4] C. Zander, J. Enderlein, R. A. Keller (eds.), Single Molecule Detection in Solution, Wiley-VCH, **2002**
- [5] T. E. Creighton, Proteins, Freeman, **1993**
- [6] M. Rabe, D. Verdes, S. Seeger, *Adv. Colloid Interface Sci.* **2011**, 162, 87-106
- [7] A. Sethuraman, G. Belfort, *Biophys. J.* **2005**, 88, 1322–1333
- [8] A. Ball, R. A. L. Jones, *Langmuir* **1995**, 11, 3542–3548
- [9] L. Caseli, R. P. M. Furriel, J. F. de Andrade, F. A. Leone, M. E. D. Zaniquelli, *Journal of Colloid and Interface Science* **2004**, 275, 123–130
- [10] M. Murray, D. Rooney, M. Van Neikerk, A. Montenegro, L.R. Weatherley, *Process Biochem* **1997**, 32, 479-486
- [11] A. S. Malinin, A. A. Rakhnyanskaya, A. V. Bacheva, A. A. Yaroslavov, *Polymer Sci.* **2011**, 53, 52-56
- [12] M. Lundqvist, I. Sethson, B.-H. Jonsson, *Langmuir* **2004**, 20, 10639-10647
- [13] C. Czeslik, *Z. Phys. Chem.* **2004**, 218, 771-801
- [14] M. Malmsten (ed.), Biopolymers at interfaces, Marcel Dekker, **2003**
- [15] N. V. Nucci, B. Fuglestad, E. A. Athanasoula, A. J. Wand, *Proc. Natl. Acad. Sci. U.S.A.*, **2014**, 111(38), 13846–13851
- [16] B. B. Boonyaratanakornkit, C. B. Park, D. S. Clark, *Biochim. Biophys. Acta* **2002**, 1595, 235-249
- [17] C. A. Royer, *Biochim. Biophys. Acta* **2002**, 1595, 201-209
- [18] M. Gross, R. Jaenicke, *Eur. J. Biochem.* **1994**, 221, 617-630
- [19] M. J. Eisenmenger, J. I. Reyes-De-Corcuera, *Enzyme Microb. Technol.* **2009**, 45, 331-347
- [20] V. V. Mozhaev, K. Heremans, J. Frank, P. Masson, C. Balny, *Trends Biotechnol.* **1994**, 12, 493-501
- [21] P. F. Cook, W. W. Cleland, Enzyme Kinetics and Mechanisms, Garland, **2007**
- [22] A. Garcia-Palazon, W. Suthanthangjai, P. Kajda, I. Zabetakis, *Food Chem.* **2004**, 88, 7-10
- [23] M. Anese, M. C. Nicoli, G. Dall’Aglia, C. R. Lericci, *J. Food Biochem.* **1995**, 18, 285-293

- [24] Y. Taniguchi, K. Suzuki, *J. Phys. Chem.* **1983**, 87, 5185-5193
- [25] V. V. Mozhaev, R. Lange, E. V. Kudryashova, C. Balny, *Biotechnol. Bioeng.* **1996**, 52, 320-331
- [26] W. Appel, *Clinical Biochemistry*, **1986**, 19, 317-322
- [27] D. M. Blow, *Accounts of Chemical Research* **1976**, 9, 145-152
- [28] B. Zerner, R.P.M. Bond, M.L. Bender, *J. of Am. Chem. Soc.* **1964**, 86, 3674-9.
- [29] M. Zimmerman, B. Asche, E. C. Yurewicz, G. Patel, *Analytical Biochemistry* **1977**, 78, 47-51
- [30] N. C. Veitch, *Phytochemistry* **2004**, 65, 249–259
- [31] K. G. Welinder, *Eur. J. Biochem.* **1979**, Y6, 483-502
- [32] J.N. Rodríguez-López, D.J. Lowe, J. Hernández-Ruiz, A.N.P. Hiner, F. García-Cánovas, R.N.F. Thorneley, *J. Am. Chem. Soc.* **2001**, 123, 11838–11847
- [33] M. Zhou, Z. Diwu, N. Panchuk-Voloshina, R.P. Haugland, *Anal Biochem.* **1997**, 253 (2), 162-168
- [34] N. R. Mohamada, N. H. C. Marzukia, N. A. Buanga, F. Huyopb, R. Abdul Wahab, *Biotechnol. Biotechnol. Equip.* **2015**, 29(2), 205-220
- [35] M.C. Flickinger, S.W. Drew, *Encyclopedia of bioprocess technology* **1999**, 1, 1st ed. New York
- [36] K.R. Jegannathan, S. Abang, D. Poncelet, E.S. Chan, P. Ravindra, *Crit. Rev. Biotechnol.* **2008**, 28, 253-264
- [37] K.A. Joshi, J.Tang, R. Haddon, J. Wang, W. Chen, A. Mulchandani, *Electroanalysis.* **2005**, 17, 54-58
- [38] L. Cao, *Carrier-bound immobilized enzymes: principles, application and design* **2005**, Weinheim: Wiley-VCH
- [39] R. Bahulekar, N.R. Ayyangar, S. Ponrathnam, *Enzyme Microb. Technol.* **1991**, 13, 858-868
- [40] V. Schuabb, S. Cinar, C. Czeslik, *Colloids Surf. B Biointerfaces* **2016**, 140, 497-504
- [41] R. Winter, F. Noll, C. Czeslik, *Methoden der Biophysikalischen Chemie* **2011**, 2nd edition, Vieweg+Teubner
- [42] J. R. Lakowicz, *Principles of Fluorescence Spectroscopy* **2006**, 3rd edition, Springer
- [43] S.N. Timasheff, H. Susi, L. Stevens, *J. Biol. Chem.* **1967**, 242, 5467–5473
- [44] D.M. Byler, H. Susi, *Biopolymers* **1986**, 25, 469–487
- [45] P.T.T. Wong, D.J. Moffat, *Appl. Spectrosc.* **1989**, 43, 1279–1281

- [46] D. Axelrod, T. P. Burghardt, N. L. Thompson, *Ann. Rev. Biophys. Bioeng.* **1984**, 13, 247-268
- [47] J. Koo, C. Czeslik, *Rev. Sci. Instrum.* **2012**, 83, 085-109
- [48] G. Decher, *Science* **1997**, 277, 1232-1237
- [49] C. Jeworrek, O. Hollmann, R. Steitz, R. Winter, C. Czeslik, *Biophys. J.* **2009**, 96, 1115-1123
- [50] J. Koo, C. Czeslik, *Colloids Surf. B Biointerfaces* **2012**, 94, 80-88
- [51] M. Tolan, *X-Ray Scattering from Soft-Matter Thin Films* **1999**, 148, Springer
- [52] A. Ratha, M. Glibowickaa, V.G. Nadeaua, G. Chena, C. M. Debera, *Proc. Natl. Acad. Sci. U.S.A* **2009**, 106, 1760-1765
- [53] C. Czeslik, C. Royer, T. Hazlett, W. Mantulin, *Biophys. J.* **2003**, 84, 2533-2541
- [54] P. Butz, K. O. Greulich, H. Ludwig, *Biochemistry* **1988**, 27, 1556-1563
- [55] A. F. García, P. Butz, B. Tauscher, *Biotechnol. Prog.* **2002**, 18, 1076-1081
- [56] T. F. Schmidt, L. Caseli, T. Viitala, O. N. Oliveira, *Biochim. Biophys. Acta* **2008**, 1778, 2291-2297
- [57] T. Kurinomaru, S. Tomita, Y. Hagihara, K. Shiraki, *Langmuir* **2014**, 20, 3826-3831
- [58] C. C. You, S. S. Agasti, M. De, M. J. Knapp, V. M. Rotello, *J. Am. Chem. Soc.* **2006**, 128, 14612-14618
- [59] C. Czeslik, R. Winter, *Phys. Chem. Chem. Phys.* **2001**, 3, 235-239
- [60] The Molecular Probes Handbook, <http://www.lifetechnologies.com>
- [61] G. Öjteg, P. Lundahl, M. Wolgast, *Biochim. Biophys. Acta* **1989**, 991, 317-323
- [62] C. Phelps, L. Forlani, E. Antonini, *Biochem. J.* **1971**, 124, 605-614
- [63] N. Ui, *Biochim. Biophys. Acta* **1971**, 229, 582-589
- [64] M. A. Marini, C. Wunsch, *Biochemistry* **1963**, 2, 1454-1460
- [65] L. Smeller, F. Meersman, J. Fidy, K. Heremans, *Biochemistry* **2003**, 42, 553-561
- [66] K. Akasaka, H. Nagahata, A. Maeno, K. Sasaki, *Biophysics* **2008**, 4, 29-32
- [67] Z. Sun, R. Winter, In *Advances in high pressure bioscience and biotechnology II*; Winter, R., Ed.; Springer: Berlin, pp 117-120
- [68] J. Koo, C. Czeslik, *Soft Matter* **2012**, 8, 11670-11676.
- [69] S. Devineau, J. M. Zanotti, C. Loupiac, L. Zargarian, F. Neiers, S. Pin, J. P. Renault, *Langmuir* **2013**, 29, 13456-13472

- [70] H. S. Pappa, A. E. G. Cass, *Eur. J. Biochem.* **1993**, 212, 227-235
- [71] D. B. Northrop, *Biochim. Biophys. Acta* **2002**, 1595, 71-79
- [72] P. S. Low, G. N. Somero, *Proc. Natl. Acad. Sci. U.S.A.* **1975**, 72, 3014-3018
- [73] D. Zheng, H. P. Lu, *J. Phys. Chem. B* **2014**, 118, 9128-9140
- [74] H. H. Gorris, D. R. Walt, *J. Am. Chem. Soc.* **2009**, 131, 6277-6282
- [75] L. Smeller, J. Fidy, *Biophys. J.* **2002**, 82, 426-436
- [76] M. Franzreb, M. Siemann-Herzberg, T. J. Hobley, O. R. T. Thomas, *Appl. Microbiol. Biotechnol.* **2006**, 70, 505-516
- [77] J. J. Gray, *Curr. Opin. Struct. Biol.*, **2004**, 14, 110-115
- [78] J. M. Harris, Poly(Ethylene Glycol) Chemistry: Biotechnical and Biomedical Applications, J. M. Harris ed., Plenum Press **1992**, New York
- [79] L. D. Unsworth, H. Sheardown, J. L. Brash, *Langmuir* **2008**, 24, 1924-1929
- [80] J. Piehler, A. Brecht, K. Hehl, G. Gauglitz, *Colloids Surf. B Biointerfaces* **1999**, 13, 325-336
- [81] P. F. Brode III, C. R. Erwin, D. S. Rauch, D. S. Lucas, D. N. Rubingh, *J. Biol. Chem.* **1994**, 269, 23538-23543
- [82] F. Caruso, C. Schüler, *Langmuir* **2000**, 16, 9595-9603
- [83] S. Disawal, J. Qiu, B. B. Elmore, Y. M. Lvov, *Colloids Surf. B Biointerfaces* **2003**, 32, 145-156
- [84] B. Haupt, T. Neumann, A. Wittemann, M. Ballauff, *Biomacromolecules* **2005**, 6, 948-955
- [85] L. Derr, R. Dringen, L. Treccani, N. Hildebrand, L. Colombi Ciacchi, K. Rezwani, *J. Colloid Interface Sci.* **2015**, 455, 236-244
- [86] T. P. Russell, *Mater. Sci. Rep.* **1990**, 5, 171-271
- [87] E. Goormaghtigh, V. Raussens, J.-M. Ruyschaert, *Biochim. Biophys. Acta* **1999**, 1422, 105-185
- [88] R. C. Neuman, W. Kauzmann, A. Zipp, *J. Phys. Chem.* **1973**, 77, 2687-2691
- [89] G. Öjteg, P. Lundahl, M. Wolgast, *Biochim. Biophys. Acta* **1989**, 991, 317-323
- [90] P. Nestler, S. Block, C. A. Helm, *J. Phys. Chem. B* **2012**, 116, 1234-1243
- [91] V. Schuabb, C. Czeslik, *Langmuir* **2014**, 30, 15496-15503
- [92] S. Cinar, C. Czeslik, *Colloids Surf. B Biointerfaces* **2015**, 129, 161-168
- [93] P. Schwinté, J.-C. Voegel, C. Picart, Y. Haikel, P. Schaaf, B. Szalontai, *J. Phys. Chem. B* **2001**, 105, 11906-11916

-
- [94] A. S. Malinin, A. A. Rakhnyanskaya, A. V. Bacheva, A. A. Yaroslavov, *Polymer Science A* **2011**, 53, 52-56
- [95] J. Koo, M. ErIkamp, S. Grobelny, R. Steitz, C. Czeslik, *Langmuir* **2013**, 29, 8025-8030
- [96] S. Suladze, S. Cinar, B. Sperlich, and R. Winter, *J. Am. Chem. Soc.* **2015**, 137, 12588-12596
- [97] S. Li, Z. Wu, M. Lu, Z. Wang, Z. Li, *Molecules* **2013**, 18, 1138-1149
- [98] C. A. Schneider, W. S. Rasband, K. W. Eliceiri, *Nature Methods* **2012**, 9, 671-675
- [99] 7-methyl-coumarin, product data sheet, Sigma-Aldrich
- [100] Q. Chen, K. G. Rausch, H. Schçnherr, G. J. Vancso, *ChemPhysChem* **2010**, 11, 3534 – 3540
- [101] Q. Chen, H. Schçnherr, G. J. Vancso, *Small* **2009**, 5, 1436 – 1445
- [102] P.Y. Bolinger, D. Stamou, H. Vogel, *Angew. Chem.* **2008**, 120, 5626.
- [103] D. M. Vriezema, P. M. L. Garcia, N. S. Oltra, N. S. Hatzakis, S. M. Kuiper, R. J. M. Nolte, A. E. Rowan, J. C. M. van Hest, *Angew. Chem.* **2007**, 119, 7522 –7526
- [104] T. Q. Luong, R. Winter, *Phys. Chem. Chem. Phys.* **2015**, 17, 23273-23278
- [105] M. L. Bender, F. J. Kezdy, F. C. Wedler, *Journal of Chemical Education* **1967**, 44, 84-88

9. Publications and presentations

Results presented in this thesis have contributed to:

PUBLICATIONS

- **V. Schuabb**, S. Cinar, C. Czeslik Effect of interfacial properties on the activation volume of adsorbed enzymes *Colloids and Surfaces B* 140 (2016) 497-504.
- **V. Schuabb**, C. Czeslik Activation volumes of enzymes adsorbed on silica particles *Langmuir* 30 (2014) 15496-15503.

TALKS

- **V. Schuabb** Activation Volumes of Enzymes Adsorbed on Silica Particles, 8th Tag der Chemie, Dortmund, Germany, 2015.
- **V. Schuabb** Effect of pressure on enzymatic activities at the water-silica interface, 8th International Conference on High Pressure Bioscience and Biotechnology, Nantes, France, 2014.

PRESENTATIONS

- **V. Schuabb**, C. Czeslik Chemically modified surfaces affect the activation volume of adsorbed enzymes, 60th Annual Meeting of Biophysical Society, Los Angeles, USA, 2016 (**Poster**).
- **V. Schuabb**, S. Cinar, C. Czeslik Effect of interfacial properties on the activation volume of adsorbed enzymes, 8th International Meeting on Biomolecules under High Pressure, Dortmund, Germany, 2016 (**Poster**).
- **V. Schuabb**, C. Czeslik Activation volume of enzymes adsorbed at solid liquid interfaces, 53th EHPRG Meeting on High Pressure Science and Technology/25th International Conference of the AIRAPT, Madrid, Spain, 2015 (**Poster**).
- **V. Schuabb**, C. Czeslik Activation volumes of enzymes adsorbed at chemically modified aqueous-solid interfaces 114th General Assembly of the German Bunsen Society for Physical Chemistry, Bochum, Germany, 2015 (**Poster**).
- **V. Schuabb**, C. Czeslik Effect of pressure on enzymatic activities at the water-silica interface 113th General Assembly of the German Bunsen Society for Physical Chemistry, Hamburg, Germany, 2014 (**Poster**).

10. *Curriculum Vitae*

Vitor Diniz Schuabb

EDUCATION

2013 - present

Technical University of Dortmund Germany

PhD in NATURAL SCIENCE

Certificate in PHYSICAL CHEMISTRY

2012

Federal University of Rio de Janeiro Brazil

Master Degree in BIOLOGICAL CHEMISTRY

Certificate in BIOLOGICAL SCIENCE

2010

Federal University of Rio de Janeiro Brazil

Complementary license in CLINICAL LABORATORY

Certificate in BIOCHEMICAL PHARMACIST

2009

Federal University of Rio de Janeiro Brazil

Bachelor Degree in PHARMACY

Certificate in PHARMACIST

AWARD

Prize of best student oral communication at 8th International Conference on High Pressure Bioscience and Biotechnology, Nantes, France, 2014

PROFESSIONAL ASSOCIATIONS

Biophysical Society, USA.

